student enquiry series D

the production properties and uses of X-rays

TELTRON

THE TEL-X-OMETER, TEL. 580

PART 1 : INSTRUCTION MANUAL.

PARA

FIGURE

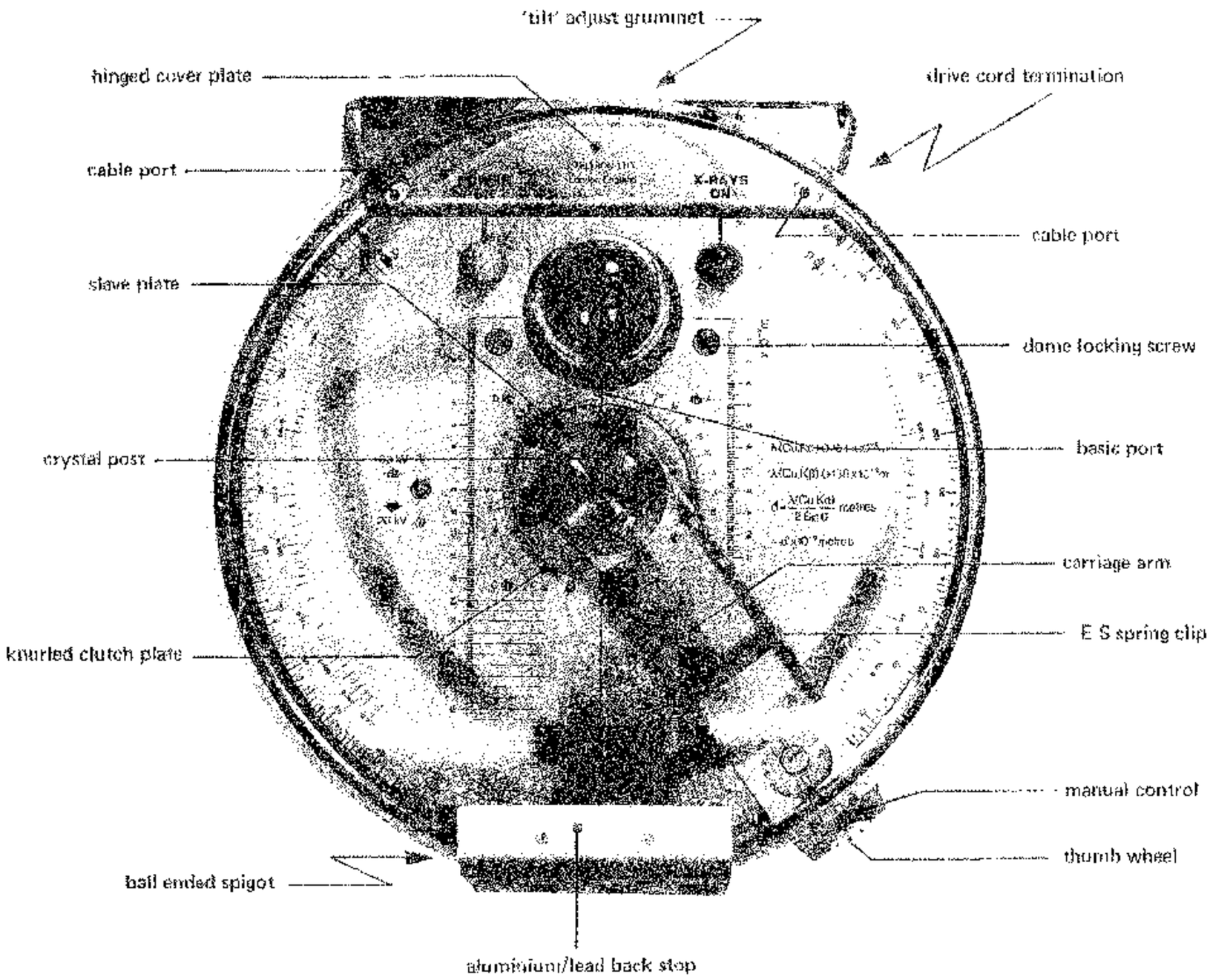

FIG. 1 – IDENTIFICATION

1.0 INTRODUCTION

The physics teachers and research scientists who helped to formulate the "TELTRON APPROACH TO ATOMIC PHYSICS" reasoned that had refractory metals and good high vacuum equipment been available to the genuises of the "golden era" at the turn of the century, then thermionic emission would have replaced the traditional gas discharge as the vehicle of atomic physics investigations.

2.0 The Free Electron

It was on this basis that the historical sequence of the evolution of this subject was disregarded and SERIES A, "THE PRODUCTION AND PROPERTIES OF THE FREE ELECTRON", was prepared; although it differs from the chronological evolution, the presentation and understanding of the argument is very much simplified and expenditure in terms of both finance and time is reduced to a minimum.

Series A starts with a simple Thermionic Effect experiment in air; this dictates the need for an evacuated experimental zone and the thermionic diode is introduced, followed by the triode and the development of a simple diode electron gun. Producing free electrons in this manner a series of crucial steps is recommended and all the experimental apparatus necessary to perform these steps is available.

The entire programme of experiments is designed such that a thorough examination of each phenomenon suggests the nature of the next crucial step.

At the culmination of Series A the electron has been produced and "weighed and measured"; but during the series, the phenomenon of the glowing of a luminous screen is not explained and similarly a limitation of 5000 volts is seemingly arbitrarily imposed for accelerating voltages. The discriminating physicist will seek both an explanation to the luminescence and a verification that the properties of the electron are unchanged by accelerations induced by more than 5000 volts.

3.0 The Bonded Electron

A re-examination of the Luminescent Tube, TEL 522 introduces SERIES B, "A CONCEPT OF THE ELECTRON WITHIN THE ATOM", leading to field emission, isotopes and electron energy levels.

4.0 High Voltage Acceleration

The employment of accelerating voltages of the order of 30,000 volts introduces SERIES D, "THE PRODUCTION, PROPERTIES AND USES OF X-RAYS".

A simple evacuated thermionic diode is postulated having an anode which can tolerate the increased wattage dissipation required when a potential difference of 30,000 volts is imposed across the cathode and anode.

In November 1895 similar very high accelerating voltages were being employed by Professor Wilhelm Röntgen in his laboratories at Würzburg in Bavaria.

Clearly the use of 30,000 volts will introduce a hazard to health and through Röntgen's work it is known that additional hazards will exist which require the use of special apparatus - the TEL-X-OMETER, TEL 580.

5.0 TEL-X-OMETER, TEL 580

The packaging of the instrument has been carefully designed to ensure that units are delivered in the same condition as they leave the factory. If any damage is apparent when the packing case is opened the supplier of the equipment should be notified immediately and the instrument should not be used.

All accessories, kits and items are packed separately but, with the exception of the Filmpaks, there is space allocated for every item in all the kits within the large Accessory Box, marked TEL 582/3/4.

6.0 COMMISSIONING THE INSTRUMENT

Lift the instrument out of the box and remove all packing materials, including the plastic bag which houses the power supply lead; place the spare fuses and the miniature jack-plug contained in the plastic bag into the Accessory Box TEL582/3/4.

6.1 Mains Power Supply

Attach a plug to the power supply cable in accordance with the wiring instruction sheet.

With the transparent plastics Scatter Shield closed, tilt the instrument onto its hinge and ensure that the Power Selector on the underside of the instrument indicates the correct mains voltage; to re-adjust the selector pull out the black plug and replace, with the arrow pointing towards the legend which corresponds to the power supply available in the laboratory.

Check that both the Power Fuse and the EHT Fuse are securely screwed in.

6.2 Radiation Warning Sign (Ref, ICRP Publication 13, para 20)

Remove the yellow, black and white radiation warning card from the top lining board of the packing case; cut out the appropriate sign and affix to "the entrance to the enclosure or room containing the Tel-X-Cmeter".

6.3 Mechanical Inspection

The transparent plastics Radiation Scatter Shield which completely encloses the experimental zone (ref: ICRP para 17) is normally locked in the 'safe" position by a ball-ended spigot.

This spigot locates in a key-hole slot situated behind the aluminium back-stop displaying the International Radiation Symbol (ref: ICRP para 19 and see Fig.1).

To open the unit the entire Scatter Shield should be displaced sideways with respect to the hinge; the spigot will automatically line up with the left hand or right hand release port and the Shield can be lifted; the cover is self-supporting when it has been lifted beyond the vertical line of the hinge.

Check that no visible screws have been loosened in transit; that the spectrometer arm can be moved around to the scale limits in both directions; that the lenses on the signal lamps are tight etc.

Lower the Shield to the locked 'operating' position; repeat the opening procedure in the opposite direction.

6.4 Safety Interlocks (ref, ICRP para 18)

To become familiar with the interlock system, displace and open the radiation Scatter Shield and remove the two screws which retain the hinge cover plate, see Fig.1; remove the plate.

Open and close the Scatter Shield observing the operation of the interlock system at the hinge; note the ball and socket indication of the central position; note that the Shield cannot be moved in a sideways direction when it is open; note the "fail-safe" duplication of interlocks. Replace and screw down the hinge cover plate.

Using a wide bladed screw driver turn the large screw-heads located at each side of the lead-glass dome, see Fig. 1; note that each screw-head controls a plastics plate which locks the glass dome in position and at the same time activates a micro-switch fixed underneath each locking plate; when these plates are unlocked the lead-glass dome can be removed for access to the X-ray tube.

Return each screw-head to the dome-locked position, close the Scatter Shield and slide to the central position.

6.5 Initial Switch On (ref: ICRP para 21)

Connect the mains supply to the unit by depressing the POWER ON switch (WHITE) on the control panel; the unit will only function when the Time Switch is rotated to the required time factor. When this is performed both the filament of the X-ray tube and the POWER-ON lamp (WHITE) will be illuminated.

6.6 Condensation

After the instrument has experienced changes in the temperature and the humidity of the surrounding air a slight condensation is sometimes apparent inside the lead-glass dome; the Tel-X-Ometer warms up after a short period in operation but at no time should any part of the instrument seem too hot to the touch of the hand.

The operating temperature is sufficient to evaporate any condensation and it is therefore recommended that only the filament is energised for the first five minutes; if, on depressing the X-RAYS ON button (RED), a faint 'crackling' noise is heard then some electrical discharge due to dampness is evident and the equipment should be allowed to run for a further five minutes with only the filament operating.

6.7 X-Rays On/X-Rays Off Procedure (ref: ICRP para 18)

To switch off the EHT, displace the Scatter Shield sideways with respect to the hinge.

Replace the Shield in the central locked position and depress the X-RAYS ON button; the X-RAYS ON lamp (RED) will be illuminated.

If, at the first attempt, the red lamp does not illuminate, check that the Shield is correctly centred; If centralisation is not properly effected the micro-switches at the hinge will not activate the EHT circuit and the red lamp will not illuminate; centralise the Shield correctly and again depress the X-RAYS ON button.

6.8 Electronic Charge Persistence

The EHT for the unit is derived from a solid state invertor circuit, followed by a Cockcroft-Walton type multiplier to provide a smooth d.c. output. In operation, the capacitors in this circuit become charged; the EHT circuit is well insulated for 30,000 volts and when the EHT is switched off the charge on these capacitors persists for many hours. In the absence of special precautions, this charge would be a hazard to technicians who may wish to perform service work on the electronic circuit or to change the X-ray tube; there would also be a radiation hazard if the filament should be energised some hours after the unit had been switched off whereupon an X-ray pulse would be emitted whether the Shield be safely in position or not.

A special protection circuit has therefore been incorporated which provides a short energy-pulse to the filament immediately after the power to the unit has been disconnected; this pulse serves to discharge the EHT circuit and can be observed as a bright flash each time the instrument is de-energised by switching off the "POWER-ON" control.

6.9 Visible and Audible Signals (ref: ICRP para 19)

The X-RAYS ON lamp (RED), the POWER ON lamp (WHITE) and the filament itself can all be readily observed from all around the instrument.

The EHT generator operates at high frequency (R.F.) which provides an audible indication that the instrument is operating.

An additional external and even remote indicator can be connected, if required, by inserting the jack-plug provided into the "monitor tube current" socket recessed in the control panel; any such external circuit must operate at 50 µA, the normal tube current.

6.10 Radiation levels (ref: ICRP para 17)

If it is desired to monitor the radiation level around the instrument, due attention should be directed to the R.F. field which can induce false readings in the radiation monitor; to verify the readings observe the effect of a piece of lead sheet in various positions about the detector; if the readings can be made to fall below 0.5 mR/hr at a distance of 50mm from the external surface without placing the lead directly between the detector and the X-ray tube anode then the R.F. field is "swamping" an otherwise "safe level" reading.

The Tel-X-Ometer is certified by the British National Radiation Protection Board as complying with all Codes of Practice recommended by the International Commission on Radiological Protection; the instrument is also approved by the British Government Department of Education and Science for use in educational establishments under the provisions of Administrative Memorandum 1/65.

6.11 Manufacturer's Serial Number

The Tel-X-Ometer is convection cooled, the air being drawn in through a wire mesh underneath the unit and expelled around the perimeter of the top of the cylindrical metal housing.

The Serial Number of each unit is visible through the wire-mesh on the underside of the instrument and is affixed to the shroud of the EHT transformer.

7.0 SERVICING & MAINTENANCE

As with all Teltron equipment the Tel-X-Ometer has been designed to withstand the abuse and misuse which all apparatus used for course demonstration and student practical work traditionally experiences and it will operate for long periods without the need for maintenance.

Some items however will require attention at some time during the useful life of the instrument - the two indicator lamps, fuses, the relay and the X-ray tube.

The indicator lamps and the X-ray tube have a nominal life in excess of 1,000 hours and replacement will be infrequent.

7.1 Replacement of "POWER-ON" and "X-RAYS ON" Lamps.

Switch off and disconnect from mains supply.

Open Shield and unscrew the coloured polystyrene lens.

With the end of a piece of stiff plastic tubing about 10mm in diameter unscrew and remove the bulb.

Similarly insert and screw in the new bulb.

Replace lens.

7.2 Replacement of "POWER FUSE" and "EHT FUSE"

These fuses are readily accessible on the underside of the instrument and will only require replacement if a fault occurs in the power unit circuits or if an incorrect fuselink has been used.

Note that the EHT fuse (see circuit diagram, FS.2) must be either a

1 Amp, Delay Type (originally supplied)

or 2 Amp, Quick Blow Type.

The only other fuselink, FS.3 is provided to protect expensive components in the event of an abnormal failure and as such it is located within the instrument.

7.3 Access to the Electronic Components

Switch off and disconnect from mains supply.

Open Shield and remove hinge cover plate.

Unscrew the lock nut retaining each end of the spectrometer-arm drive cord, located at the back of the apparatus underneath the hinges, see Fig.1.

Carefully release, in turn, each end of the drive cord, keeping it under tension and affix it with a piece of adhesive tape to the respective vertical side of the Manual Control, made of orange plastics material.

From inside the hinge chamber remove the two screws used for terminating the drive-cord.

Close the Scatter Shield.

Invert the instrument onto a piece of soft cloth and remove the four screws fixing the flange of the cylindrical body to the base-casting of the spectrometer table.

Lift the flanged cylindrical housing by tilting it upwards and away from the hinge region and carefully guide it away from the multi-plug cable connector; disconnect the cable connector.

The electronic components on the printed circuit board are now accessible.

7.4 Replacement of Fuselink FS. 3

This fuse protects the supply to the heater voltage stabiliser and is fitted in an open fuseholder mounted on the printed circuit board close to one of the transistor cooling plates.

It will require replacement only if the output terminals of the stabiliser are shorted externally or if an internal short occurs in the stabiliser circuit itself.

FUSE TYPE: 2 Amp Quick Blow Type.

7.5 Replacement of Interlock Relay

The relay controls the interlocked switching of the EHT generator and the correct function of the safety discharge circuit.

Spring off the retaining clip; unplug and replace the relay; replace spring clip.

8.0 FAULT FINDING

It is recommended that unless professional facilities are available the rectification of only minor and obvious faults are attempted by the user; for more obscure faults the instrument should be returned to the supplier.

8.1 Elementary Fault: Indicator lamp fails to operate and the tube filament fails to illuminate.

Possible Causes: Mains plug defective.
Timer switch not operated.
Power fuse defective.
Diode bridge D2 -D5 or D6 -D9 defective.
Transformer T.1 defective.

8.2 Elementary Fault: "POWER ON" lamp fails to operate but tube filament does illuminate.

Possible Causes: Indicator lamp defective.
EHT fuse defective.
EHT stabiliser defective.
EHT oscillator defective.

Operate "X-RAYS ON" momentarily and observe "X-RAYS ON" lamp - switch off instrument.

If lamp operates, then "POWER ON" lamp or the associated wiring is defective.

If X-Rays On lamp does not illuminate, check EHT fuse; if replacement fuse blows when power is switched on, check EHT stabiliser.

If EHT fuse blows check oscillator transistors for VCE short or collector to chassis short.

8.3 Elementary Fault: "POWER ON" lamp operates but tube filament fails to illuminate.

Possible Causes: Tube pin contact defective.
Tube heater coil defective; check continuity.
Filament supply fuse defective.
Filament supply stabiliser defective; check input voltage before fuselink.
Filament supply wiring defective; check heater supply on pins 6 and 13.

9.0 REPLACEMENT OF X-RAY TUBE, TEL 581

IMPORTANT: If a tube is being replaced due to a faulty filament, ensure that at least 6 hours has elapsed since the instrument was last operated; the discharge protection circuit (see 6.8) depends on the illumination of the filament for correct operation; if the filament is not operating, the capacitors in the EHT circuit must be allowed sufficient time to discharge.

9.1 Disconnect the unit from main supply.

9.2 Displace and open the Scatter Shield (see 6.3) and remove the lead glass dome (see 6.4).

9.3 If a tube is being replaced, carefully lift off the top cap connector and remove the tube by pulling in a vertical direction.

9.4 Examine the new tube and ensure that the anode has not been dislocated in transit.

9.5 Orient the new tube such that the bubble window is facing the crystal post; then push the pins of the tube into the base connector, ensuring that the axis of the helical filament is in the direction $2\theta = \theta = 0^{\circ}$.

NOTE: The bubble window may be slightly offset, but the important feature to line up is the filament.

9.6 Carefully replace the top cap connector.

9.7 Replace the lead glass dome and lock in position.

9.8 Place the 1 mm Collimator, TEL 582.001 in the Basic Port with the slot HORIZONTAL.

9.9 Place the 1 mm Collimator Slide, TEL 562.015 at E.S.13 with the slot HORIZONTAL.

9.10 Mount the G/M tube and holder at E.S.22. Connect to the Ratemeter (polarising supply about 420 volts).

9.11 Select 30KV and close and centre the Scatter Shield with the Carriage Arm in the zero position.

9.12 Connect a 100 µA meter to the 'Monitor Tube Current' jack socket on the control panel, using the jack plug provided.

9.13 Switch Power On; the filament should be illuminated if the time switch is not in the off position; if it does not illuminate, proceed as in para. 8.0.

9.14 Operate 'X-Rays On' button; the Red Indicator Lamp should illuminate (see 6.7).

9.15 Check that the tube current can be varied from 20 to 80 µA and set at 50 µA.

IF THE TUBE CURRENT CANNOT BE VARIED UP TO 80 µA REPORT THIS TO THE SUPPLIER OF THE INSTRUMENT. (Adjustment can be undertaken by a trained technician).

9.16 'Height' Adjustment

Remove the lower black rubber grummet located just below the hinge extension.

The screw-head thus exposed controls the "height" of the X-ray tube.

9.17 Using a screwdriver, slowly rotate the screwhead and at the same time observe the Ratemeter.

Note that the count rate depends on the height of the tube; obtain a peak count rate and replace the black grummet.

Before commencing experimental work with the Tel-X-Ometer, carry out the "tilt" adjustment procedure as detailed in para 14.0.

10.0 EXPERIMENTAL TECHNIQUES

10.1 Primary Beam:

The X-ray emission from the tube is collimated at the lead glass dome to be a circular beam of 5mm diameter, see Fig.1; this primary beam diverges from the Basic Port to give a useful beam diameter at the Crystal Post of 15mm diameter, at Experimental Station (ES) 13 of 20mm diameter and at Experimental Station (ES) 30 of 38mm diameter.

Where the primary beam impinges on the lead back-stop it has a diameter of 60mm and a penumbral width of approximately 20mm.

With the unit operating at 30kV and 50 µA the intensity of radiation in the useful beam at 20cm (ES.28) from the focus is about 2 rads per minute.

10.2 Primary Collimators:

The primary beam can be collimated to a fine circular beam using the 1mm diameter Collimator TEL 582.002 and to a ribbon beam using the 1mm Slot Collimator, TEL 582.001; each of these collimators is installed by inserting the 'O' ring shank into the Basic Port and pushing it home; the 'O' ring retains the collimator in position and allows exchange of the collimators even when they become warm.

The collimators should be rotated when they are inserted to unsure that they are securely seated.

The 1mm Slot Collimator can be rotated in position to provide a vertical ribbon of X-rays, a horizontal ribbon or any diametrical ribbon.

10.3 Secondary Collimators:

There are two secondary collimators, a 1mm Slot Collimator, TEL 562.015 and a 3mm Slot Collimator, TEL 562.016.

Each of these collimators is slide mounted and can be positioned in any E.S. on the Spectrometer Arm.

Always use an E.S. Spring Clip, see Fig.1, when positioning these collimators (and indeed any of the experimental slides) to ensure that all the slides are centred on the X-ray beam by pressing them against the numbered side of the carriage which acts as a datum.

The E.S. Spring Clips can be easily repositioned by springing open the toothed jaw on the outside face of the plastics carriage. Six of these E.S. Spring Clips are provided, four on the Spectrometer Arm and two on the Auxiliary Carriage.

10.4 Auxiliary Slide Carriage, TEL 582.005:

A demountable Auxiliary Slide Carriage is included.

Using this carriage, Experimental Stations 1 to 4 can be placed in the X-ray beam in a variety of positions.

Some of the experiments recommended in this booklet require this carriage to be mounted in two particular modes.

Mode H (Horizontal) The hole in the end face of the Auxiliary Carriage is placed over the Basic Port in the glass dome and then held in that position by one or other of the Primary Collimators. In this mode the axis of the centre of each experimental slide is HORIZONTAL and is transcribed by the X-ray beam.

Note that the Carriage Arm is now restricted to a maximum 2θ angle of 100°.

Mode V (Vertical) The end face of the Auxiliary Carriage is placed over the minor diameter of the Knurled Clutch Plate screwed over the Crystal Post, see Fig.1; the crystal mounting jaw and screw should be removed. In this mode the axis of the centre of each experimental slide is VERTICAL and co-incident with the pivot axis of the spectrometer table.

The X-ray beam now passes through the slides at right angles to the centre line axis. The height of the Auxiliary Carriage can be adjusted by screwing the Clutch Plate up or down accordingly.

10.5 Knurled Clutch Plate

When the Clutch Plate is screwed down it exerts pressure on a spring plate which in turn engages the 2:1 spectrometer drive mechanism. When it is unscrewed it disengages the drive mechanism. This permits the Crystal Post to be manually positioned in any desired orientation with respect to the Carriage Arm.

10.6 The 2:1 Spectrometer Mechanism:

Open the Scatter Shield and rotate the Carriage Arm until the cursor gives an accurate no-parallax zero reading on the 2θ scale.

Release the drive by unscrewing the Clutch Plate and push the Slave Plate (the inner rotating plate engraved with two datum lines, see Fig.1) round until the datum lines are accurately opposite the zeros on the θ scale. It may be necessary to "mean out" small zero-reading differences on each side of the θ scale.

Check that the Carriage Arm cursor is still at zero on the 2θ scale and screw in the Clutch Plate to engage the 2:1 drive mechanism.

Now rotate the Carriage Arm through 90° (2θ) and note that the crystal Slave Plate moves through 45° (θ).

10.7 Choice of operating side:

Close the Scatter Shield - note that the Shield can be displaced in two directions; always slide the Shield to the same side as that of the Carriage Arm. Note that the gap between the Shield and the spectrometer table, where the Carriage Arm normally freely rotates, is eliminated on one side of the instrument, depending on the direction of displacement at the hinge.

To transfer the Carriage Arm to the opposite side, rotate the arm to the smallest angle possible, about 11° (2θ); now open the Shield by sliding away from the Carriage Arm and then rotate the arm through the zero axis to the opposite side.

10.8 Fine and Coarse Controls:

The Carriage Arm is terminated outside the Shield with an orange plastics Manual Control; measurements can be made at the cursor to an accuracy of 15 minutes of arc.

To achieve fine adjustment of the Carriage Arm, rest the hand on the base flange of the Tel-X-Ometer or on the bench top and using the thumb rotate the knurled aluminium drive wheel protruding from the Manual Control.

To achieve fine measurements line up the cursor exactly on the most convenient 2θ graduation which is central within the region requiring detailed examination; hold the Manual Control rigidly in this position and "slip" the Thumb Wheel against the friction of the drive cord until the zero on the Thumb Wheel scale aligns exactly with the pointer.

Now the Thumb Wheel can be moved $\pm 4^{\circ}$ (2θ) about the preset centre line by an amount which can be measured at the Thumb Wheel scale to an accuracy of 5 minutes of arc; this amount should be added or subtracted from the selected cursor setting according to the direction of movement of the arm.

10.9 Mounting of cubic crystals:

Select the LiF crystal (BLUE) from the box of accessories and place one of the short edges onto the step in the Crystal Post; ensure that a long broad face, a (100) cleavage plane, is butting against the chamfered protrusion of the post, see Fig.2. Screw up the clamp until the crystal is held securely by the rubber jaw.

Ensure that the crystal is vertical and flat on the step.

THE EXPERIMENTAL FACE OF THE CRYSTAL IS THAT FACE WHICH IS COINCIDENT WITH THE CHAMFER ON THE POST.

10.10 Mounting of Geiger Muller Tube:

Plug the G/M tube MX168 (TEL 546) into the Holder, TEL 547.

Place the square flange of the holder in E.S.26 on the carriage arm without use of an ES Spring Clip, ensuring that the co-axial cable is leading out from the underside and that the end-window of the G/M tube is facing the Crystal Post. It is advisable to leave the plastics guard over the end-window unless very feeble count rates are to be monitored.

The co-axial cable can be trailed out from the Shield beside the Manual Control.

10.11 General Facilities:

There are two radiation-proof ports located at each end of the hinge cover plate for introducing large cables, vacuum pipes, etc. into the experimental zone.

There are four blind holes on the surface of the spectrometer table for the mounting of innovative experiments of the teachers' or pupils' choice; these holes are 4mm diameter, located around the θ Scale and marked A, B, C and D.

11.0 MONITORING INSTRUMENTS:

During Bragg Diffraction experiments (from Experiment D.14) count rates of 800 to 1,000 counts per second are experienced for CuKα reflections from the Lithium Fluoride crystal. Count rates of up to 500 cps are more normal for the other three crystals, NaCl, KCl or RbCl.

Background count rates vary from up to 300 cps at the top of the "whale-back" down to 10 cps at the tail-off.

For crystallography experiments therefore a Ratemeter capable of integrating up to 2000 cps is recommended.

For measurements in the main X-ray beam it should be noted that the normal intensity of radiation will saturate the G/M tube; the MX168 has a dead time of 100 microseconds and hence the G/M tube will saturate at a count rate of 10,000 cps; the X-ray tube current must be reduced to about 5 μA to prevent saturation and achieve a count rate of about 7,000 cps. For quantitative experiments in the main beam therefore a Ratemeter capable of integrating up to 7/8000 cps is recommended.

The X-ray tube current should NOT be adjusted without monitoring the current, using the jack-plug provided and an external 100 μA or 150 μA meter.

NEVER EXCEED 80 MICROAMPS.

The polarising supply for the MX168 G/M tube should be variable from 250 to 450 volts d.c.; the threshhold voltage is about 370 volts d.c.

When varying the tube current from 20 to 80 μA the EHT will remain constant within 5% of the selected value, 20 or 30 kV. Conversely, when varying the EHT from 30 to 20 kV the regulation is such that the tube current will remain constant within 5%.

12.0 OPERATIONAL ALIGNMENT:

The Tel-X-Cmeter has been carefully aligned during the final stages of factory inspection; but to verify that the pre-set-alignment has not been disturbed during transit it is recommended that the following tests be performed.

12.1 Place the 1mm Collimator, TEL 582.001 in the Basic Port and the 1mm Collimator Slide, TEL 562.015 at E.S.30 and ensure that both collimators are vertical.

12.2 Zero-set and lock the Slave Plate and the Carriage Arm cursor as precisely as possible.

12.3 Spring a Spindle Clip TEL 567.008 over the chamfered Crystal Post and carefully insert a Glass Fibre TEL 567.004 to be truly vertical, see Fig.3.

12.4 With the Scatter Shield open, operate the POWER ON switch and sight through the collimators to view the reflection of the tube filament in the copper target anode.

The Glass Fibre should normally be observed as central in the "viewing column" created by the two collimators, i.e. the direction of the primary beam and it should be possible to obtain an uninterrupted view of the anode past each side of the fibre; the glass dome can be rotated by a small amount if the two dome-locks are unscrewed.

12.5 Remove the Glass Fibre and the Spindle Clip.

13.0 EXPERIMENTAL VERIFICATION:

Mount the LiF Crystal (Blue) in the Crystal Post (see "Induced Dislocation", Part 2, para D.27.30).

13.1 Check that the cursor is at zero reading (2θ) and again sight through the collimators; the direction of the primary beam should lie in the surface of the crystal, as does the axis of rotation.

13.2 The normal to the reflecting face of the crystal should bisect the angle between the primary beam and the centre line of the Carriage Arm; for Bragg reflection experiments the arm should always be moved to the same side of the crystal as that occupied by the chamfered Crystal Post protrusion.

13.3 Move Collimator (1mm) 562.015 to E.S.18 and mount Collimator (3mm) 562.016 at E.S.13. Mount the G/M tube and Holder at E.S.26.

Connect to the Ratemeter and energise the polarising supply to the G/M tube (400 - 420 volts d.c).

13.4 Check that the voltage selector indicates 30kV.

13.5 Move the Carriage Arm through at least 15° (2θ) in the direction to detect Bragg Reflection.

13.6 Close and centre the Scatter Shield.

13.7 Depress the "X-RAYS ON" button; the RFD signal lamp should be illuminated.

13.8 Verify that a strong CuKα reflection (high ratemeter count rate) is evident at a 2θ angle of $45^{\circ} \pm 30'$.

Record the 2θ angle of the peak reflection.

IF THE PEAK OF THE REFLECTION LIES OUTSIDE THIS TOLERANCE THEN THE X-RAY TUBE SHOULD BE ADJUSTED FOR 'TILT' AS IN PARA. 14.

Now record the equivalent reflection on the opposite side of the table.

13.9 Return the Carriage Arm to about 12^{o} (2θ) and open the Shield by displacing it away from the arm.

13.10 Unscrew the Clutch Plate, rotate the Slave Plate (and thereby the Crystal) through 180^{o} and again zero-set the Slave Plate and the Carriage Arm as precisely as possible.

13.11 Repeat stages 13.5 to 13.8 and record the 2θ angle of the peak CuKα reflection.

13.12 The Mean Reading of the reflections recorded at 13.8 and 13.11 should be 44^{o} 56' ± 12'.

WHEN MAKING ACCURATE ANGULAR MEASUREMENTS EXPERIMENTAL ERRORS SHOULD BE MINIMISED BY EMPLOYING THIS TECHNIQUE OF TAKING A MEAN OF THE EQUIVALENT READING AT EACH SIDE OF THE SPECTROMETER TABLE.

13.13 The Tel-X-Ometer is now commissioned and certified as capable of measuring angular deflections (2θ) to an accuracy of ± ½'.

14.0 "TILT" ADJUSTMENT OF X-RAY TUBE:

Before proceeding with this adjustment carefully repeat both paras 12 and 13 to ensure that no alignment errors have been introduced.

14.1 Remove the upper black rubber grummet located just below the hinge extension.

The screw-head thus exposed controls the "tilt" of the X-ray tube about a central position.

14.2 Set the cursor of the Carriage Arm at the exact mean of the reading measured at para. 13.8 and the true Bragg angle (2θ) for LiF of 44^{o} 56'.

14.3 Obtain a peak count rate by carefully adjusting ONLY the 'tilt-control' without displacing the Carriage Arm.

14.4 Now seek and record a peak reflection by displacing the Carriage Arm only, without operating the tube tilt-control.

14.5 Set the cursor at the exact mean of the reading measured at para 14.4 and the true Bragg angle 44^{o} 56' (2θ).

14.6 Iteratively repeat paras 14.2, 14.3 and 14.4 until the cursor peak reading falls within the tolerance 45^{o} ± 30'.

14.7 Replace the black rubber grummet and carry out recommendations 13.9 to 13.12.

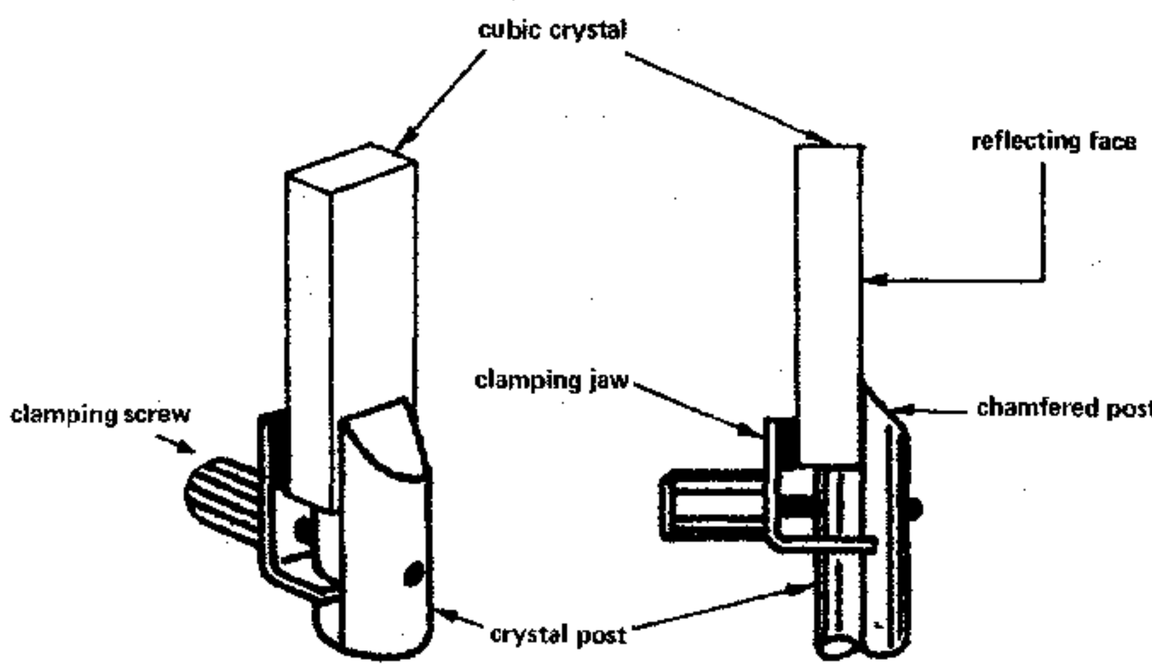

FIG. 2 MOUNTING OF CUBIC CRYSTALS

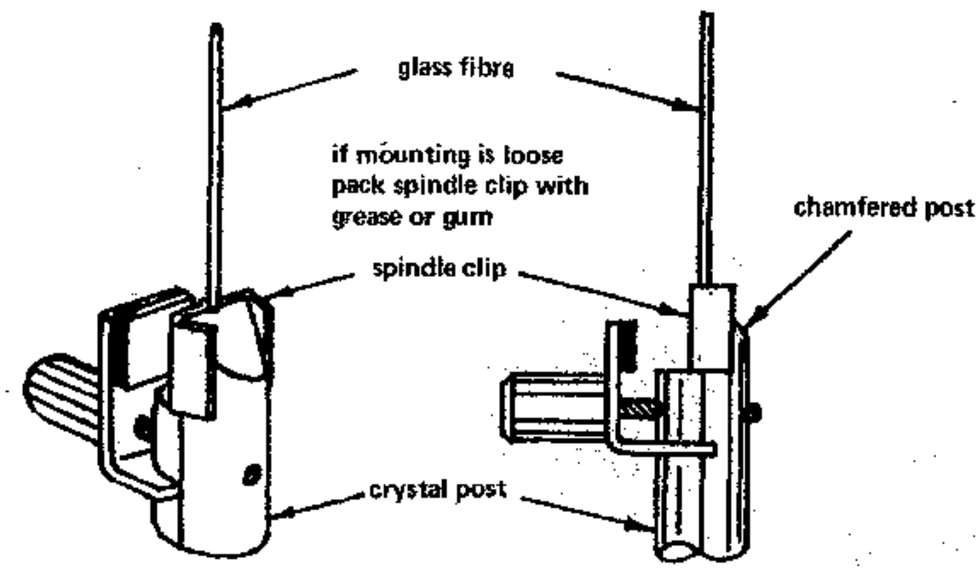

FIG. 3 MOUNTING OF GLASS FIBRES

LIAISON WITH ELECTRON ANALYSIS
(High Energy electrons?)

D.1 THE RONTGEN OBSERVATION
(The Luminescent Screen)

DETECTION

D.2 THE SPARK GAP

D.3 THE IONISATION CHAMBER*

D.4 THE GEIGER-MULLER TUBE*

D.5 EXCITATION OF PHOTOEMULSION

D.6 THE PHOTOGRAPHIC PROCESS

PROPERTIES

D.7 RECTILINEAR PROPOGATION

D.8 INVERSE SQUARE LAW

D.9 DEFLECTION EFFECTS

D.10 PENETRATION & ABSORPTION
(The Linear Absorption Co-efficient)
(Introduction to White Radiation)

D.11 THE PHANTOM
(1/2 and 1/10 value thickness)

ELECTROMAGNETIC RADIATION and THE QUANTUM THEORY

D.12 DIFFRACTION EVIDENCE, LAUE

D.13 WAVELENGTH MEASUREMENT
(Nuffield Film on Diffraction Grating)

D.14 THE BRAGG RELATIONSHIP
(Avogadro's Number)

D.15 X-RAY EMISSION
(Planck's Constant)
(The inverse Photo-electric effect)

D.16 X-RAY ABSORPTION
(Absorption Edges)
(Mass Absorption Co-efficient)

D.17 X-RAY SCATTERING
(Secondary Emission)

PHYSICS

D.18 MOSELEY'S LAW
(Material Analysis)

D.19 FINE STRUCTURE
($K\alpha_1$ and $K\alpha_2$)
(Emission Intensities)

Under Development

D.20 ELECTRON ENERGY LEVELS
Robinson/De Broglie

D.21 THE COMPTON EFFECT
A quantitative measurement

CRYSTALLOGRAPHY

D.22 ATOMIC SIZE
(The Alkaline halide sequence)

D.23 THE UNIT CELL
(One, dimension, a)
(Single Crystal, Bragg)

D.24 CO-ORDINATES
(The Reciprocal Lattice)
(The Circle of Reflection)

D.25 THE UNIT CELL
(Two dimensions, a and b)
(Single Crystal, Bragg)

D.26 THE UNIT CELL
(Third dimension, c)
(The Sphere of Reflection)
(Rotating Single Crystal Photograph)

D.27 POWDER ANALYSIS
(Extinctions and Intensity)
(Debye-Scherrer photographs)

D.28 CRYSTAL SYSTEMS
(Simple, face, body-centred)
(Debye-Scherrer photographs)

D.29 MATERIAL STATE
(Orientation and Laue spots)
(Drawn monofilament)
(Particle size)

D.30 MATERIAL COMPOSITIONS
(The X-ray Powder Data File)
(Debye-Scherrer photographs)

RADIOGRAPHY

Film Techniques

D.31 CONTRAST
(Exposure Times)
(Wavelength, kV Considerations)
(Choice of Filters)
(Scatter)

D.32 DEFINITION
(Size of Focal Spot)
(Film/Tube/Object Distance)
(Viewing angle)

D.33 SENSITIVITY
(The Penetrameter)
(Negative Diagnosis)

D.34 RESOLUTION
(Feature Recognition)

RADIATION UNITS & MEASUREMENTS

THE ROENTGEN, R

D.35 EXPOSURE DOSE RATE*

D.36 THE *RAD**

D.37 QUALITY FACTOR, QF*

D.38 THE *REM**

D.39 BUILD UP FACTOR*

D.40 S.I. UNITS

* Optional Experiments: an ionization chamber and picoammmeter or a high voltage power supply will be required

General Introduction:

It is recognised that those educational Institutions teaching pure physics probably possess neither the time nor the desire to concentrate much attention on the application of X-ray technology to industry or medicine; the converse may well apply to those teaching X-ray radiography.

The range of accessories has therefore been divided into 3 groups, Kit TEL 582 being of basic universal use and Kits 583 and 584 being for specialised application.

The experiments detailed in this booklet follow the teaching sequence of Series D, The Production, Properties and Uses of X-rays; no claim is made that this sequence can provide adequate coverage of the subject for all levels of education and it is recommended that experiments are selected, disregarded or embellished in accordance with the requirements of the curriculum.

Experimental Notes:

For each Experimental Programme the recommended voltage and current setting for the X-ray tube is indicated, together with the relevant accessory kit required to perform the experiment.

A summary of this latter information is tabled , Appendix A.

Note that no reliance should be placed upon the timer for photographic exposures of less than 5 minutes duration; the timer has been incorporated as a safety device and it is not sufficiently accurate for short exposures. Such exposures can be initiated by depressing the 'X-RAYS ON' button (RED), timed using a watch and terminated by displacing the Scatter Shield sideways, with respect to the hinge, or by operating the 'POWER ON' switch.

EXPERIMENTAL PROGRAMME D1 TO D6, DETECTION (2 HOURS)

D1 — THE RONTGEN OBSERVATION (15 MINUTES):

Remove Crystal Post and Jaw.

KIT 582+584	30 kV	50 μA	DARKENED LAB

Cover the Lead Glass Dome and both signal lamps with a piece of black cloth and perform these experiments in a well darkened room ; allow sufficient time for observers to become dark-adapted.

D1.1 Insert Luminescent Screen, TEL 582.003 in E.S.13 with the phosphor coating facing the X-ray tube; locate the Carriage Arm in the axis of the beam, (2θ = 0).

Switch on X-rays and observe the circle of luminescence.

D1.2 Insert Screen in E.S.20. Remove the metal back plate from Film Cassette TEL 562.031 and place the Backstop of the Cassette in E.S.13.

Observe an image of the backstop and its supporting wires on the screen.

That barium platino-cyanide could be made to "fluoresce" when placed close to a high voltage discharge in a tube containing rarified gas was discovered by Rontgen in 1895, two years before J. J. Thomson succeeded in isolating the electron. Arguments were raging at that time regarding the nature of cathode rays and the relative merits of particle and wave theories and Rontgen shrewdly labelled the new 'radiation effect' as X-radiation, pending further enquiry as to its nature.

The name X-rays is still in general use today although the title "Rontgen radiation" is also used.

Prof. Rontgen wrote: "..... behind a bound book of about one thousand pages I saw the fluorescent screen light up brightly, the printer's ink offering scarcely a noticeable hindrance".

D1.3 Invert the Screen at E.S.20 such that the phosphor coating faces away from the X-ray tube and place two or three pieces of printed news sheet between the screen and the tube.

Observe luminescence.

In his paper published in 1895, Rontgen also wrote "... the X-rays proceed from that spot where the cathode rays strike the glass wall. If the cathode rays within the discharge apparatus are deflected by means of a magnet, it is observed that the X-rays proceed from another spot - namely, from that which is the new terminus of the cathode rays".

D1.4 Perform "Pin-hole Camera Experiment" as detailed in Experimental Programme D.32.

D1.5 Make a right-angle bend in a piece of steel strip of length about 15 cms and place the two magnets 562.008 together at the extremity of one arm so constructed; pass the other arm through a Cable Port on the hinge plate - the magnet can be rotated from below the Cable Port from a position near the Scatter Shield side-wall to close to the Glass Dome, still covered with the black cloth.

Replace the film cassette backstop in position E.S.13.

Locate the Collimator, 582.001, in the Basic Port and rotate the 1mm slot to the vertical position.

Observe the image on the screen and its variation when the magnets are moved close to the X-ray tube thereby deflecting the source of X-radiation.

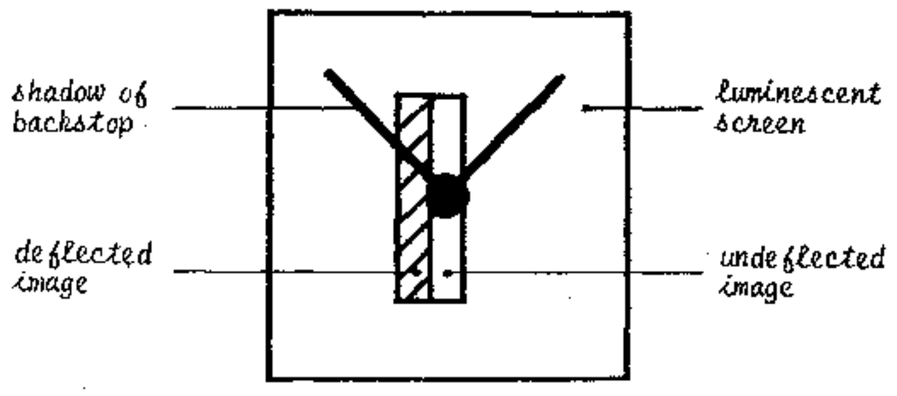

The magnets should approach the dome as low as possible to the base flange in order to obtain maximum deflection.

This series of experiments follows Series A where the production and the properties of the free electron have been studied; the student will probably anticipate some evidence of high energy electrons; he might justifiably believe that a hitherto undiscovered property of the electron is that at high energies it can penetrate the glass of the X-ray tube, the black cloth, the newsheet and indeed the intervening air.

Series A commenced with the Thermionic Effect where ionisation of air brought about the discharge of an electroscope; if X-rays are high speed electrons then can air be ionised in a similar manner?

D2 — THE SPARK GAP (10 MINUTES, OPTIONAL):

5 KV power supply required

KIT 582	kV as specified 50 µA	NORMAL LAB

Attach two steel needles to the Auxiliary Slide Carriage, TEL 582.005 using adhesive tape as illustrated, with points placed 3mm apart.

Connect the pins to the positive and negative terminals of a 5,000 volt d.c. power supply, passing the cables through the Cable Ports at the Hinge Plate.

Locate the Spark Gap assembly as illustrated such that the needle points lie in the X-ray beam.

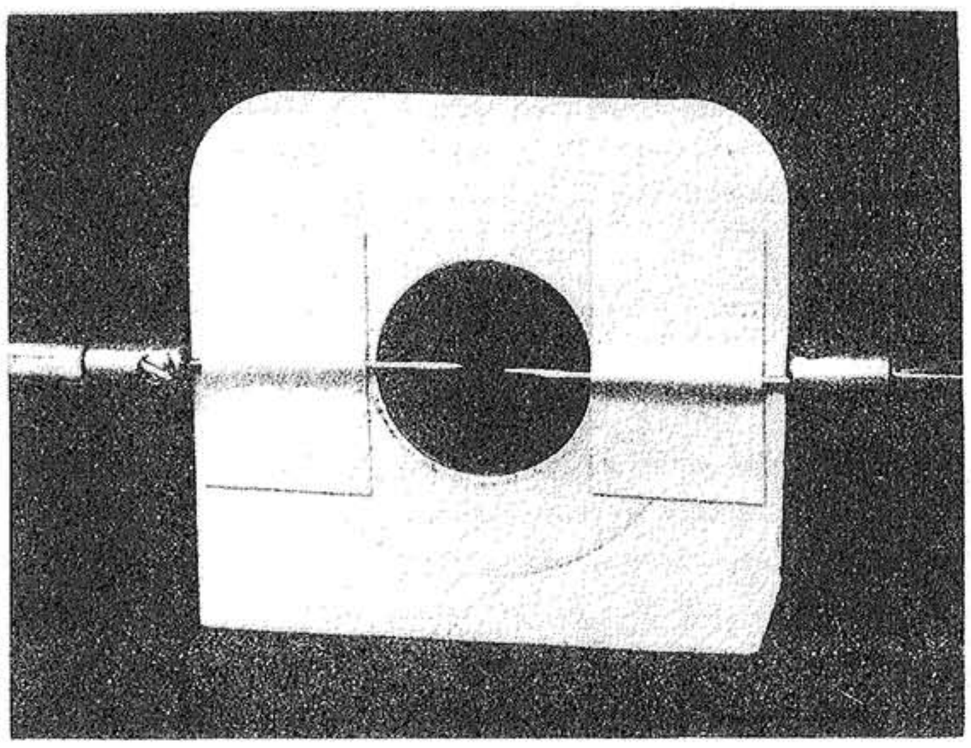

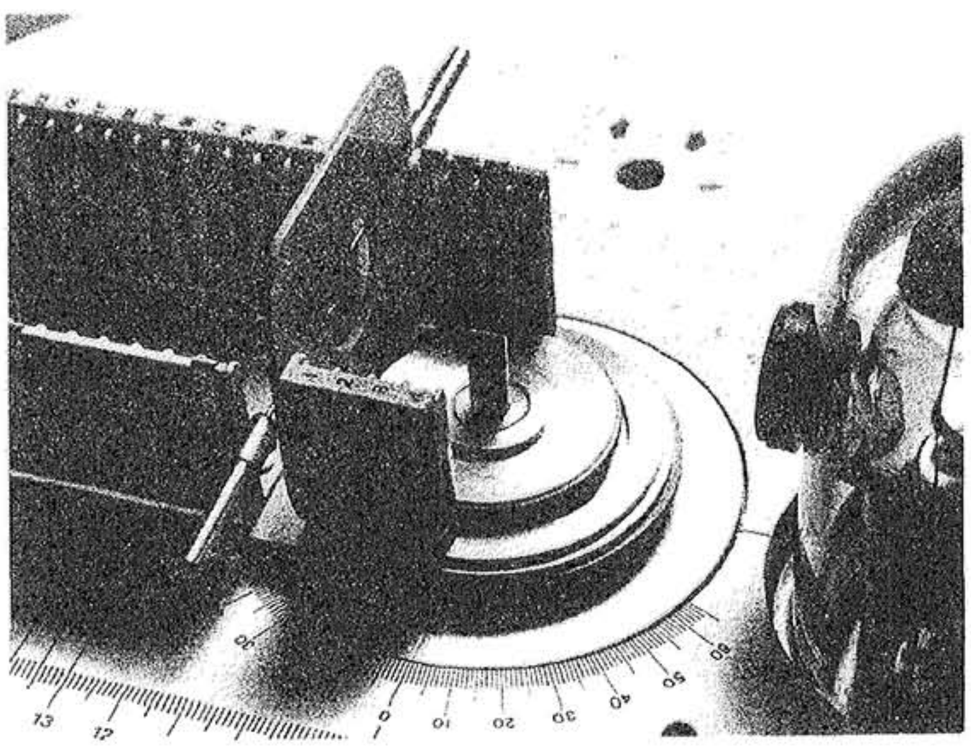

D2.1 In the absence of ary X-radiation, increase the d.c. voltage from zero and note that a spark discharge occurs at about 4kV; now reduce the voltage until the spark ceases.

D2.2 Select 3CkV and operate the 'X-PAYS ON' button.

Note that the presence of the X-rays precipitates the spark discharge.

Switch off the X-rays by dislocating the Scatter Shield and note that again the discharge ceases.

D2.3 Select 2CkV and switch on the X-rays; the discharge will only pass if the potential difference across the gap is INCREASED.

The X-radiation causes ionisation of the air in the spark gap, the degree of which depends on the voltage across the X-ray tube electrodes; it is evident, qualitatively, that X-rays cause ionising events but the technique needs to be developed for meaningful quantitative results.

D3 — THE IONISATION CHAMBER (1 HOUR, OPTIONAL):

Ionization Chamber, Picoammeter, and 5 KV power supply required

Remove Crystal Post and Jaw.

TEL 588	kV & µA as specified	NORMAL LAB

Mount the Ionisation Chamber, TEL 588 in E.S.13 and 26 with the insulator supporting the central electrode at E.S.26 and the Carriage Arm in the Primary Beam.

Connect up the circuit as illustrated to a D.C. Amplifier with a facility to measure currents down to 10^{-11} amps., and polarise the Ionisation Chamber using a power supply with a d.c. output variable to 2000 volts.

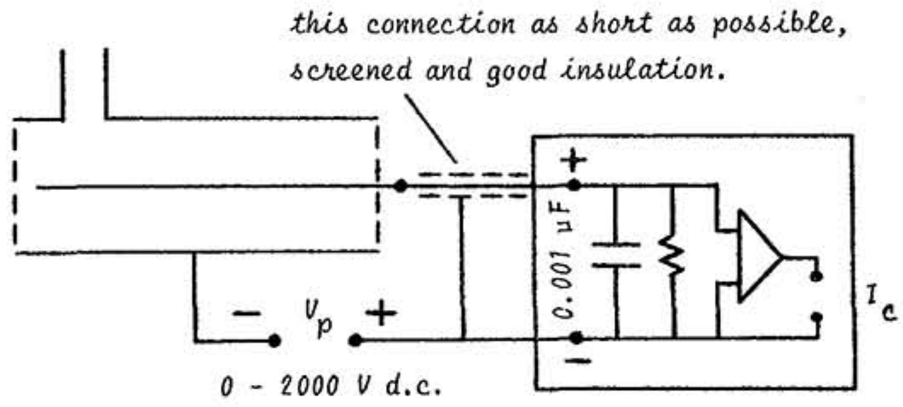

D3.1 Ionisation at Atmospheric Pressure

Tabulate the collector current I_c for increments of polarising voltage V_p and plot graphs A to D.

Table A		Table B		Table C		Table D	
30kV 50 µA		20kV 50 µA		30kV 20 µA		30kV 80 µA	
V_p	I_c	V_p	I_c	V_p	I_c	V_p	I_c

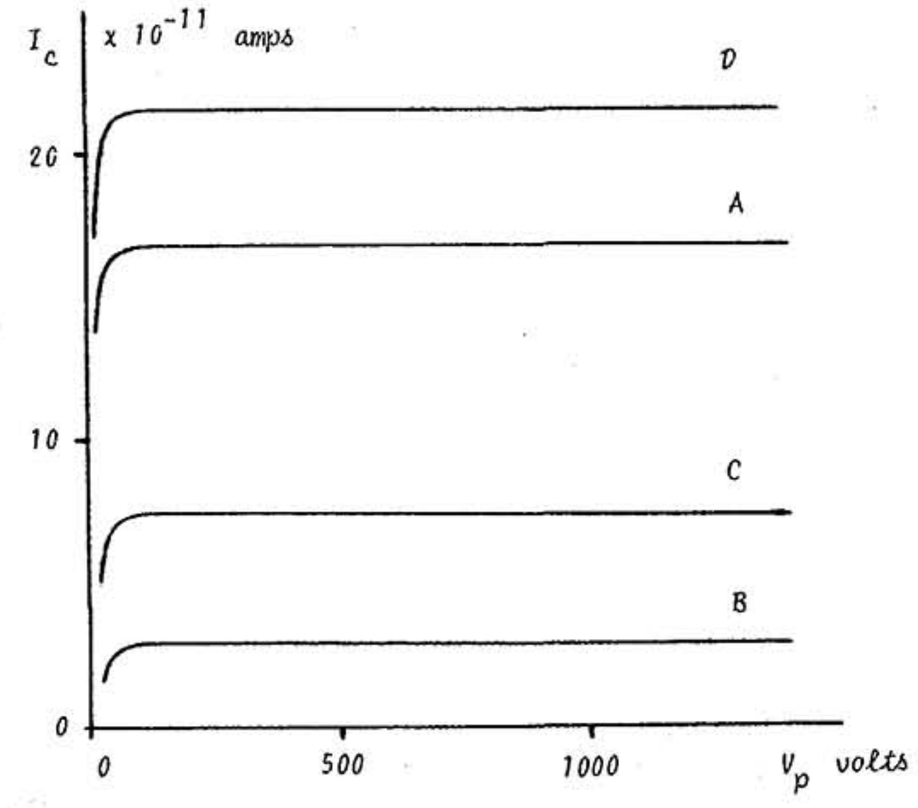

NOTE: Do not touch the Scatter Shield during these experiments as the effect on stray capacitance due to electrostatic charging can disturb the uniformity of the results.

This simple ionisation chamber can be calibrated to provide an X-ray measuring instrument capable of much greater quantitative results than the Spark Gap; changes in both X-ray tube current and voltage produce measurably different ionisation currents within the chamber.

See Experimental Programme D.35

In Series A the Thermionic Effect experiment was complicated by the presence of air; in the instance of this ionisation chamber, for the given geometry of the detector, the only parameter that has not been varied is the nature of the gas being ionised and does this similarly complicate the results?

D3.2 Ionisation at Low Pressure

Connect the exhaust manifold of the Ionisation chamber to a rotary vacuum pump by passing thick-walled rubber vacuum tubing through a Cable Port at the Hinge Plate; interconnect a needle-valve between the Ionisation chamber and the rotary pump so that a controlled leak of air can be made to vary the pressure in the chamber.

Before tabulating any results set the polarising voltage, V_p at 1,000 volts and adjust the pressure in the chamber by means of the needle-valve until the collector current reads about 5×10^{-11} amps; allow the system to stabilise in this condition for two or three minutes to permit the vacuum pump to warm up; the pressure at this point is about 1mm Hg.

Vary the voltage V_p from zero to about 1600 volts; tabulate and plot graphs as in D3.1.

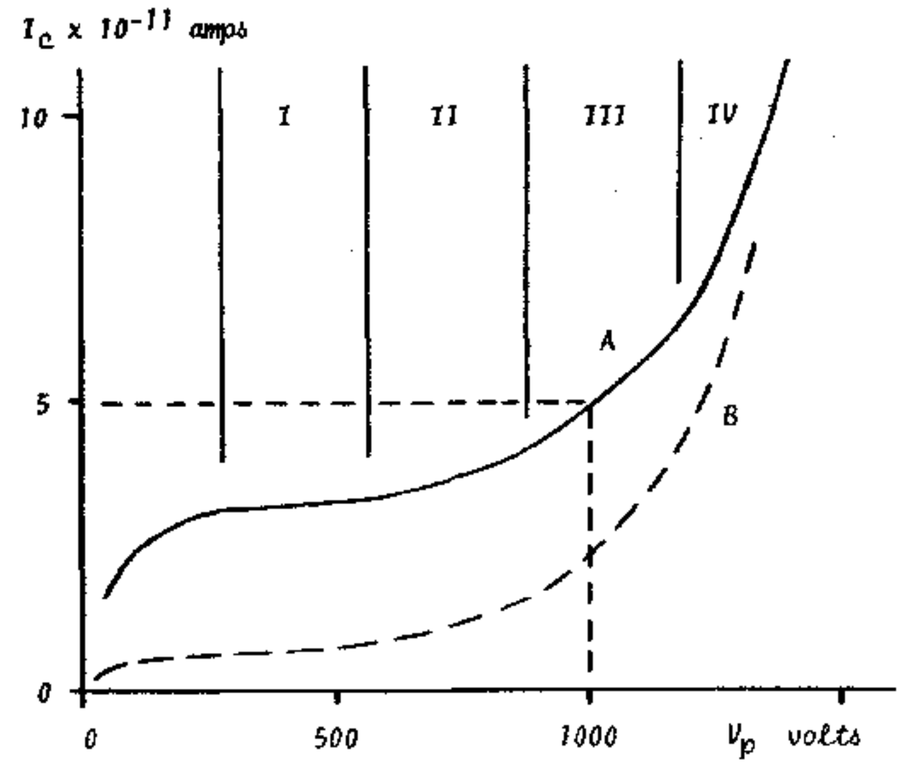

Set - up: 5 mins.

Experimental Time: Graph A , 30 kV , 50 µA 10 mins.

Graph B , 20 kV , 50 µA 5 mins.

To verify that a continuous discharge occurs at about 1600 volts reduce V_p to 1400 volts and switch off X-rays; now increase V_p until I_c avalanches without any external ionising influence (quickly reduce V_p after this verification of continuous discharge to avoid damage to the d.c. amplifier).

For a comprehensive analysis of Ionisation Characteristics reference should be made to standard text-books.

The Regions of Ionisation (I), Proportionality (II) and Limited Proportionality (III) are clearly illustrated; for the purposes of Series D the mode of ionisation giving the greatest collector current, the Geiger Region (IV), will be preferred as a convenient and sensitive detector of X-radiation.

For further quantitative studies see D.35.

D4 – X-RAY DETECTION BY GEIGER-MULLER TUBE (20 MINUTES)

For a detailed study of the theory and construction of Counter Tubes reference should be made to standard text-books.

The ionisation chamber was first developed by Johannes Geiger whilst working with Professor E. Rutherford at Manchester in 1908 to become a detector which could count individual ionising events and his work was subsequently further developed by Walther Muller in 1928 at Kiel University with the then Professor Geiger.

In experiment D3.2 the nature of the gas experiencing ionisation due to X-radiation was varied in pressure only; more detailed research reveals that 'individual ionising events' are occurring due to the X-radiation and that the total number of events in a given period of time can be recorded, using a Scaler or integrated, to register the number of counts-per-second, using a Ratemeter. The duration of the effect of the ionising event depends not only on the pressure but also on the actual gas or mixture of gases used; after the detection of an 'individual ionising event' ("count") the Geiger-Muller tube must be 'quenched' in order to be ready as quickly as possible to receive the next event; the Counter Tube, TEL 546 (MX168), is self-quenched by means of a mixture of Halogen gases at low pressure.

D4.1 Optimum Operating Voltage (Optional)

Scaler Required

Insert the G.M. Tube in the Holder, TEL 547, and mount the assembly at E.S.22 (see Part 1, para 10.10) and connect to a Ratemeter/Polarising Supply (see Part 1, para 11.0).

Set X-ray tube volts at 30kV; reduce the tube current to minimum and slowly increase the current until a count rate of about 4,000 cps is achieved.

Tabulate and plot a graph (A) of the number of counts per second registered for increments of polarising voltage (most Ratemeters have an integral polarising supply with 'practical' limits of about 300 and 500 volts and the full G.M. tube ionisation characteristic cannot be recorded).

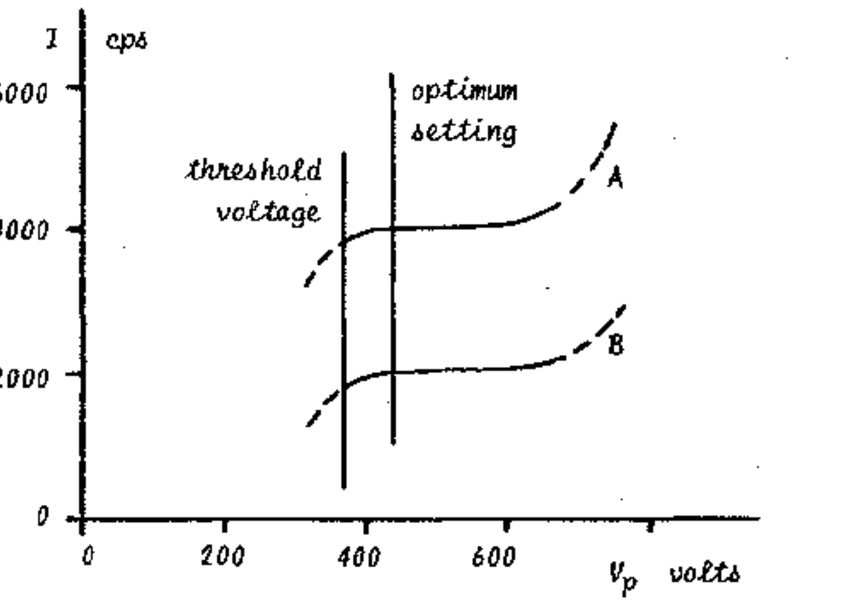

The optimum voltage at which to operate the Counter Tube is on the low voltage end of the 'plateau' about 420 volts.

D4.2 Dependence of Count Rate on kV

Plot two or three points about 400 volts with the Tel-X-Ometer set at 20kV and observe that although the count rate varies, the value of the threshhold voltage remains constant.

D4.3 Saturation

Set the Tel-X-Ometer at 30kV and again reduce the tube current to a minimum; slowly and progressively increase the current and observe that a peak count is reached after which the count rate falls away; this peak is the saturation point of the G.M. Tube and the G.M. Tube must always be used below this peak on the side of positive gradient for meaningful results.

The 'Resolution Time' of the G. M. Tube is defined as

$$\frac{I}{I_{max}} \quad \text{microseconds}$$

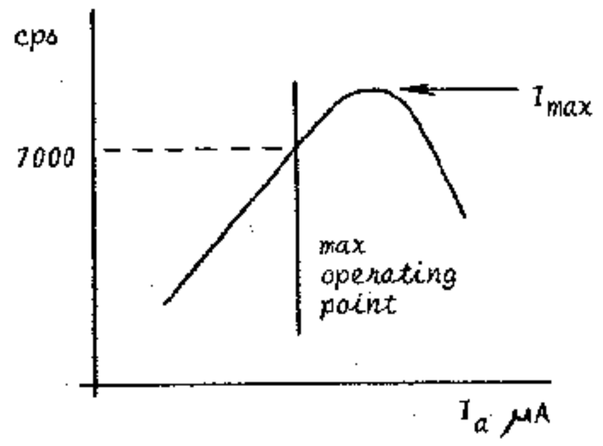

See also para. D38

The detection of individual or 'quantised' events supports the student's anticipation that the X-rays are high energy electrons and this should be further investigated now that a suitable detector of the phenomenon has been developed.

The G.M. tube permits a permanent numerical record to be made of the ionising effect of X-rays; can the effect on the Luminescent Screen, as a visual detector of X-rays, be made permanent by allowing the emitted 'light' to stimulate a photographic emulsion?

D5 — PHOTOGRAPHIC DETECTION (15 MINUTES)

Remove Crystal Post and Jaw.

KIT 582	30 kV	50 μA	DARKROOM

Cut out and fold a photographic film envelope as illustrated, using thin black paper.

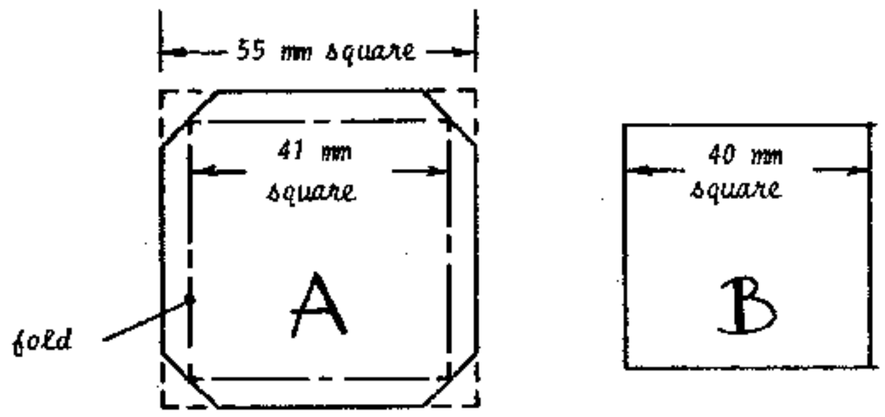

Fold along dotted lines.

In a darkroom, remove the film from a Filmpak 750/2; place the piece of film in the black paper envelope A and fold the four edges over the film; remove the Luminescent Screen, 582.003, from its slide and place the screen on the enveloped film with the phosphor coating in contact with the film.

The white card on which the screen is mounted is relatively light transparent and so the piece of black paper, with the letter B marked in pencil on one side, should be used to 'back' the screen; ensure that the letter B is on the outside face.

Place the film/salt screen assembly in Film Cassette 562.013.

D5.1 In a normally lit laboratory locate the Film Cassette at E.S.30 with the pencilled letter B facing the X-ray tube and the Back Stop only of Cassette 562.031 at E.S.29 with the Carriage Arm in the zero beam axis. Expose to X-rays for 5 seconds and remove to the dark room for processing. The developed film clearly illustrates that an image of the Back Stop has been registered but a penumbra exists around the film which coincides with the folds of the black paper envelope.

The paper envelope is impervious to light and so it must be inferred that the penetrating beam of X-rays has been responsible for 'energising' the penumbral area of the film and not the light from the salt screen.

D5.2 Reload the Film Cassette and repeat D5.1 but with the pencilled letter B facing away from the X-ray tube.

Apart from an increase in blackening the developed film is identical to that D5.1; the film has been traversed and energised by the X-ray beam but the penumbra are still present; the light emitted by the salt screen is thus 'intonsifying' the exposure of the central area of the film.

X-radiation causes the exposure of photographic film and this exposure can be 'intensified' using light-emitting salt screens.

As with ionisation chambers, the technique of photography has been researched uniquely for X-ray detection and many special types of film and intensifyer screens have been developed.

D6 — THE PHOTOGRAPHIC PROCESS (5 MINUTES)

Remove Crystal Post and Jaw.

KIT 582+584	30 kV	50 μA	NORMAL LAB

Remove the circular frame plate from Film Cassette 562.013, load with a Teltron Filmpak 750/2 and locate at E.S.30.

Place Maltese Cross 562.007 at E.S.29.

Expose to X-rays for 10 seconds and develop.

The special double sided X-ray film has registered an image of the cross.

A similar iterative experiment involving increments in exposure time would reveal the "characteristic curve" of the emulsion of the film. If it is required to perform this experiment, an externally operated shutter must be placed at the Basic Port to prevent the 'flash pulse' (see Part I, para 6.8) from obscuring the true exposure results.

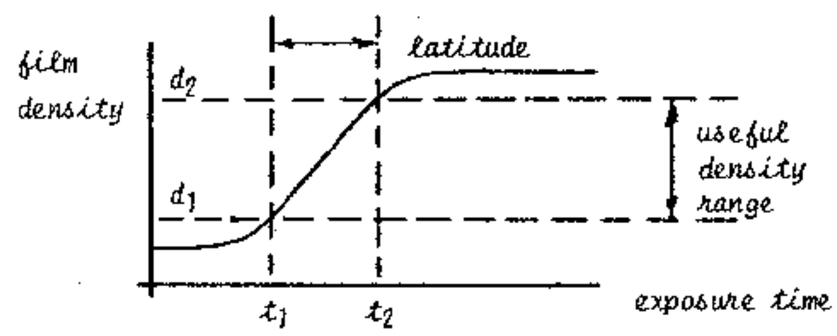

X-radiographers are mainly concerned with the slope or "gamma" of the characteristic curve; the gamma of an emulsion is defined as the ratio of the "useful density range", d, to the "latitude", t, and the greater the value of gamma the larger becomes the contrast of the emulsion:

$$\gamma_{emulsion} = \frac{d_2 - d_1}{t_2 - t_1}$$

The upper limit d_2 is governed by the intensity of light from the viewing box and the ability to discriminate in the blacker regions of the film; the practical lower limit is governed by the smallest change in object thickness that can be detected, the "sensitivity".

The stimulation of photographic film by exposure to X-rays has revealed a similarity between the X-ray phenomenon and light rays or electromagnetic radiation.

In order to attempt to differentiate between the 'high-energy electron' and the 'electromagnetic' postulations the four classical tests so often used in physics should be performed; rectilinear propogation; the inverse square law; deflection due to electric and magnetic fields; diffraction.

EXPERIMENTAL PROGRAMME D7 TO D11, PROPERTIES (2 HOURS)

D7 — RECTILINEAR PROPOGATION (10 MINUTES)

Remove Crystal Post and Jaw.

KIT 582	30 kV	50 μA	NORMAL LAB

D7.1 Attach two steel needles to the Auxiliary Slide Carriage 582.005 using Adhesive Tape, as illustrated.

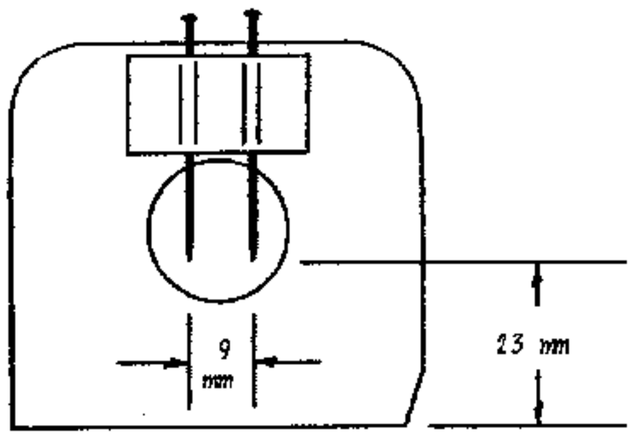

D7.2 Locate the assembly such that the needle points lie in the X-ray beam as illustrated in para D2.

D7.3 Load Film Cassette 562.013 with Filmpak 750/2 and locate at E.S.14 with the circular frame facing the X-ray tube.

Expose to X-rays for 2 seconds.

D7.4 Remove Film Cassette to E.S.22, expose for 4 seconds.

D7.5 Remove to E.S.30, expose for 6 seconds.

D7.6 Measure the distances between E.S.14 and E.S.22 and between E.S.22 and E.S.30.

D7.7 Develop the film and measure the distances between the needle points for each of the three superimposed images.

D7.8 Construct a diagram of the experimental layout.

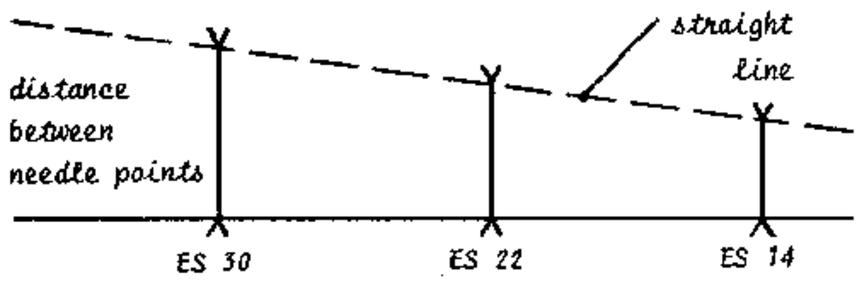

Confirm that the images of the needle points obey the law of rectilinear propogation.

The developed film provides evidence that, like light, the intensity of the three exposures obey the Inverse Square Law.

D8 — INVERSE SQUARE LAW (15 MINUTES):

Remove Crystal Post and Jaw.

KIT 582	30 kV	50 μA	NORMAL LAB

The intensity, I of radiation coming from a point source is inversely proportional to the square of the distance, ℓ, from the source; as in optical physics,

$$I = 6\left(\frac{1}{\ell^2}\right) \qquad \text{and from para D.6} \qquad d = I\,t$$

the Law of Reciprocity, where d is the density of the blackening of the film in time t.

A photographic film exposed at 20 cms from the anode of the X-ray tube requires, therefore, four times the exposure to show the same density as does a film which is exposed to the same radiation at a distance of 10 cms.

$$t_b = \frac{d}{I_b} = \frac{I_a\,t_a}{I_b} = \left(\frac{\ell_b}{\ell_a}\right)^2 t_a$$

D8.1 Load Film Cassette 562.013 with a Filmpak 750/2 and locate at E.S.14.

D8.2 Place the Lead Mask, 584.006, at E.S.13 such that the exposed portion of the film will be in the top right hand quadrant.

Expose to X-rays for 4 seconds.

D8.3 Remove the Lead Mask to E.S.18 with the exposure quadrant now in the bottom right hand quadrant.

D8.4 Remove the Film Cassette to E.S.19.

D8.5 Measure the distances of the film from the anode at E.S.14 and E.S.19 and calculate the exposure required at E.S.19 to give the same film density as at E.S.14.

Expose to X-rays for the calculated time.

D8.6 Repeat the procedure at E.S.24 and E.S.29, each time with the Lead Mask just in front of the film and rotated by 90 degrees to expose another quadrant of the film for the respective calculated time.

D8.7 Develop the film and observe that there is equal blackening of the four quadrants, confirming that X-radiation obeys the Inverse Square Law.

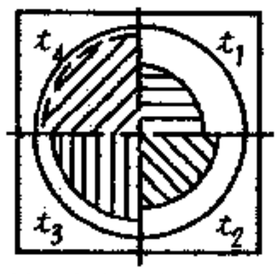

Observe also that at the outside limit of the beam the image is progressively more blurred and not sharp, indicating that scattering of the X-ray beam by the intervening air is taking place and this is more prevalent the greater the length of air traversed.

D9 — DEFLECTION EFFECTS (15 MINUTES, OPTIONAL):

5 KV power supply required

Remove Crystal Post and Jaw.

KIT 582+584	30 kV	50 μA	DARKENED LAB

D9.1 Locate Plain Electrodes 562.009 in E.S.2 and 4 of the Auxiliary Slide Carriage, with the circular plates facing each other.

D9.2 Mount this assembly in Mode V (see Part 1, para 10.4).

D9.3 Insert the 1mm Slot Collimator, 582.001, into the Basic Port with the slot horizontal.

D9.4 Adjust the Clutch Plate until the slot is central between the Electrode Plates.

D9.5 Connect the lower electrode to the earthed negative of a 2,000 volt d.c. voltage supply and the upper electrode to positive; pass the cables through the Cable Ports at the Hinge Plate.

D9.6 Locate the Backstop only of Cassette 562.031 at E.S.13, the Luminescent Screen 582.003 facing the X-ray tube at E.S.20 and cover the Glass Dome and the signal lamps with a black cloth.

D9.7 Switch on X-rays and observe that there is NO deflection of the image even with a potential difference across the electrodes of 2,000 volts.

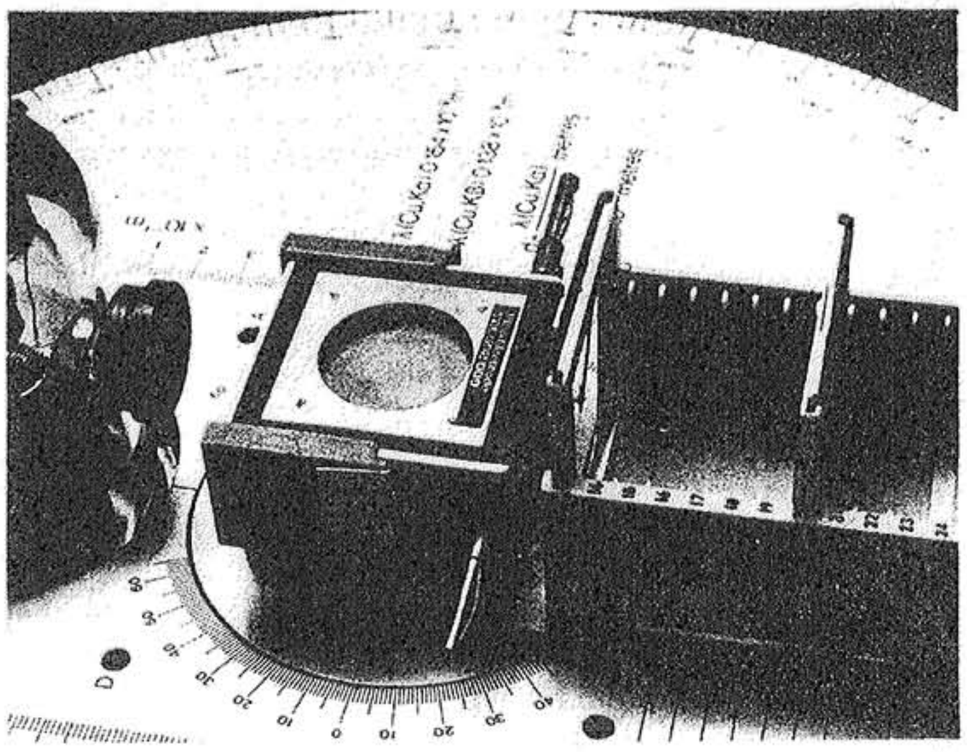

D9.8 Switch off and disconnect the voltage supply to the electrcdes but leave the electrodes at E.S.2 and E.S.4.

Place one of the Magnets 562.008 under the overhang of the lower electrode and othe other magnet similarly above the upper electrode as illustrated, to create a strong magnetic field between the electrodes; test this with a strip of ferrous metal or a needle.

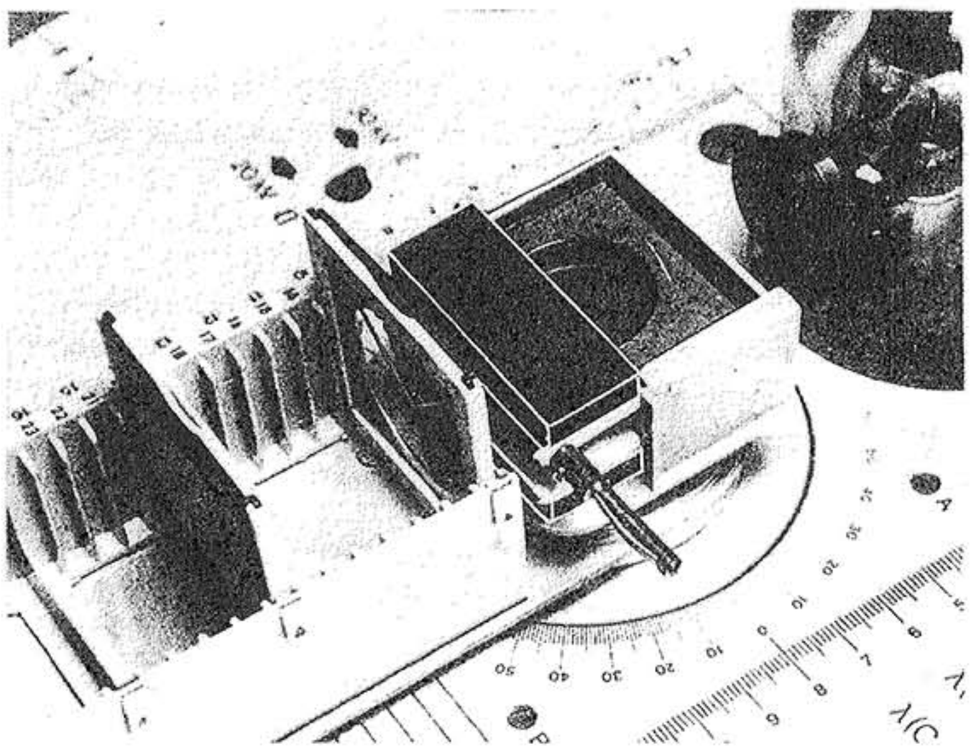

D9.9 Switch on X-rays and observe that there is NO deflection of the image on the screen.

It is evident from these 'nil-effects' that X-rays do not consist of high-energy electrons or other charged particles.

If X-radiation is electromagnetic in nature then diffraction will occur using a suitable grating; to achieve optical diffraction the spacing of the grating must be of the same order as the wavelength of the incident light.

In the absence of any knowledge of the wavelength of radiation no decision can be made regarding the type of grating to be used.

Further studies must be made in order to assess the 'quality' of the X-radiation.

D10 — PENETRATION AND ABSORPTION (45 MINUTES);

Remove Crystal Post and Jaw.

KIT 582+584	kV and µA as specified	NORMAL LAB

In the previous experiments X-rays have penetrated the glass of the X-ray tube (as does light), the black cloth, paper, cardboard and plastics ; but not the metal of the needles, the Maltese Cross, the Film Cassette Backstop and the Lead Mask.

D10.1 Place the Lead Mask 584.006 at ES.28 to expose the top right hand quadrant.

D10.2 Place Aluminium Wedge, 562.014, at E.S.29 with a pin trapped in the plastic of the surrounding slide to provide a datum on the exposed film; the datum should appear in the first exposure in the top right hand quadrant.

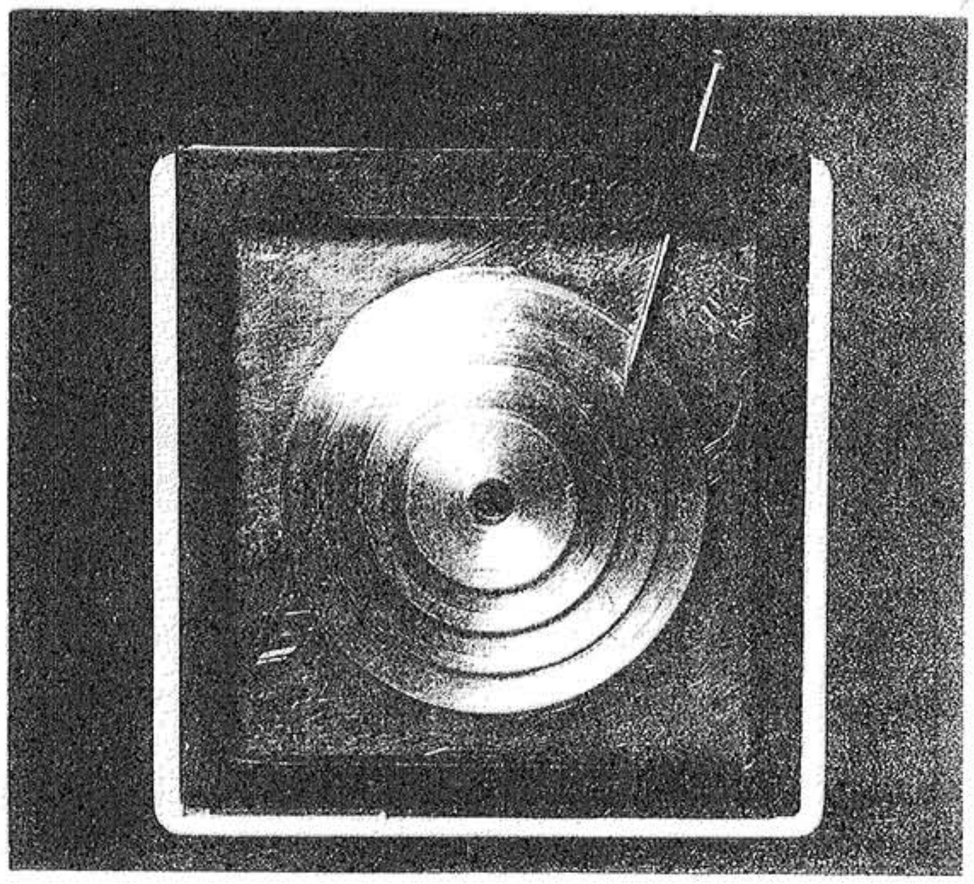

D10.3 Connect a 100 µA meter to the 'monitor tube current' jack socket and with 30kV selected, adjust the tube current to 80 µA.

D10.4 Locate Cassette 562.013 with Filmpak 750/2 at E.S.30.

D10.5 Expose to X-rays for 1½ minutes.

D10.6 Select 20kV and rotate the Lead Mask 90 degrees tc expose the bottom right hand quadrant.

D10.7 Expose to X-rays for 1½ minutes.

D10.8 Remove the Film Cassette, select 30kV and adjust for 40 µA tube current.

D10.9 Rotate the Lead Mask to quadrant 3,replace the Film Cassette and expose for 2 minutes.

D10.10 Repeat in Quadrant 4 with the tube current set to 60 µA and expose for 2 minutes.

The developed film reveals that X-rays can penetrate a light metal such as aluminium but the degree of penetration depends not only on the thickness of the material but also on the voltage applied to the X-ray tube; quadrants 1 and 2.
Variations in the tube current does not effect the degree of penetration but only the density of film blackening and therefore the intensity of radiation in the beam; quadrants 3, 4 and 1.

The greater the tube voltage the greater the penetration and the greater the tube current the less the exposure time for a given intensity.

D10.11 Hard and Soft Radiation

Early researchers noticed that the better the vacuum in an X-ray tube the greater the power of penetration.

The gas discharge X-ray tubes of the period, with a low order of vacuum and relatively 'gassy', were known as 'soft' tubes

and discharged at relatively low voltages and conversely, tubes with a high order of vacuum were 'hard' tubes and only discharged at high voltages. X-radiation from the tubes was called 'hard' or 'soft' and these terms are still used. The higher the voltage applied to the X-ray tube the 'harder' the resultant radiation. The selection of 20 kV with the Tel-X-Ometer will result in softer radiation than that emitted at the 30 kV selection.

D10.12 Linear absorption.

KIT 582+584	30 kV	50 µA	NORMAL LAB

Insert the G.M. Tube, TEL 546, in the Holder, TEL 547, mount the assembly at E.S.22 and connect to a Ratemeter or Scaler.

Mount the Auxiliary Slide Carriage in Mode H using the 1mm diameter Collimator 582.002; reduce the tube current until a count rate of about 10,000 counts per second is achived.

D10.13 Locate in turn the slides indicated in the following table and record the intensity of radiation (counts per second).

Slide No.	ES	Thickness mm	I cps	Log I	Log I_0 - Log I
582.033	4	0			——
.017	4	0.10			
.018	4	0.25			
.019	4	0.50			
.018 .019	3 4	0.75			
.020	4	1.00			
.018 .020	3 4	1.25			
.019 .020	3 4	1.50			
.018 .019 .020	2 3 4	1.75			
.021	4	2.00			
.020 .021	3 4	3.00			
.019 .020 .021	2 3 4	3.50			

D10.14 Plot Graph as illustrated.

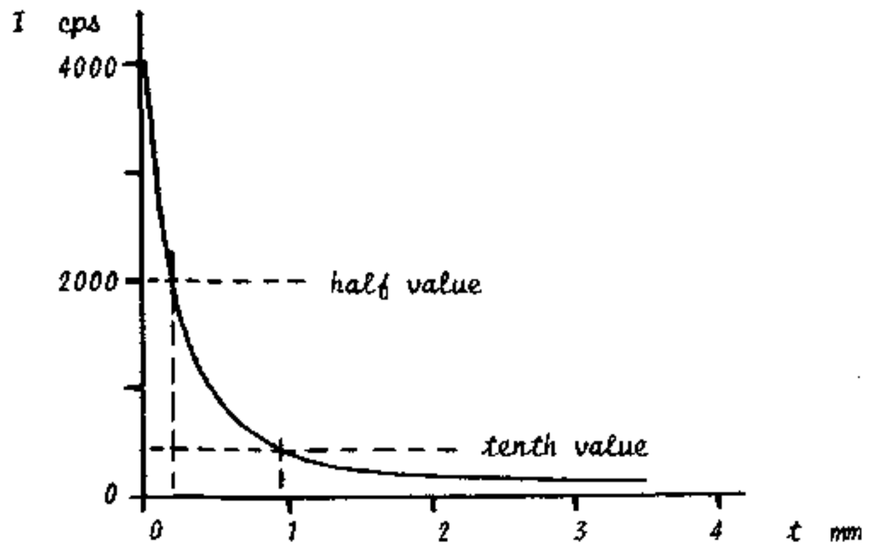

The graph is characteristic of an exponential curve

where $I = I_0 e^{-\mu t}$

and μ is the linear or total absorption coefficient

$$\mu = \frac{\log I_0/I}{t} \quad , \quad m^{-1} \quad .$$

D10.15 Tabulate and plot the graph of $\log I_0/I$ as a function of t ; if the practical curve of D10.14 is truly exponential then all points on the 'log' curve should lie on a straight line passing through zero.

Observe that this is not so and the curve has a tendency to fall away at greater values of t .

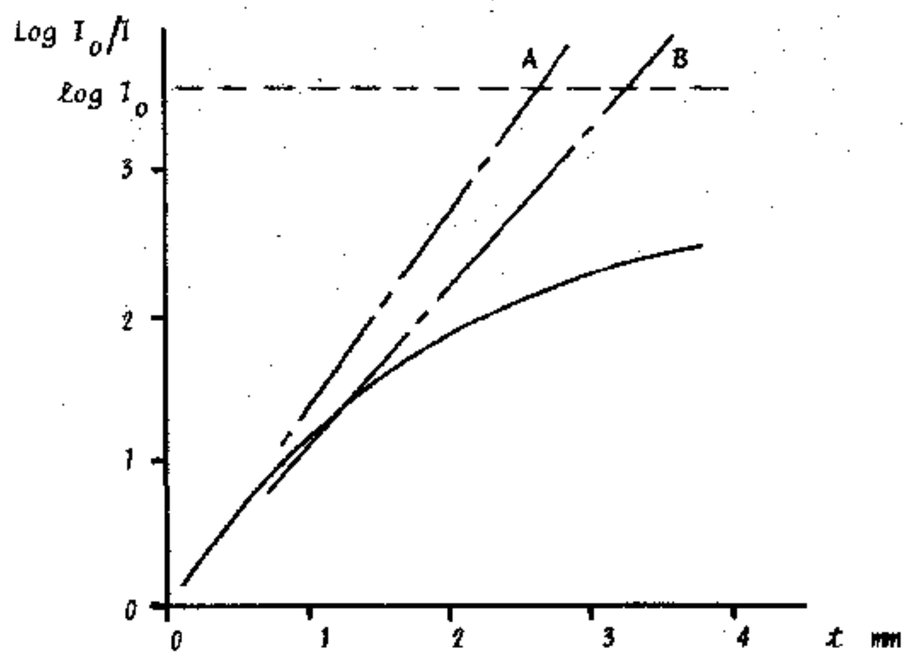

Since log [Io/I] is smaller than the correct exponential value, then I alone must be responsible for the deviation and is larger than theory predicts; this in turn infers that the X-radiation is becoming more penetrating as it passes through the aluminium. This is only consistent with the law of conservation of energy if not just one homogeneous wavelength but a heterogeneous mixture of wavelengths comprises the primary X-ray beam. This is similar to white light and such heterogeneous X-radiation is called 'white' radiation.

The least energetic, soft radiation (longer wavelength) is progressively absorbed by the aluminium such that the mean wavelength of the transmitted beam progressively decreases; it thus appears that the quality of the radiation gets harder the deeper the penetration.

To avoid the necessity to constantly analyse the whole spectrum of the white radiation, radiographers refer to an "effective wavelength" of the heterogeneous primary beam; the "effective wavelength" is defined as that wavelength which requires the same thickness of absorbing medium to reduce the intensity to one half of that of the incident beam as does the 'white' heterogeneous beam.

D10.16 Half-Value and Tenth-Value Thickness.

From D10.14 (I_0/I) or D10.15 (where $\log I_0/I = \log 2 = 0.301$) the Half-Value Thickness in aluminium for 30 kV radiation is about 0.2 mm . If a theoretically exponential 'log-line', A is plotted on graph D10.15 through (0.2, 0.3010) and zero the radiation will be theoretically completely absorbed by 2.4 mm of aluminium where $\log I = 0$ and so $\log I_0 - \log I$ is a maximum.

Since the value 2.4 mm is seriously in error it is apparent that Half-Value Thickness is mainly of relevance to radiographers concerned with the effects of soft radiation, for example in medicine where the damage to the outer body tissues due to absorption of soft radiation is closely studied.

Radiographers concerned with hard radiation and with protection calculations more commonly use the Tenth Value Thickness where $I = I_0/10$; from graph D10.14 the Tenth Value Thickness in aluminium for 30 kV radiation is about 0.9 mm.

The straight line B through zero and the point (0.9, 1.0) where $\log I_0/I = \log 10 = 1.0$ predicts that the radiation will be completely absorbed by about 3.25 mm of aluminium which more nearly approximates to practice. See also para 039.

D11 — THE PHANTOM (40 MINUTES)

Remove Crystal Post and Jaw.

KIT 582+584	30 kV	80 µA	NORMAL LAB

Carefully locate Auxiliary Slide Carriage in Mode H without using either of the Basic Port Collimators.

Mount the Phantom TEL 562.012 at E.S.29.

D11.1 Locate Blank Slide 562.033 at E.S.4.

Place a Filmpak 750/2 in Cassette 562.013 and locate at E.S.30, with carriage arm in zero axis.

Expose for 2 minutes.

D11.2 Replace the Blank Slide with Aluminium Slide 562.018 (0.25mm) at E.S.4.

Reload new Filmpak in Cassette 562.013.

Calculate, using Graph D10.14, the exposure required to give the same film density as in D11.1 (this will be more than twice since 0.25mm of aluminium is greater than the Half-Value Thickness).

Expose for calculated time.

D11.3 Add Aluminium Slides 562.017 (0.1mm) and 562.019 (0.50mm) at E.S.3 and E.S.2 - the total thickness of aluminium is 0.85mm which is almost exactly the Tenth Value Thickness.

Reload new Filmpak in Cassette 562.013.

Expose for 20 minutes (2 x 10 minutes).

Compare the three developed films.

Although these experiments were intended to give equivalent intensities, that this is not so is proof of the heterogeneous nature of the X-rays; the more energetic wavelengths are not absorbed resulting in greater film densities.

The construction of the phantom is a sandwich of three equal thicknesses of plastics material which is approximately "tissue equivalent" with respect to absorption.

The central layer of the sandwich has a bone-shaped hole cut in it which is filled with calcium carbonate, approximately "bone equivalent", and three pieces of lead shot.

Different thicknesses of calcium carbonate are traversed by the X-rays; 1) the thickness of the filling in the bone-hole, 2) the voids created by the movement of the lead shot in the powder and 3) the seepage into the separation planes of the plastics layers.

At the Fourth International Congress of Radiology in Zurich Dr. Christen made use of the Half-Value Thickness to define the homogeneity of a radiation beam.

If radiation at the Half-Value Thickness, t_1 = 0.2 of D10.14 is considered as incident radiation for penetrating a subsequent thickness of aluminium then a progressive second Half-Value Thickness, t_2 can be read off the curve at

$\frac{I_0/2}{2} = I_0/4$. The value for t_2 is about 0.5-0.2 = 0.3 mm.

Dr. Christen defined, for biological purposes only, a beam of radiation as being homogenous when $t_2/t_1 = 1$ and for all values greater then 1 the incident beam is heterogeneous.

From graph D10.14 $t_2/t_1 = 0.3/0.2 = 1.5$, confirming that the radiation emitted at 30 kV is heterogeneous.

See also para. D 37.

D12 — DIFFRACTION OF X-RAYS; LAUE (45 OR 75 MINUTES)

Adopting now the rational assumption that the beam is heterogeneous and electromagnetic, then the emission from the X-ray tube should obey the laws of wave motion; the most classical experimental criterion for wave motion is the demonstration of constructive or destructive interference, the diffraction effect.

All the early attempts around 1901 to obtain diffraction patterns, based on known optical techniques, were not generally accepted as conclusive. The careful manufacture of the finest possible gratings proved ineffective.

In 1912, Prof. Max von Laue postulated that the wavelength of X-rays was much shorter than most experimenters believed; he suggested that the basic granularity of matter was imposing restrictions on the construction of gratings fine enough to cause diffraction; he concluded that this very granularity might provide a 3-dimensional grating for the diffraction of X-rays.

In 1913, Professor Laue's theoretical proposal was successfully tested by Friedrich and Knipping.

KIT 582	30 kV	80 µA	NORMAL LAB

D12.1 Using tweezers if available, carefully select one of the Mini Crystals, TEL 582.007; the Crystals are Lithium Fluoride and are very fragile.

D12.2 By means of clear adhesive tape mount the mini crystal over the existing aperture of the 1mm diameter Primary Beam Collimator 582.002.

D12.3 Mount the Auxiliary Slide Carriage in Mode H (see Part I, para 10.4) using the Crystal/Collimator assembly, assuring that the long axis of the crystal is vertical.

D12.4 Load a Filmpak 750/2 into the Cassette, 562.013.

D12.5 A good Laue pattern can be recorded with the Cassette located at E.S.2 and exposed for 20 minutes.

Greater dispersion and film density is obtained with the Cassette located at E.S.3 and exposed for 1 hour.

The Laue pattern, an array of dots around an intense central spot, illustrates, with discernible symmetry, interference of wave motion due to diffraction.

Late in 1913, W. L. Bragg sought to explain the basic formation of the Laue diagram very simply; the primary beam of waves is scattered by the atoms in successive crystal planes and where the path-lengths differ by an integral multiple n of the wavelength λ, then strong re-inforcement occurs.

The Laue pattern in this experiment is intended to illustrate diffraction of X-rays in a qualitative sense only - in order to interpret a Laue configuration, apart from the complexity of the mathematical analysis, the wavelength of the primary radiation must be known. This wavelength, λ, is still to be established.

D13 — WAVELENGTH BY DIFFRACTION GRATING

Although suitable man-made gratings were not available to Friedrich and Knipping (1912) they are now manufactured but they are expensive; furthermore, considerable time-consuming precision is required to set up such experimental apparatus.

The Nuffield 8MM Filmloop, PENGUIN NO.XXI,666 on this subject is recommended; explanatory notes are included with each film.

D14 – WAVELENGTH MEASUREMENT: BRAGG METHOD (1½ HOURS)

Sir Lawrence Bragg presumed that the atoms of a crystal such as Sodium Chloride were arranged in a cubic and regular three-dimensional pattern.

The mass of a molecule of *NaCℓ* is M/N Kg, where M is the molecular weight (58.46×10^{-3} kg per mole) and N is Avogadro's number (6.02×10^{23} molecules per mole).

The number of molecules per unit volume is $\rho/\frac{M}{N}$ molecules per cubic metre, where ρ is the density (2.16×10^{3} kg m^{-3}).

Since *NaCℓ* is diatomic the number of atoms per unit volume is $2\rho N/M$ atoms per cubic metre.

The distance therefore between adjacent atoms, d in the lattice is derived from the equation

$$d^3 = \frac{1}{2\rho N/M} \quad \text{or} \quad d = \sqrt[3]{M/2\rho N}$$

and for *NaCℓ*, $d = 0.282$ nm.

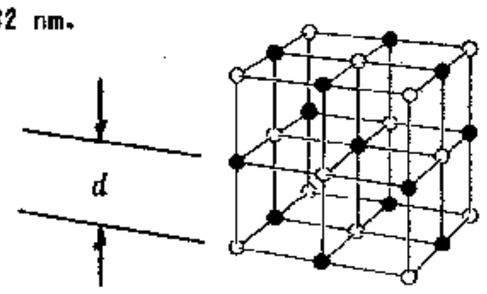

The first condition, for Bragg "reflection" is that the angle of incidence θ equals the angle of reflection – this is as for optical reflection and infers that any detector of the reflected rays must move through an angle 2θ, the 2:1 spectrometer relationship.

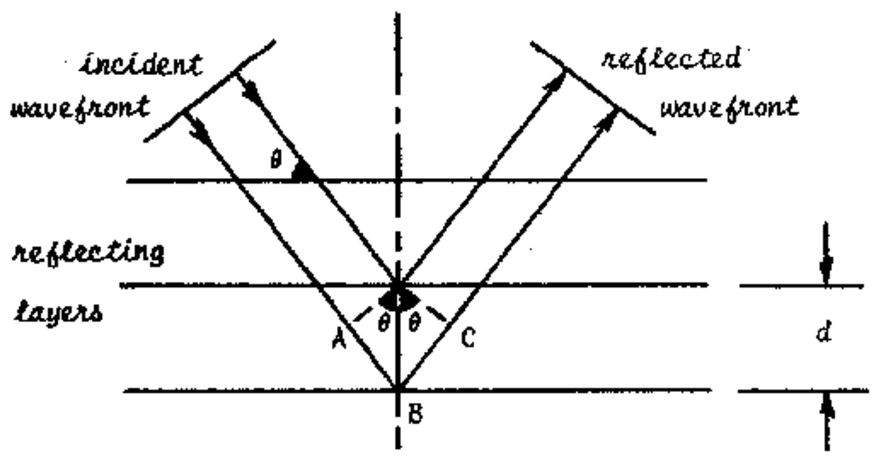

The second condition is that reflections from several layers must combine constructively :-

$$n\lambda = AB + BC = 2d \sin\theta$$

KIT 582	30/20 kV	50 μA	NORMAL LAB

D14.1 Mount the *NaCℓ* crystal, TEL 582.004, in the crystal post (see Part 1, para 10.9) ensuring that the major face having "flat matt" appearance is in the reflecting position (see Para D27.30).

D14.2 Locate Primary Beam Collimator 582.001 in the Basic Port with the 1mm slot vertical.

D14.3 Mount Slide Collimator (3mm) 562.016 at E.S.13 and Collimator (1mm) 562.015 at E.S.18.

D14.4 Zero-set and lock the Slave Plate and the Carriage Arm cursor as precisely as possible (see Part 1, para. 10.6).

D14.5 Sight through the collimating slits and observe that the primary beam direction lies in the surface of the crystal.

D14.6 Mount the G.M tube and it's holder at E.S.26.

D14.7 Using a Ratemeter track the Carriage Arm round from it's minimum setting (about 11°, 2θ) to maximum setting (about 124°, 2θ).

Plot on graph paper the count rate per second at 1° (2θ) intervals, allowing time at each reading to estimate the mean of the fluctuations of the needle.

The Carriage Arm should be indexed to 15° (2θ) and the thumb wheel set to zero; when the Scatter Shield is closed, settings from 11° to 19° can be achieved using only thumb-wheel indications.

If the ratemeter has a loud speaker, note the random "quantum" nature of the beam of radiation at low count rates.

Where the count rate appears to peak, plot intervals of only 10' arc using the thumb-wheel (see Part 1, para 10.8); at each peak, measure and record the maximum count rate and the angle 2θ as precisely as possible.

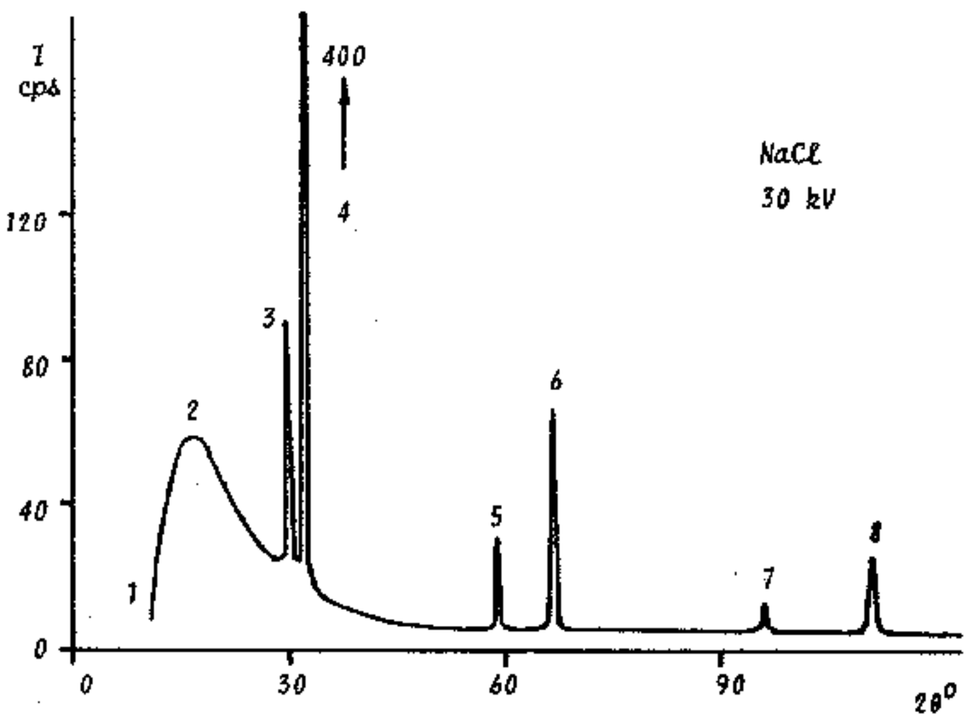

D14.8 Select 20kV and repeat D14.7.

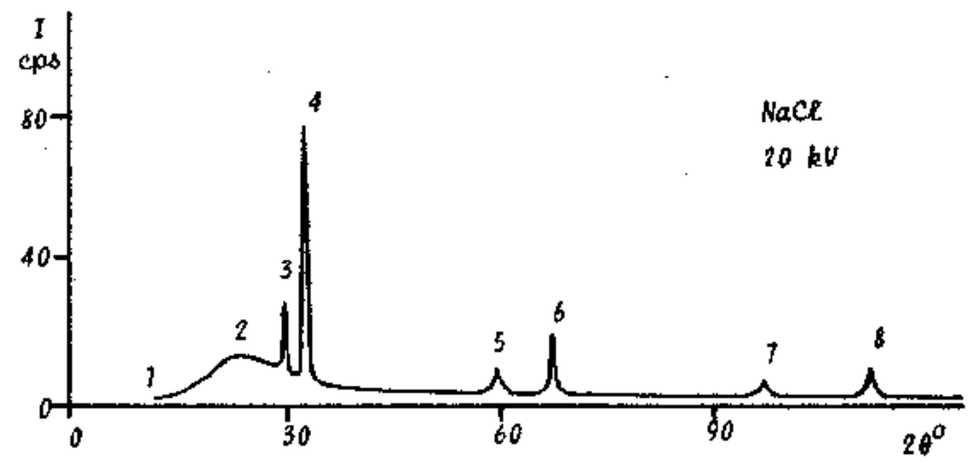

Observe that the continuous spectra of "white" radiation exhibit peak intensities (feature 2) and intercepts on the 2θ axis (feature 1) which only vary with the voltage setting of the X-ray tube.

The six peaks, features 3 to 8, superimposed on the continuous spectrum do not vary in angle 2θ with voltage setting, but only in amplitude.

D14.9 Tabulate the results from the six superimposed peaks of the graph and calculate λ and n.

Feature	2 θ	θ	sin θ	2 d	n λ	n
3				0.564		
4				0.564		
5				0.564		

Observe that the sharp peaks are a pair of "emission lines" which re-appear in second and third orders of diffraction.

The more energetic radiation, termed Kβ, is successively less intense than the longer wavelength, Kα, line.

In the absence of micro-gratings, the "reasonable argument" was formulated by Sir Lawrence Bragg that the NaCl crystal could be used as a 3-dimensional grating which would reveal diffraction information by means of which the wavelength of the primary radiation could be established; but in the second sentence of D14 a bland assumption is made for Avogadro's number. If, however, the wavelength of the radiation is obtained by using a man-made grating, as in D13 then a contemporary approach is to reverse the sequence of the Bragg argument to provide an accurate evaluation of Avogadro's number.

Whichever didactic sequence is adopted, the Bragg experiment verifies that the incident radiation is both electromagnetic and heterogeneous and that co-operative interference can be induced using a crystal as a diffraction grating.

The crystal itself cannot be considered as the source of the 'dual' spectrum due to photon bombardment; the continuous spectrum is modified in both minimum wavelength and general intensity only by changing the X-ray tube accelerating voltage, without any variations in crystal parameters; the "emission lines" are particularly discreet in angle (2θ) whereas radiation from the crystal due to photon bombardment would be multi-directional.

The radiation must be derived through some "inverse photo-electric effect" from the impact of the thermionic electrons on the Copper target within the X-ray tube.

D15 — X-RAY EMISSION (1¼ HOURS)

In striking the Copper anode the majority of electrons experience nothing spectacular; they undergo sequential glancing collisions with particles of matter, lose their energy a little at a time and merely increase the average kinetic energy of the particles in the target ; the target gets hot.

The minority of electrons will undergo a variety of glancing collisions of varying severity; the electrons are decelerated imparting some of their energy to the target particle and some in the form of electromagnetic radiation equivalent in energy to the energy loss experienced at each collision.

Since these collisions usually occur at a slight depth within the target the longer, less energetic, wavelengths are absorbed within the target material.

This "bremsstrahlung" or "braking radiation" is thus a continuous spread of wavelengths, the minimum wavelength (or maximum energy) being determined by the accelerating voltage of the tube.

$$\lambda_{min} = f\left(\frac{1}{V}\right) \quad \text{or} \quad V\lambda_{min} = k$$

where V is the X-ray tube voltage selected.

D15.1 Minimum Wavelength, Planck's Constant.

KIT 582	30/20 kV	80 μA	NORMAL LAB

An accurate determination of the minimum wavelength Intercept on the x-axis requires that the Ratemeter be replaced by a Scaler; counts should be recorded over at least 10 second durations, the longer the counting period the greater the accuracy of the results.

D15.2 Mount the auxiliary slide carriage in Mode H (see Part 1, para 10.4) using the 1mm slot Primary Beam Collimator, vertical.

D15.3 Position the Slide Collimator, (1mm slot) 562.015 at E.S.4 and Slide Collimator (3mm) 562.016 at E.S.13.

D15.4 With the *NaCl* crystal mounted as in 14.1, set up as for 14.4, 5 and 6; select 30kV.

D15.5 Measure, tabulate and plot the count rate at every 30' arc, commencing at 11°, 30', until the "whale back" appears to fall off.

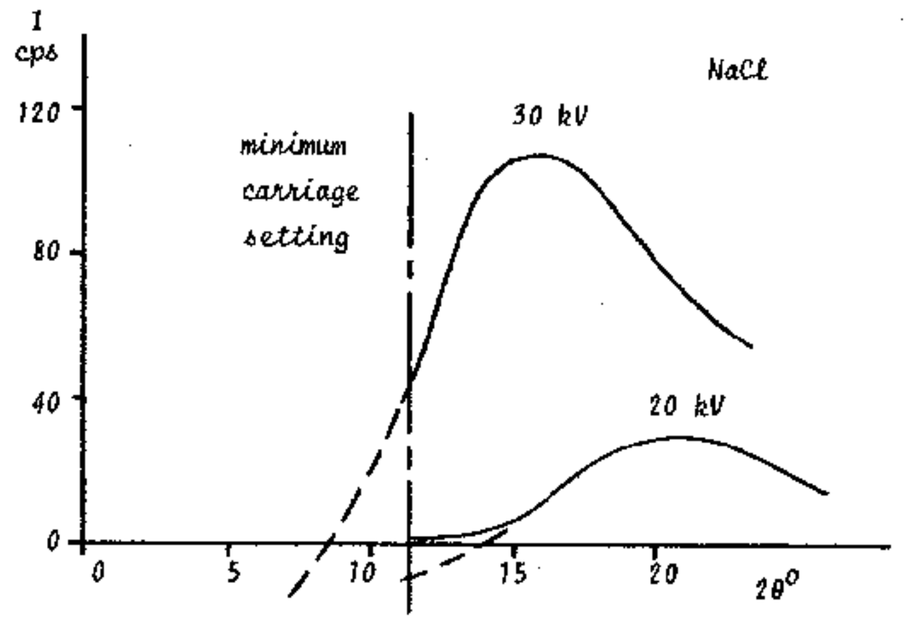

D15.6 Repeat for 20kV.

Observe that the minimum setting of the Carriage Arm requires an extended extrapolation of the 30kV curve to obtain and intercept on the x-axis ; curves of similar nature can be drawn for the *KCl* and the *RbCl* crystals.

With *LiF* however a more precise intercept can be plotted.

D15.7 Replace *NaCl* crystal by the *LiF* crystal, zero set and repeat 15.5 and 15.6.

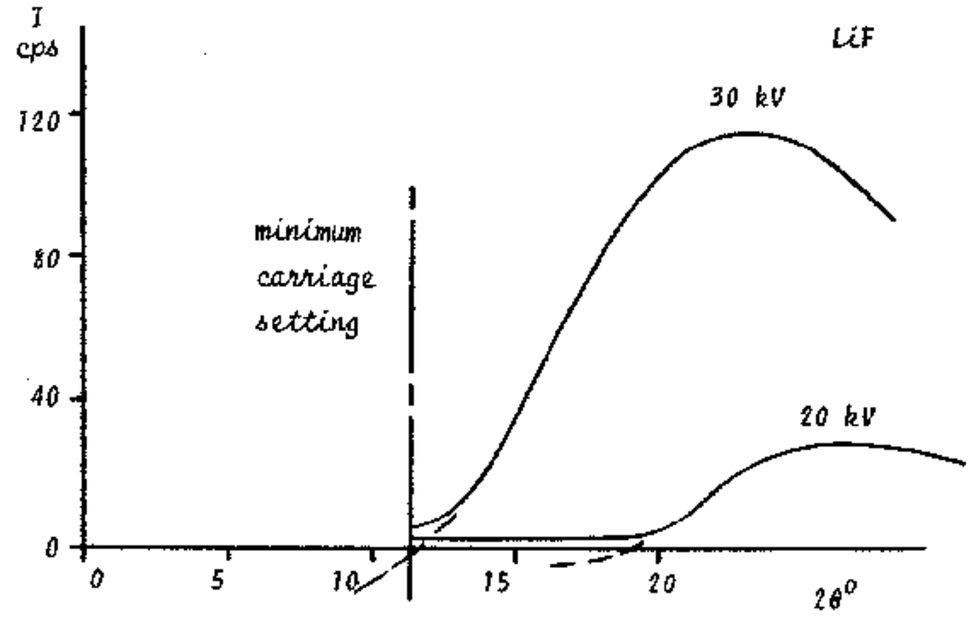

Observe that the curves flatten out before intercepting the axis, due to the contribution of the general background radiation.

D15.8 Extrapolate the theoretical intercepts and tabulate the results:

Crystal	V	2θ	θ	sin θ	2d	λ nm	Vλ
NaCl	30 kV				0.564		
NaCl	20 kV				0.564		
LiF	30 kV				0.403		
LiF	20 kV				0.403		

If the theory of the "inverse photoelectric effect" is valid then Einstein's assumption of 1905, that both emission and absorption are "quantised", must be tested in relation to Planck's formula for photo-electron emission

$$w = h\upsilon \text{ joules}$$

where w is the energy associated with each quanta, υ is the frequency of radiation and h is Planck's constant.

Since $\upsilon = c/\lambda$ for electromagnetic radiation where c is the velocity of light, and $w = Ve$, the maximum energy that can be acquired by any electron within the X-ray tube system, then

$$Ve = hc/\lambda \quad \text{or} \quad h = V\lambda\left(\frac{e}{c}\right).$$

D15.9 Calculate the mean value for $V\lambda$ from D15.8 and evaluate h.

($e = 1.60 \times 10^{-19}$ coulombs ; $c = 3.00 \times 10^{8}$ m sec^{-1})

Compare with the international value for h of

$$6.62 \times 10^{-34} \text{ joule-sec}$$

The difference between the accepted standard value and the evaluated result for h of about 5% is well within experimental limits and illustrates why the 'inverse photo-electric effect' is considered to be a very accurate method of determining h, the fundamental constant in the Quantum Theory.

It is assumed that previous studies of optical spectra have established that "characteristic lines" in the visible region of the electromagnetic spectrum are emitted from atomic energy-levels of high principal quantum number, the N, O, P and Q levels; the relatively much shorter wavelengths of the characteristic Kβ and Kα lines indicate that these shorter emissions are due to electron transitions at energy-levels of low principal quantum number. Any electron from the X-ray tube filament having sufficient energy to eject a K electron in a collision process will ionise the Copper atom; the ionised atom will revert to it's stable state through electron transitions, each transition being accompanied by the emission of a photon of equivalent energy.

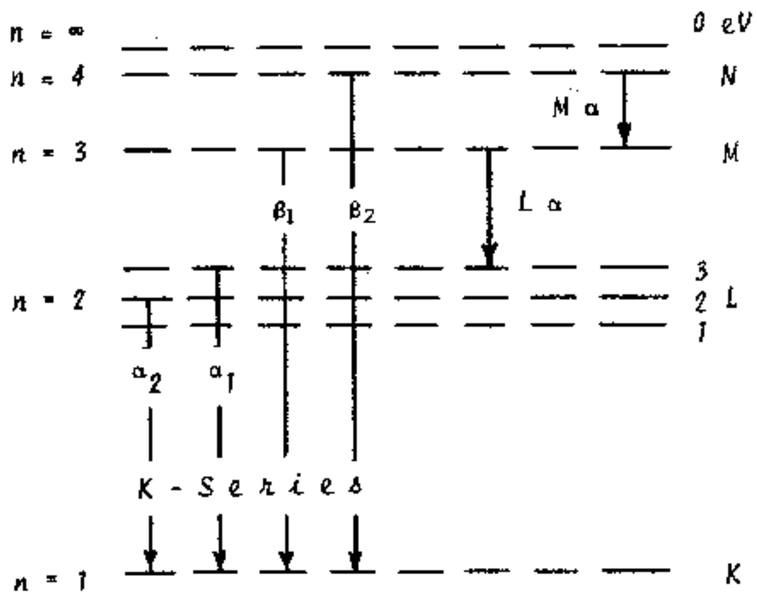

By definition, the Kβ emission results from transitions from the N and M levels to the K level and Kα from transitions from the L to the K level (see para. D19); the N and M levels have a greater energy difference with respect to the K level than does the L level and hence the wavelength of the Kβ photon is shorter and more energetic than that of Kα. But the closer proximity of the L and K levels results in more frequent transitions than for the N or M levels and hence there is a greater "population" of Kα exhibited by the relative intensities of the peaks 3 and 4 of graphs D14.7 and 8. (See also para. D19.7).

The Bragg experiment has established that a crystal can be used to demonstrate the co-operative interference of X-rays; the wavelength limit of the continuous "white" spectrum is dependent uniquely on the energy imposed upon the electrons by the potential difference between the electron emitting filament and the anode, regardless of it's material; the "characteristic" line spectrum, superimposed upon the white spectrum is due to the elemental composition of the anode and the energy-levels associated with it's individual electron system.

The lines are unique to emission from a Copper target and are thus termed CuKβ and CuKα emission lines.

Spectral analysis by the Bragg technique can accurately evaluate a) an unidentified voltage, using both a known crystal and anode material, b) an unknown crystal structure using an identified voltage and anode material and c) the chemical composition of a material serving as an anode to emit characteristic radiation, using an established crystal and an accurately defined voltage.

The process of X-ray emission is such that the wavelength may well overlap both the ultra-violet and the Gamma regions of the broad electromagnetic spectrum; in the "Teltron Approach to Atomic Physics" the phenomenon of Gamma radiation has yet to be studied.

By its mode of emission X-radiation is therefore defined, through the "inverse photoelectric effect", and not by wavelength; "ultra-violet" radiation results from classical photoelectric events and "Gamma" radiation from nuclear disintegrations.

However, consequent upon the similarities between diffraction of optical and X-ray wavelengths, the student will surely anticipate 'absorption' effects in X-ray, as in optical, spectra.

D16 — X-RAY ABSORPTION (1 HOUR)

KIT 582	30 kV	80 μA	NORMAL LAB

D16.1 Locate the NaCl crystal in the crystal post as in 14.1.

D16.2 Mount the Auxiliary Slide Carriage in Mode H (see Part 1, para 10.4) using the 1mm slot Primary Beam Collimator, vertical. Locate the Slide Collimator (3mm slot) 562.016 at E.S.4.

D16.3 Position Slide Collimator (1mm) 562.015 at E.S.18 and the G.M. Tube Holder assembly at E.S.26; connect the G.M. Tube to a Scaler; due to the low count rates of this experiment, counts should be recorded over at least 10 second durations; the longer the counting period the greater the accuracy of the results; it is also advisable to monitor the tube current and adjust as necessary to 80 μA.

Ensure that 30kV is correctly selected.

D16.4 Tabulate counts, I_o from 20° (2θ) to 40° at 1° intervals.

$2\theta^o$	I_o cps	I_{cu} cps	I_{cu}/I_o %
20			
21			
22			

D16.5 Locate the Copper Filter 564.006 at E.S.2 and tabulate counts I_{cu}.

D16.6 Calculate the ratio I_{cu}/I_0 and plot as a Percentage Transmission against angle 2θ.

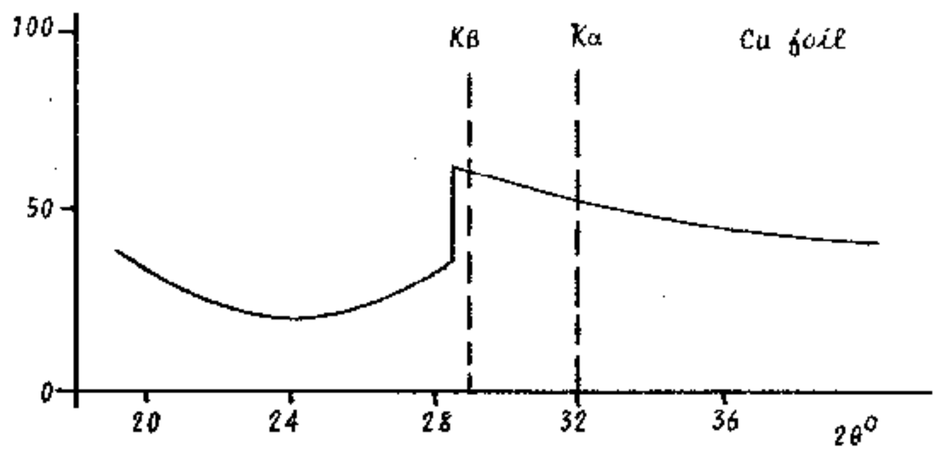

Observe that the whole spectrum has been reduced in intensity but that the expected "self-reversal" of the Kβ and Kα lines is not evident; a very abrupt discontinuity is revealed however at a wavelength just shorter than the Kβ line.

D16.7 From the graph, determine the angle 2θ at which this discontinuity occurs and calculate the equivalent wavelength in accordance with the Bragg equation:

$$\lambda = 2\, d \sin \theta$$

The Copper Foil interposed at E.S.2 has a finite thickness, 12.5×10^{-6} metres and, applying the Linear Absorption Co-efficient as studied at D10.14 some absorption of the spectrum must be expected.

That Copper does not 'reversibly' absorb it's own characteristic emission lines Kβ and Kα is in agreement with the theory outlined in the comments following D15.9. To ionise an atom of the Copper target in the tube any electron from the filament must have sufficient energy to liberate an electron in the K level or indeed the L level for Lβ or Lα emission not detectable with the compact geometry of the Tel-X-Ometer. Thus, in hypothetical terms:

$$W_o \geqslant W_{k \to \infty} = -10 \times 10^3 \text{ eV}.$$

Following an M to K electron transition a Kβ photon is emitted having energy $W_{m \to k}$ or -9.9×10^3 eV (ie −10,000 + 100 eV); there is therefore a relatively small energy difference of 100 eV.

The discontinuity occurs at a wavelength of 0.138 nm (from D16.7) which is just shorter in wavelength than the Kβ emission (about 0.140 nm from D14.9) and it is evident therefore that a "classical photoelectric effect" has occurred wherein some photons in the primary X-ray beam have sufficient energy to ionise the Copper atoms in the foil placed at E.S.2.

Furthermore, the value of the wavelength indicates that the incident photons must be a component part of the "white" radiation; the inference is therefore that the Copper foil will exhibit the "absorption edge" when exposed to radiation containing energies equivalent to 0.138 nm, regardless of the material of the source.

The discontinuity is thus unique to the system and is referred to as the CuK Absorption Edge.

Since the elements in the periodic table have different energy-level structures and densities the student could now expect to find an element which will discreetly absorb Copper K emission by a systematic study using foils of different elements, but equal thickness.

D16.8 Remove the Copper Filter from E.S.2 and replace with the Zinc Filter 563.009.

Repeat 16.5, 16.6 and 16.7.

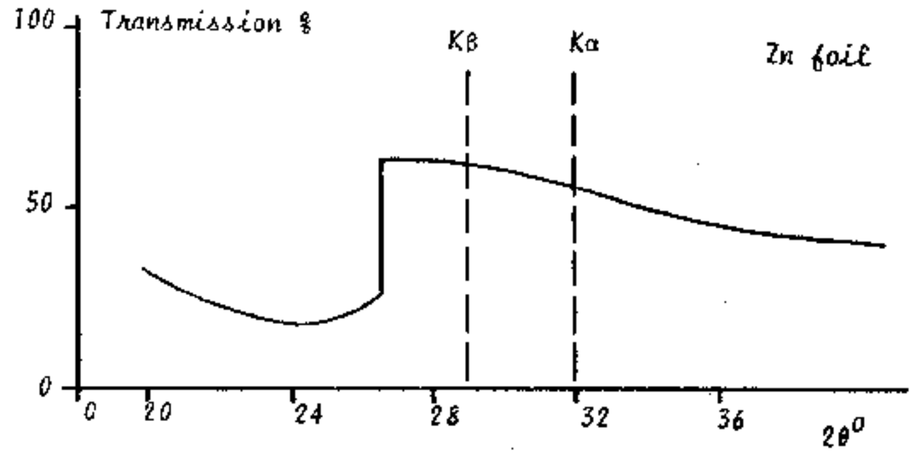

D16.9 Remove the Zinc Filter and replace with the Nickel Filter 564.004.

Repeat 16.5, 16.6 and 16.7.

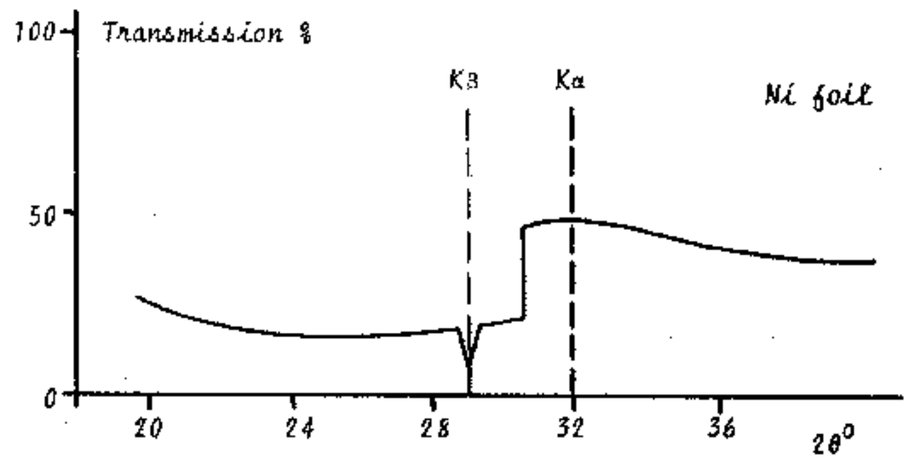

D16.10 Remove the Nickel Filter and replace with the Cobalt Filter 564.008.

Repeat 16.5, 16.6 and 16.7.

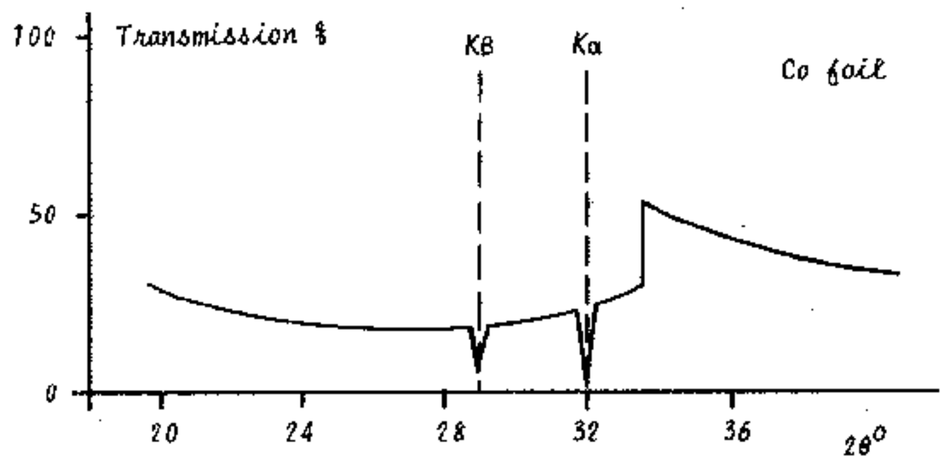

Observe that only the Cobalt Foil has absorbed or "filtered out" both the CuK emission lines but that Nickel has dramatically discriminated between the Kβ and Kα radiation.

Clearly the absorption of X-rays is dependent not only on the thickness of the absorbing material but also on the nature of the material itself.

The Linear Absorption Co-efficient is not therefore sufficiently definitive for X-ray purposes, especially with thin foils where the effect due to the material is greater than that due to thickness.

The thickness t is related to the material itself by the equation $t = m/\rho$ per unit area, where m is the mass and ρ is the mass density of the material.

D16.11 The equation for the Absorption Co-efficient can therefore be re-written

$$I = I_0 e^{-\mu m/\rho} \quad \text{or} \quad \mu/\rho = \frac{Log\ I_0/I}{m} = \mu_m\ , m^2\ kg^{-1}$$

μ_m is defined as the Mass Absorption Co-efficient

On examination of the transmission graphs drawn during the experiment, it is apparent that μ_m is dependent not only on mass but also on wavelength; where an absorption edge occurs two values of μ_m a maximum and a minimum, are defined for the particular wavelength.

The student may determine the maximum and minimum Mass Absorption Co-efficients from the graphs for each absorption edge but due to the relatively broad width of the beam, accounting also for the lack of linearity in the practical curves, the results will bear little relationship to published standards.

The experiments have demonstrated that Characteristic Radiation is only emitted when the energy of the incident photon or electron equals or exceeds that of the Characteristic Absorption Edge.

Conversely if an Absorption Edge is observed there must be X-radiation present which is characteristic of the absorbing material; this radiation will "fluoresce" indiscriminately in all directions, but the wavelength of this "secondary emission" will always be slightly longer than that of the incident radiation.

D16.12 Set up for Bragg Reflections as in D14.1 to 7. Without plotting the results on paper, insert each of the 4 filters at E.S.14 and observe the effect on count rate at features 3 and 4.

D17 — X-RAY SCATTERING (50 MINUTES)

KIT 582	30 kV	50 μA	NORMAL LAB

Foils of the elements Zn, Cu, Co and Ni are affixed to four of the faces of a moulded plastics octagonal drum and the drum located to rotate within a moulded plastics outer case which locates in the crystal post; this is the Rotary Radiator: 564.001.

The other four faces are occupied by metal elements which are sequential when classified according to their ATOMIC WEIGHTS, as prescribed by the study of the Mass Absorption Co-efficient in D.16.

Zinc	(Zn)	65.37	Iron	(Fe)	55.85
Copper	(Cu)	63.54	Manganese	(Mn)	54.94
Cobalt	(Co)	58.93	Chromium	(Cr)	52.00
Nickel	(Ni)	58.71	Vanadium	(V)	50.94

The drum has eight rest positions; an attempt can be made to "fluoresce" the characteristic X-radiation of each element by placing them in turn into the window in the cover which is irradiated by the primary beam from the Copper target tube. The symbol of the element in the irradiation window is shown in a second window at the rear of the Rotary Radiator.

D17.1 Remove the jaw clamp from the Crystal Post; mount the Rotary Radiator and fix with the clamping screw without replacing the jaw.

D17.2 Turn the Carriage Arm to rest at 90° (2θ) to the X-ray beam axis and verify that the Rotary Radiator presents the irradiation window to the Basic Port at an angle of 45°.

Screw the flexible actuator cable into the socket on the Rotary Radiator and lead it out of the experimental zone to a convenient operating position outside the Scatter Shield.

Successive rotations of the foil drum can now be achieved without disturbing any electrical parameters.

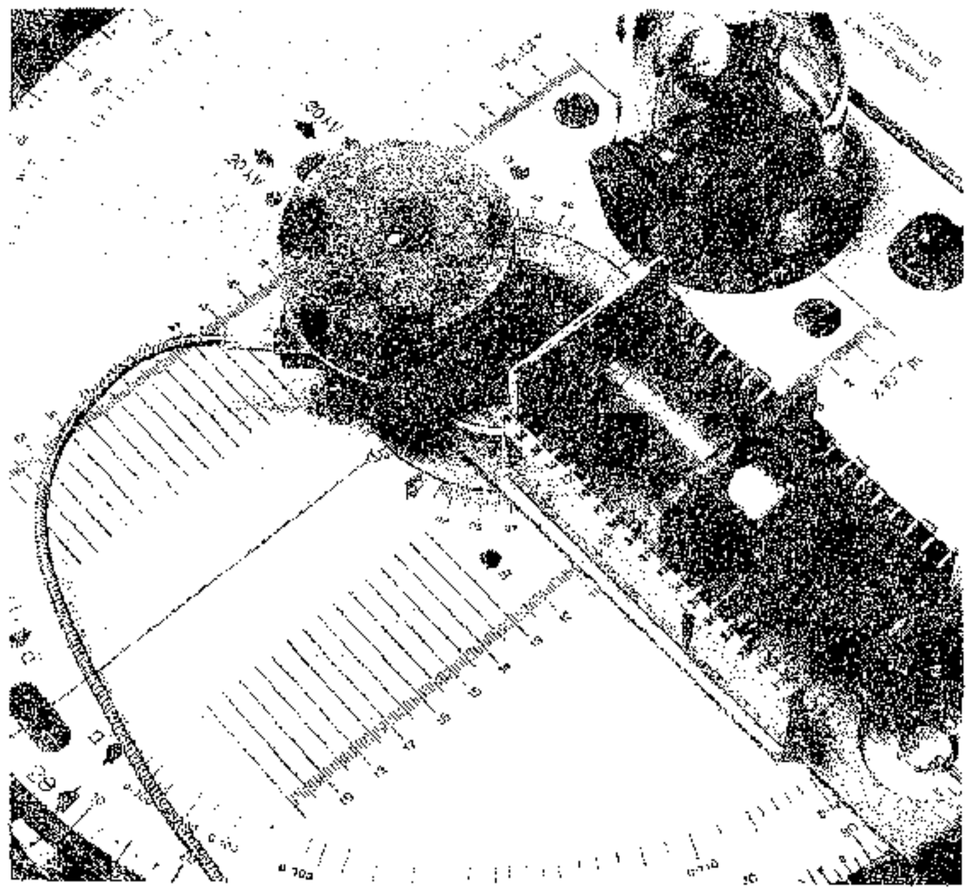

D17.3 Insert the Primary Beam Collimator 582.001 into the Basic Port with the 1mm slot in the horizontal position.

D17.4 Locate the G.M. Tube and Holder Assembly at E.S.22.

Meaningful results can be obtained with a Ratemeter but a Scaler provides greater accuracy.

D17.5 Locate the Blank Slide 562.033 at E.S.13.

Measure and tabulate the intensity, I_0 for each of the elements on the Rotary Radiator:

RADIATOR		I_0	I	I/I_0
At. Wt.	Element	cps	cps	
50.94	V			
52.00	Cr			
54.94	Mn			
55.85	Fe			
58.71	Ni			
58.93	Co			
63.54	Cu			
65.37	Zn			

Observe that the values of intensity I_0 vary considerably.

It is interesting that there is any "secondary emission" at all from the Zn and Cu radiators; experiment D16 has illustrated that CuK emission is too long in wavelength to excite the Absorption Edge of either Zn or Cu. If short wavelength "white" radiation was exciting the Zn or Cu then

the level of intensity would be very much less than that of the Ni or Co radiators, known to be excited by the CuK radiation which constitutes a large proportion of the primary incident beam.

It must be concluded therefore that some incident photons experience merely elastic collisions and are "scattered" out of the direction of the primary beam but without appreciable loss of energy.

D17.6 Remove the Blank Slide at E.S.13 and replace with the Zinc Filter 564.009.

Measure and tabulate the intensity, I for each element on the Rotary Radiator as in 16.5.

D17.7 Calculate the ratio I/I_o and plot a graph of this ratio against Atomic Weight

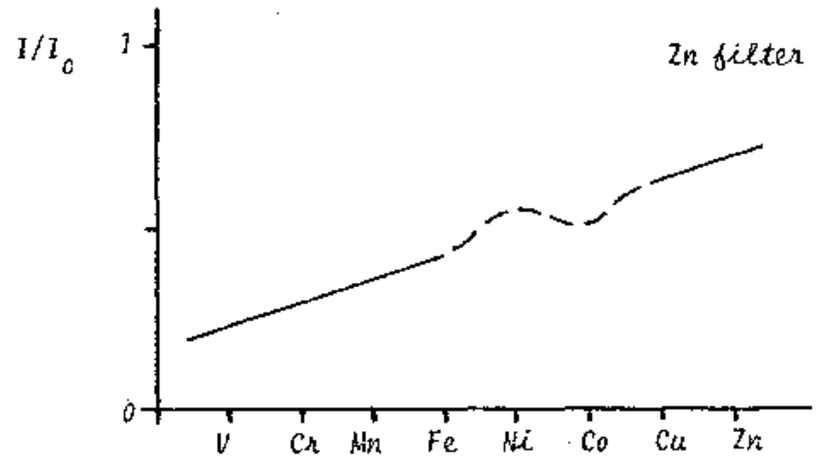

Observe that all the points lie in a straight line with a discrepancy near the centre; a rapid repeat of the experiment verifies that this 'kink' is consistent and is not an experimental error.

Observe also that although the values for I_o varied considerably, when expressed as transmission there is a continuous increase in I/I_o as the atomic weight of the "fluorescing" element increases.

As the Atomic Weight increases so the "population" of electrons in the element increases and this gives rise to an increase in the intensity of "scattered" radiation following elastic collisions.

D17.8 Replace the Zn Filter with the Copper Filter, 564.006, tabulate the results, calculate I/I_o and plot the transmission graph.

Observe that the unexplained 'kink' is still present but that the hitherto straight line curves downwards at the high Atomic Weight End.

Evidently the radiation "fluorescing" from the Zn element is being partially absorbed by the Cu filter.

"Scattering" as the prime cause of this reduction can be eliminated since the effect is not likely to be radically different for neighbouring elements such as Cu and Zn.

Similarly the "kink" cannot be due to differential scattering since it is unchanged whether the Cu or the Zn filter is present.

D17.9 Replace the Cu Filter with the Cobalt Filter 564.008, tabulate the results and plot the transmission graph.

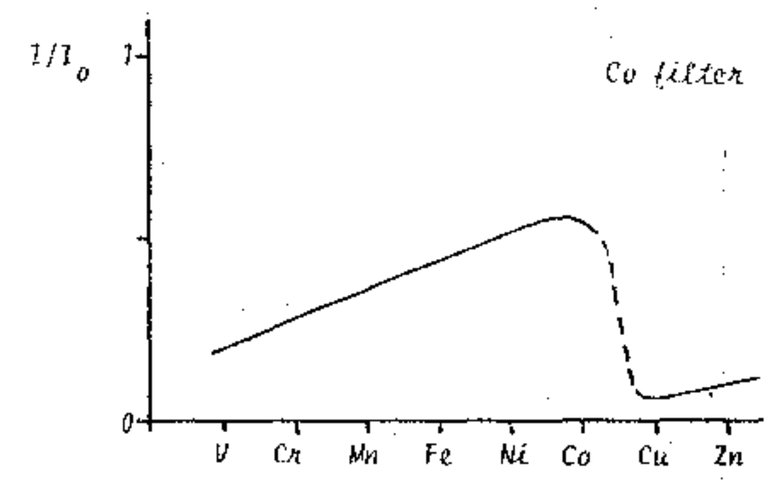

Observe that an abrupt discontinuity has appeared, although a curve-down before the discontinuity is evident (for emission from the Co radiator) and the 'kink' has disappeared.

Following D16 it is to be expected that emission "fluorescing" from the Zn and Cu radiators will excite the element Co; but the Cobalt emission seems to be partly exciting itself!

Together with the absence of the 'kink' the results are becoming difficult to interpret, as indeed Henry Moseley discovered around 1910; it would be prudent to continue the series of experiments before making further conclusions!

D17.10 Replace the Co Filter with the Nickel Filter 564.004 and tabulate and graph.

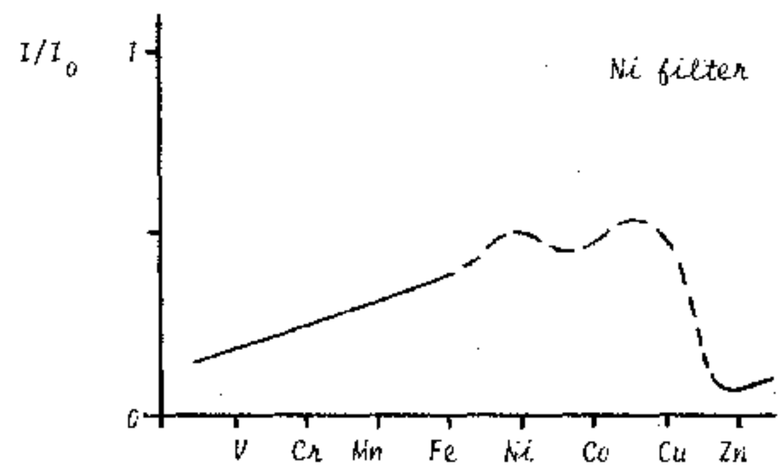

MOSELEY PERCEIVED THAT IF THE PERIODIC CLASSIFICATION OF Ni AND Co WERE REVERSED ALL THE EXPERIMENTAL RESULTS WOULD EXHIBIT A SIMPLE PROGRESSION.

D17.11 Redraw the Graphs of 17.7, 17.8, 17.9 and 17.10 with the classification of Ni and Co reversed.

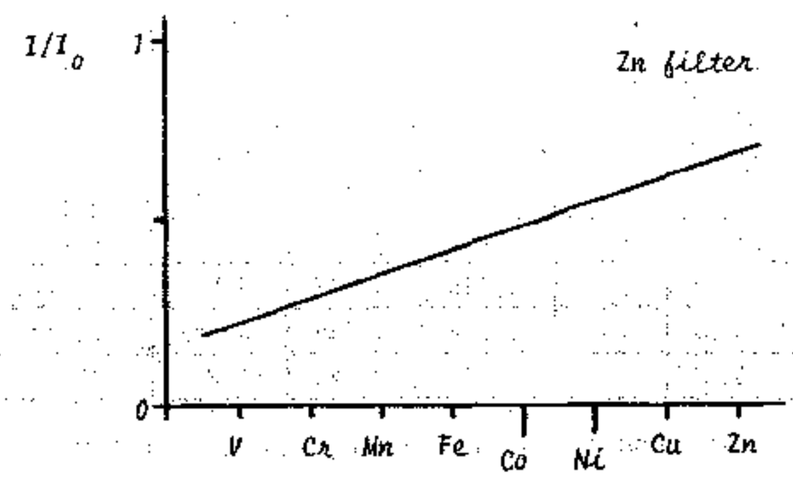

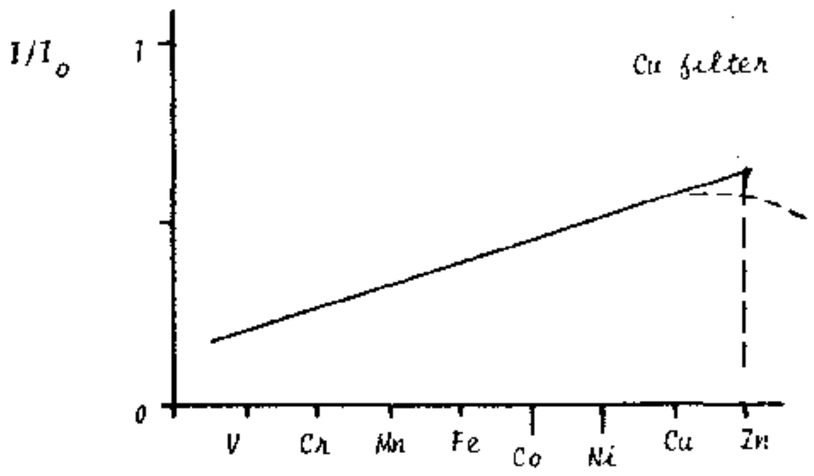

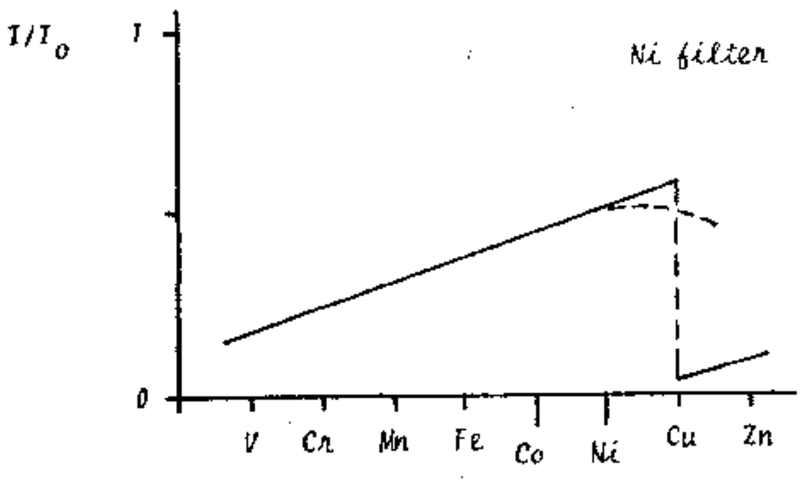

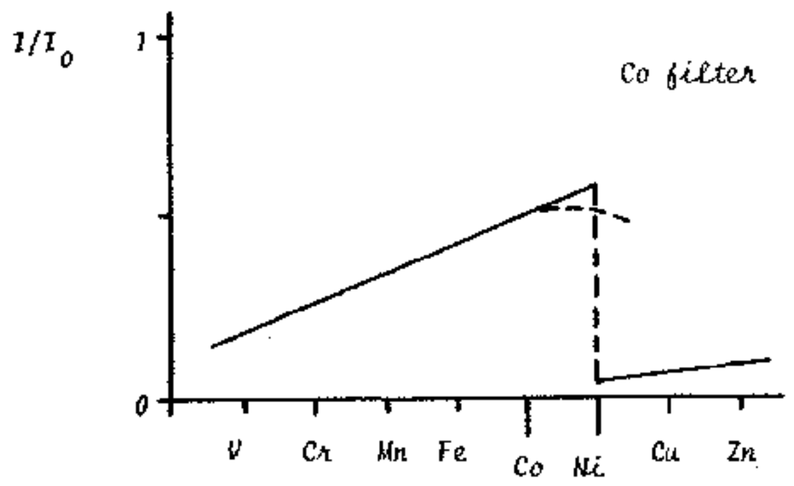

Observe that the 'kink' in all cases is eliminated and that the curving-down of the lines progresses systematically with the new classification, as does the abrupt discontinuity.

A review of graph 16.9 and 16.10 provides the explanation for the curving-down; only the less intense Kβ radiation is absorbed by the Ni whereas the much more intense Kα radiation is also absorbed by the Co filter.

It is evident that the absorption edge of each element occurs between the Kα and Kβ lines of the neighbouring element in increasing atomic number direction; this technique is frequently used to filter out Kβ lines to obtain a beam of essentially monochromatic, Kα, radiation.

The positions of Cobalt and Nickel in the Periodic Table of Elements should be determined by the relative values of their characteristic spectra and not by their atomic weights.

ELEMENT			EMISSION, nm			ABSORPTION
At.No	At. Wt.	SYMBOL	Kα	Kβ	Mean	K edge
23	50.94	V	0.255	0.228	0.242	0.227
24	52.00	Cr	0.229	0.208	0.218	0.207
25	54.94	Mn	0.210	0.191	0.200	0.189
26	55.85	Fe	0.194	0.176	0.185	0.174
27	58.93*	Co	0.179	0.162	0.170	0.161
28	58.71*	Ni	0.166	0.149	0.157	0.148
29	63.54	Cu	0.154	0.139	0.146	0.138
30	65.37	Zn	0.144	0.129	0.137	0.128

The above table shows the Kα and Kβ emission lines and the absorption edge wavelengths for each of the eight elements used in the experiments and has been tabulated from very accurate measurements; these figures have been extracted from the International Tables.

Compare the Absorption Edge figures given for Zn, Cu, Ni and Co with the results obtained in D16 and note the relative accuracy of the experiment.

The study of scattering, due to "elastic" and "inelastic" collisions provides evidence that the wavelength of the absorption edge is different and discreet for each element and that the elements can be arranged in order of decreasing wavelength.

The discreet disposition of electrons in an atom depends on the population of the electrons and this in turn is associated with the nucleus. Moseley boldly postulated that "..... we have here a proof that there is in the atom a fundamental quantity which increases by regular steps as we pass from one element to the next. This quantity can only be the charge associated with the central positive nucleus."

D18 — MOSELEY'S LAW (30 MINUTES)

In 1913 and 1914 Henry Moseley made a systematic study, using photographic techniques, of the X-ray emission line spectra of all known elements from Aluminium to Gold, placed at that time in the Periodic Classification of the Elements according to their Atomic Weights. He presented a simple series wherein every element emits an X-ray spectrum which is predictable from the spectrum of its neighbours and which is determined by an integer Z, its atomic number, in accordance with the equation

$$\sqrt{1/\lambda} = k\,(Z - s)$$

where λ is the wavelength of the spectral line and K and s are constants.

With this theory, Moseley predicted that not only Cobalt but also Argon and Tellurium were misplaced in the Periodic Table and that there were elements as yet undiscovered having Atomic Numbers 43, 61, 72 and 75.

Since Moseley worked with characteristic emission spectra, to reproduce his work would require a range of X-ray tubes each having different target anodes and, apart from being costly, this would be extremely time consuming.

Experiment D17 illustrates that absorption edges are slightly different from, but just as discreet as, the emission wavelengths; it is therefore possible to both cost - and time - effectively simulate Moseley's work through an analysis of absorption edges.

A preliminary enquiry into Moseley's Law has thus already been contributed by Experimental Programme D17.

D18.1 Analysis of the elements (30 minutes)

KIT 582+583	30 kV	50 μA	NORMAL LAB

Using the Iron, Manganese, Chromium and Vanadium Filters and the Rotary Radiator, TEL 564/001, the analysis of fluorescent radiation can be extended to provide four more graphs.

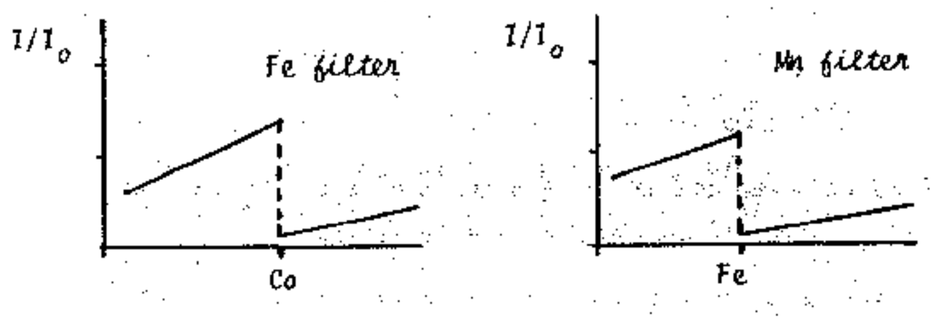

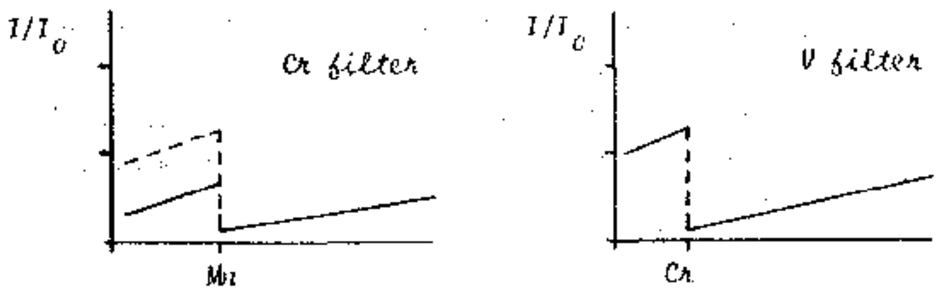

The experimental procedure is as for programme D17.

It is perhaps a more interesting practical exercise to remove the identification from say 3 of the 8 filters and ask the student to identify the elements by comparing at which wavelengths their absorption edges occur in relation to those of known elements.

The labels on the eight filters have been designed such that the Atomic Symbol can be cut away to leave only the catalogue number for identification; the numerical sequence of these numbers bears no relationship to the sequence in the Periodic Table.

Nomograph of Moseley's Law

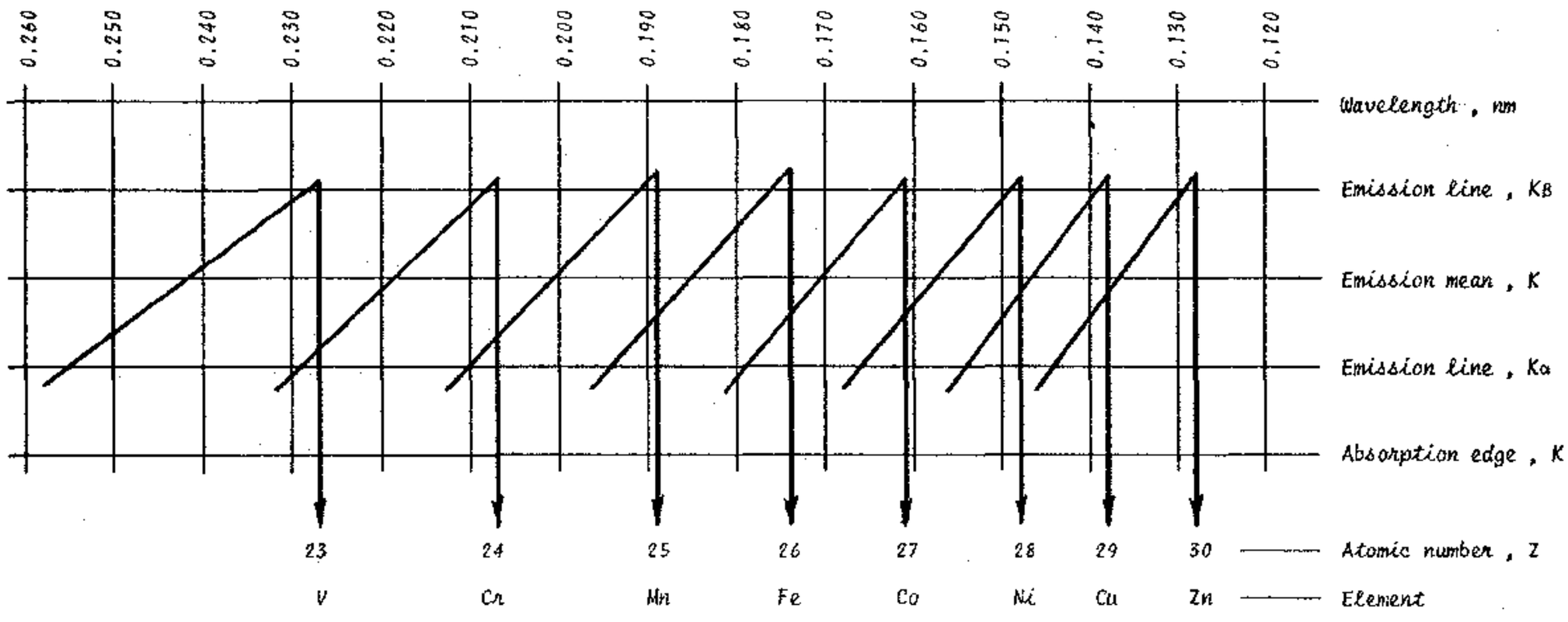

No thorough investigation of absorption and scattering should be terminated without some consideration being directed to the "secondary electron emission" present when an absorption process is detected or the probability of there being some loss of energy experienced by X-ray photons when undergoing merely elastic collisions.

The accessories necessary to perform experiments D20 and D21 are not yet available.

D19 — FINE STRUCTURE (4 HOURS)

At D15.9 electron transitions at energy-levels of low principal quantum number were studied in relation to the emission of Kβ and Kα radiation.

In spite of the compact geometry of the Tel-X-Ometer it is possible to separate the CuKα into its fine structure.

KIT 582-583	30 kV	80 μA	NORMAL LAB

D19.1 Mount the Auxiliary Slide Carriage in Mode H (see Part 1, para. 10.4) using the 1mm diameter Primary Beam Collimator 582.002.

D19.2 Cut open a Filmpak 750/2 in a dark room and using a sharp cork-punch make a hole in the centre of the film of 10mm diameter.

D19.3 Mount the film within a black paper envelope, as described in para D5; do not incorporate the Luminescent Screen. Mount the prepared envelope in the Frame of Cassette 562.013 but with the square metal backing plate removed. Mount the assembly at E.S.4.

D19.4 Carefully mount a length of Aluminium Wire 585.005 on the crystal post by means of a Spindle Clip 567.008; ensure that the wire is straight and vertical.

D19.5 Select 30kV and 80 μA. Expose for 3 hours.

Return to the darkroom and process the film.

Observe the Debye Scherrer type pattern of two concentric rings recorded from back reflections of high order angle from the Al wire (see para D27 and 28).

D19.6 Reconstruct the experiment and measure the distance from the centre of the crystal post to the film, ℓ mm.

Measure also the diameters D_A and D_B.

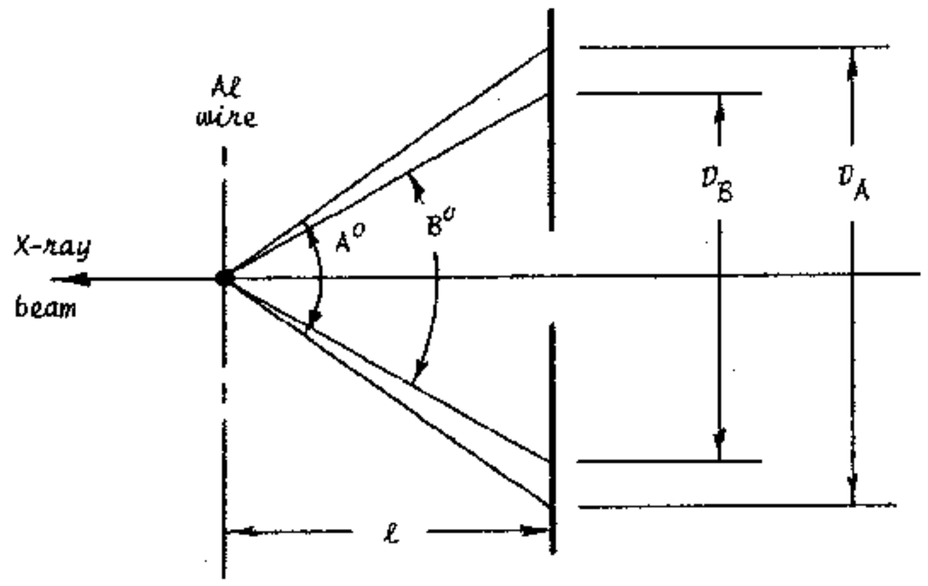

The angle A is $360 - 4\theta_1$ where θ is the Bragg angle ; similarly B is $360 - 4\theta_2$.

Thus $\tan\{180 - 2\theta_1\} = \frac{D_A}{2\ell}$

and $\tan\{180 - 2\theta_2\} = \frac{D_B}{2\ell}$.

Evaluate θ_1 and θ_2 and given that the reflections are due to the (511) planes at a spacing of 0.0779 nm , calculate λ_1 and λ_2 .

$\lambda = 2d/n \sin\theta$ where $d/n = 0.0779$ (see D28)

Calculate to four significant figures.
($\lambda_1 = 0.1541$ and $\lambda_2 = 0.1544$ nm).

D19.7 Observe that the intensity of the circle due to α_2 is less than that due to α_1 .

At D15.9 the difference in intensity between the Kα and Kβ reflections was attributed to the relative proximities of L and the N and M levels to the K level; the greater the energy difference of the electron transition the shorter the wavelength but the less the intensity.

The quantum theory postulates three possible energy states for electrons in the L level due to the effect of both orbital and spin angular momentum.

At the K level, where quantum number n = 1 and ℓ = 0, the selection rules permit only one value, ½, for j and so there is only one energy level. At the L level where n = 2, the value of ℓ can be 0 or 1 and thus j can be ½ (ℓ = 0 or 1) and 1½ (ℓ = 1).

Energy Level	Sub Level	Quantum Number n	ℓ	j	Radiation Emitted	Relative Intensity
L	3	2	1	1½	Ka_1	2
	2	2	1	½	Ka_2	1
	1	2	0	½	-	-
K	-	1	0	½	-	-

The selection rules require that δℓ be ±1 for electron transitions; this is not satisfied by $L_1 \rightarrow K$ transitions hence there can be no emission of energy. Transitions $L_3 \rightarrow K$ and $L_2 \rightarrow K$ both satisfy the selection rules for δℓ and also for δj. Energy is thus emitted in the form of Ka_1 and Ka_2 radiation and, in accordance with Summerfeld's intensity rule, the relative intensity of the emissions is 2:1.

The relative intensities of the Kα and Kβ reflections can similarly be deduced to be 5:1; this ratio is not observed exactly in the graphs of experiment D14 due to the greater absorption of the softer Kα radiation.

EXPERIMENTAL PROGRAMME D22 TO D30, CRSTALLOGRAPHY (45 HOURS)

The performance of programme D22 to D30 is intended to familiarise the student with the basic principles of crystallographic analysis.

For a comprehensive treatment of X-ray Crystallography, reference should be made to standard text books.

It is general practice in higher education to allocate 4 hours for student practical work periods; the techniques and materials used in this section have been carefully selected to provide the student with meaningful results within this period of time ; where possible Debye-Scherrer exposures are limited to 3 hours thus allowing 1 hour for setting-up, for film development, for discussion etc.

In experimental programme D15 the LiF crystal is used to accurately determine Planch's constant; measurements of the intercept on the x-axis of the graph are more precise than with NaCl due to the larger angle 2θ; the crystal spacing given in D15.8 indicates smaller spacing for LiF and hence larger 2θ; this is in accordance with the Bragg equation.

Both Li and F lie in the second period of the Periodic Chart where electrons are present at the K and L levels; Na and Cl are in the third period and electrons are not only present in the K and L states but also at the M level; the addition of electrons in the M state seems to result in a larger crystal spacing 'd'.

D22 — ATOMIC SIZE (20 MINUTES)

KIT 582+583	30 kV	80 μA	NORMAL LAB

D22.1 Set up for Bragg reflection as in D14.1 to D14.6.

D22.2 Minimise the CuKβ radiation by inserting the Ni filter TEL 564.004 at E.S.17.

D22.3 Increase the tube current to 80 μA.

D22.4 Using a Ratemeter, search and record the 2θ angle for the first diffraction peak for CuKα radiation, $\lambda = 0.154$ nm.

Tabulate and calculate d, assuming $n = 1$ in the Bragg equation $n\lambda = 2 d \sin \theta$.

Crystal	2θ	θ	$\sin \theta$	$\lambda/2$	d nm
NaCl (yellow)				*0.077*	
KCl (green)				*0.077*	
RbCl (red)				*0.077*	

D22.5 Repeat the experiment using the KCl crystal (Green).

D22.6 Repeat the experiment using the RbCl crystal (Red).

Observe that the crystal spacing, d increases with the Atomic Number of the Alkaline metals; Na in the third period has eleven electrons at K, L and M levels; K in the fourth period has nineteen electrons but in the K, L, M and N states, whereas Rb has thirty seven electrons in the five energy states, K, L, M, N and O. Chlorine is common to the three compounds and thus the evidence suggests that the size of individual atoms increases with atomic number.

Crystallography is not a 'direct' science; crystal structures are postulated after interpretation of all the evidence available including the morphological, the optical and the chemical properties of the specimen; the alkaline halides are both morphologically and chemically similar and the student could expect that these salts will exhibit similar crystal structures.

The experimental evidence so far indicates that the Bragg postulation (that NaCl is of cubic structure) is acceptable; it is rewarding at this stage for the student to build atomic models but it is recommended that contacting spheres are used rather than point-centre lattices; this reminds the student that the phenomenon of X-ray diffraction is a function of electron densities and locations and is not due to the relatively point-centred nucleus; the student will also find it less confusing when studying the reciprocal lattice, which will be seen to be necessarily point-centred.

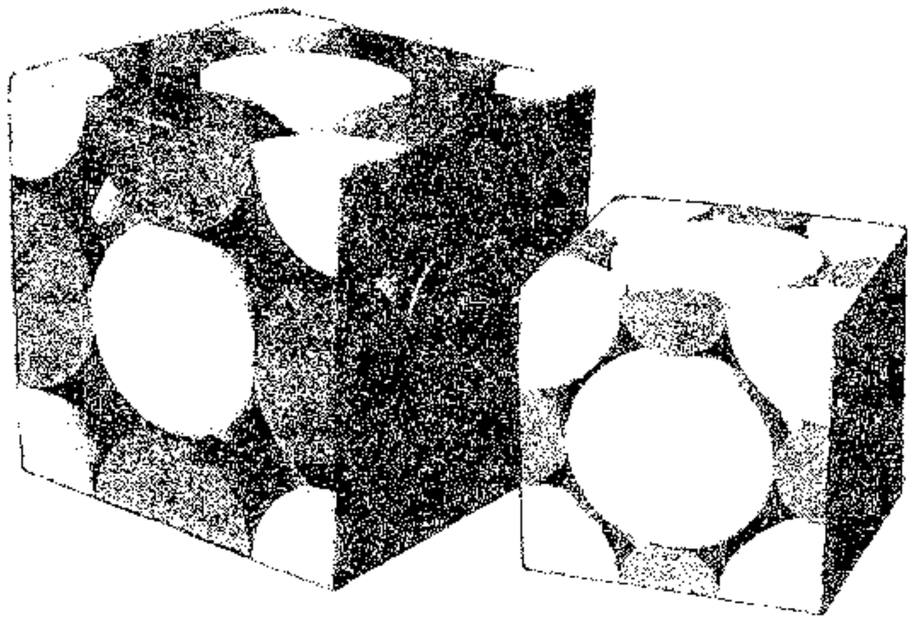

D22.7 The Na atom, with 11 electrons, is thus smaller than the Cl atom (17 electrons); the K atom, in sharing an electron with Cl is of equal size and the Rb atom (37 electrons) is larger than that of Chlorine; the three models should depict these relative sizes.

D22.8 The size of atoms is of great importance in metallurgy when studying crystal cohesion and in the development of alloys having specific mechanical properties.

D23 — UNIT CELL (CALCULATIONS — 5 MINUTES)

D23.1 The table of D22.4 was drawn up from angular measurements of the first Bragg peaks and defines the largest spacing within the three crystals which give rise to constructive interference.

Clearly sets of planes can be chosen which have greater spacing, but in the absence of any Bragg reflections, the interference must be destructive and not constructive.

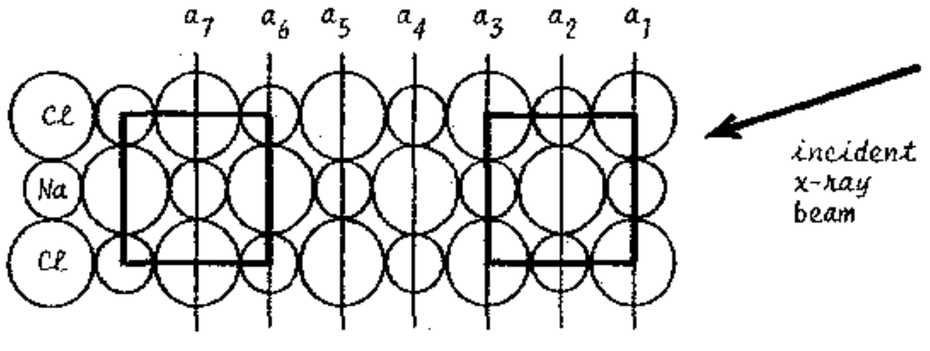

D23.2 A plan view of a model of NaCl exhibits a pattern of repetitive symmetry; a pattern of symmetry is apparent in the Laue photographs of experiment D12 and one of the first objectives in crystallography is to establish the linear repetition frequency of a symmetrical pattern in each of three dimensions.

In the a-direction illustrated, the symmetrical structure bordered by layers a_1 and a_3 is repeated by a_3 and a_5, by a_5 and a_7 etc; an identical geometric form can be repeated by choosing a_2/a_4, a_4/a_6 etc.

D23.3 Accepting the cubic proposal a symmetrical pattern should be evident in both the b- and c-axes and hence a "building block" can be defined as indicated by the bold line, the nature of the atoms at the vertices being consistently either *Cℓ* or *Na*.

In D14 the distance between adjacent unlike atoms, *Na* and *Cℓ*, *d* was calculated to be 0.282 nm; the distance between two like atoms, *Cℓ* and *Cℓ* is twice this spacing and hence the length of the side of the "building block" is 0.564 nm.

This repetitive geometric figure, when established in 3-dimensions, is defined as the UNIT CELL. Where a choice exists with geometric forms of identical area then the form most clearly approaching rectangular is usually adopted.

D23.4 Experiment D22.4 establishes that the length of the edge of the Unit Cell of *NaCℓ* in the arbitrary a-direction is *2d*. Similarly 'a' can be established for the Unit Cells of *KCℓ* and *RbCℓ*.

Crystal	*Unit Cell Side a nm*
NaCℓ	
KCℓ	
RbCℓ	

D23.5 Reflections are not observed for spacings equivalent to the side of the Unit Cell by virtue of destructive interference.

When waves from layer a_3 are one wavelength behind those from layer a_1, then waves from layer a_2 must be half a wavelength lagging on those from layer a_1 and exactly opposite in phase; since the layers throughout the crystal contain the same combination of atoms of Na and Cl, the electron densities are the same and so the diffractive power of the layers is identical; the waves from layer a_2 therefore exactly cancel out those from a_1.

It is necessary to verify that the crystals are of cubic form and to evaluate the length of the sides of the Unit Cell in the b and c directions; once all these shapes and dimensions have been determined, the position of the atoms within it must be discovered; to achieve this both a datum and a suitable system of co-ordinates is required.

D24 – CO-ORDINATES (30 MINUTES)

D24.1 Now that a Unit Cell for each of the three alkaline halide crystals has been proposed, the groups of layers a_3/a_5 and above can be defined as mere repetitions of all diffracting electron layers of the Unit Cell group a_1 to a_3, all having a spacing of 'a' nanometers. If the facing layer of the crystal is defined as a_1, as in the illustration of D23.1, then all layers with an odd suffix can be redesignated as repetition a_1 layers.

Note that the datum is arbitrary and an a_1 layer could equally have *Cℓ* or *Na* as vertices but once the decision has been made it must be consistently applied.

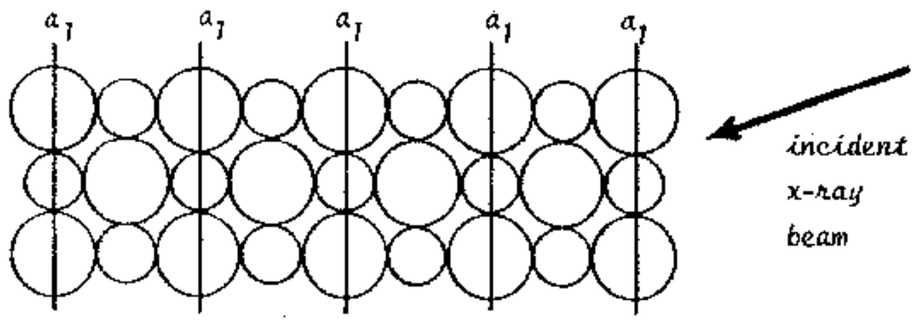

D24.2 The essential condition for diffraction from the a_1 layers is that the Bragg law is satisfied :

$$n\lambda = 2\,a\,\sin\theta\,.$$

The equation can be written in terms of $\sin\theta$:

$$\sin\theta = \frac{n/a}{2/\lambda}$$

and represented diagrammatically :

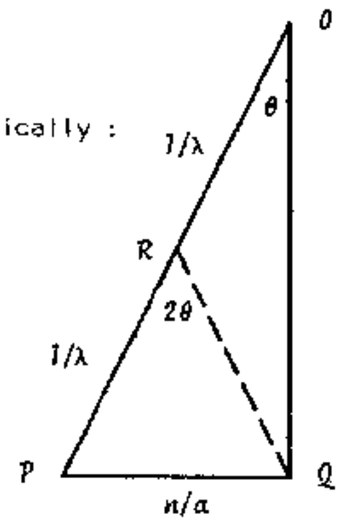

The point R bisects the side PO and if R is joined to Q, $Q\hat{R}P$ is equal to 2θ.

When $2\theta = 0^\circ = \theta$, Q coincides with P and $\vec{OP}$ can thus be considered as the DIRECTION of the primary X-ray wavefront ; similarly $\vec{RQ}$ represents the DIRECTION of the diffracted wavefront due to constructive interference of reflections from P and Q, having a separation of n/a ; this is a reciprocal dimension and in real terms the separation of P and Q is a/n nanometers.

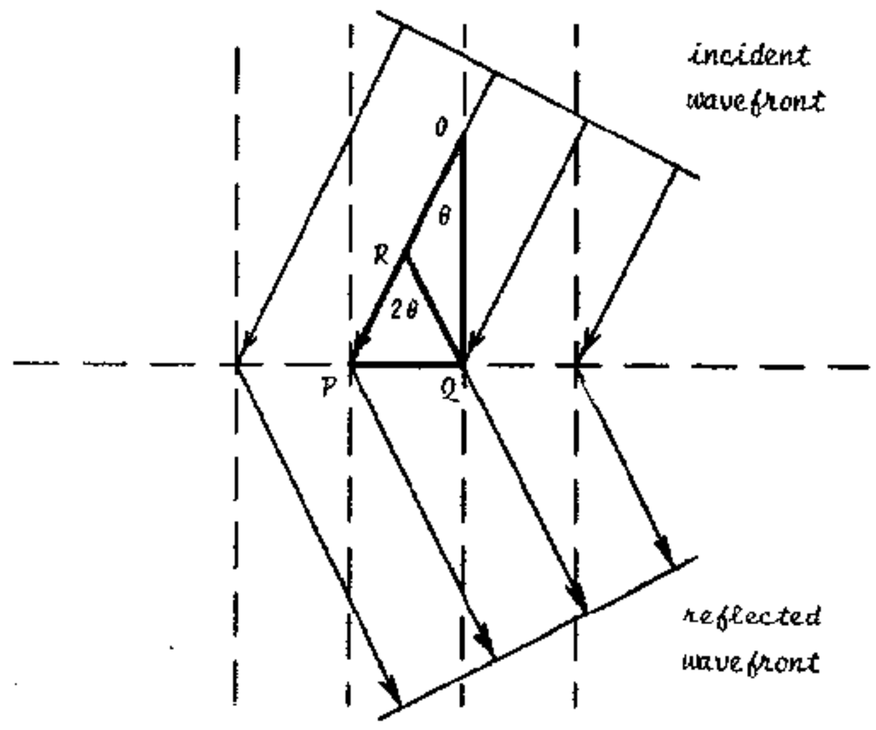

Since n must be an integer PQ can be represented by a reciprocal linear scale in terms of n/a.

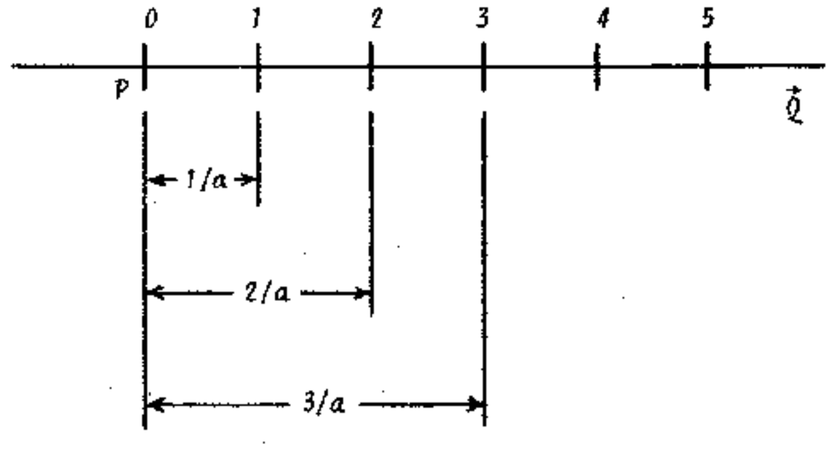

D24.3 PQ̂O is always a right angle and for a fixed wavelength, λ the locus of the point Q is a "Circle of Reflection" of radius $\frac{1}{\lambda}$ and centred at R; by choosing a convenient scale a diagram can be constructed and measurements of angles of reflection and reciprocal spacings can be "read-off" without the need to constantly solve the Bragg equation for θ or d.

Let $1/a$ nm^{-1} = 2 cm ; then 1 nm^{-1} = $2a$ cm and λ nm^{-1} = $2a/\lambda$ cm .

Hence RP = $1/\lambda$ = $2a/\lambda$ cm and for

NaCl where a = 0.564 nm , RP = 7.30 cm , for

KCl where a = 0.629 nm , RP = 8.16 cm and for

RbCl where a = 0.655 nm , RP = 8.53 cm .

D24.4 Construct a Circle of Reflection for *NaCl* ;

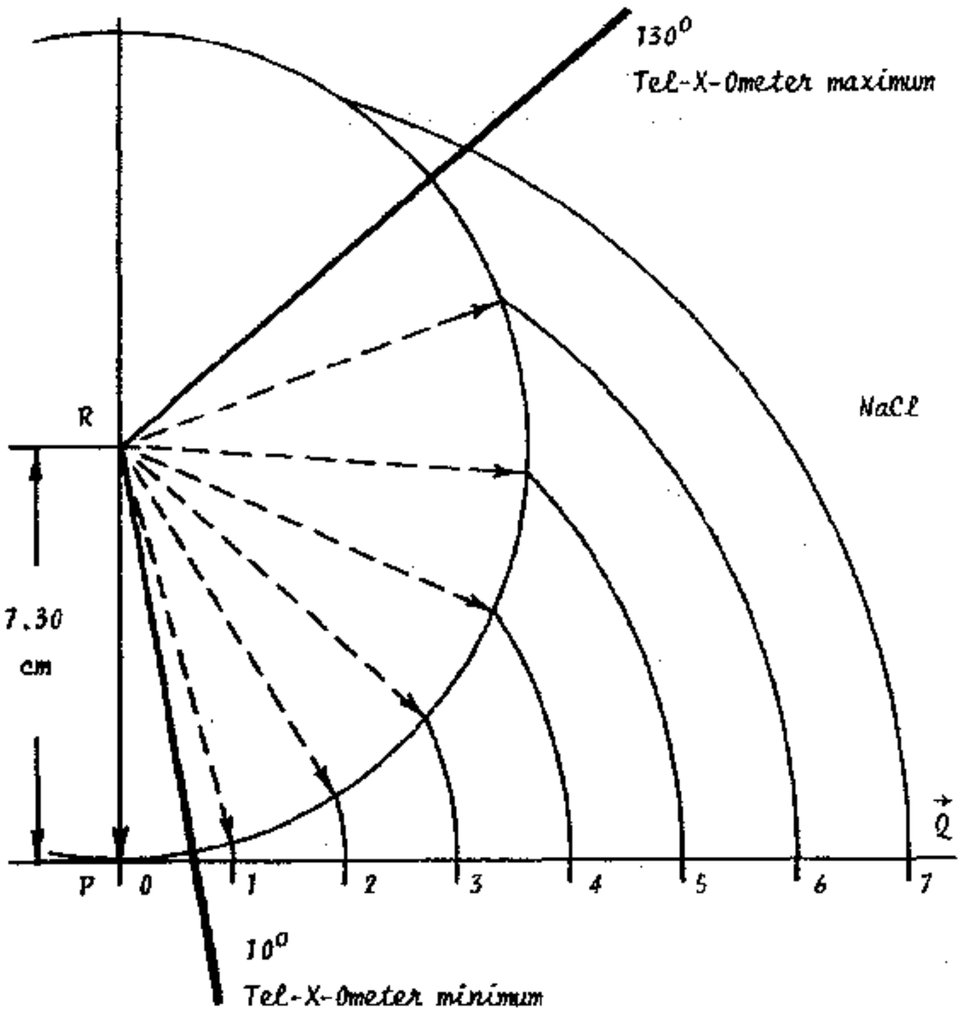

If the centre linear scale PQ were rotated about the Origin P and the Circle of Reflection constructed to the same scale but printed on transparent material and graduated in degrees for increasing angles of 2θ then the points for predictable diffraction Q_1, Q_2 etc. could be read directly.

D24.5 The Reciprocal Lattice Calculator TEL 583.003 is constructed in this manner; only the arcs of the circles relevant to the Tel-X-Ometer geometry are printed for each of the alkaline halide crystals.

Small pin-holes are drilled at the origin, P, for each circle of reflection.

Lay the Calculator on the diagram of D24.4 and locate the *NaCl* origin on the point P of the diagram using a mapping pin. Rotate the diagram underneath the Calculator and observe the intersection on the circle of the integer intervals for n on the line PQ.

D24.6 Tabulate the measured angles in the 'Theoretical' column for 2θ.

D24.7 Set up for Bragg reflection as in D22.1 to D22.3

D24.8 Using a Ratemeter, search in the theoretically predicted regions for diffraction peaks; tabulate the results in the 'Actual' colume for 2θ, noting also the absence of any predicted peaks.

n	2 θ	
	theoretical	*actual*
1		
2		
3		
4		

D24.9 Repeat the experiment with the other crystals but using only the Calculator and centimetre graph paper, graduated to the scale of 2 cms on one side of the graph paper (further constructions follow later).

The absence of peaks when n = 1 has been discussed in D23.5; it is reasonable to assume that the observed absence of peaks whenever n is odd must similarly be due to destructive interferences.

D25 — THE UNIT CELL, TWO DIMENSIONS (40 MINUTES)

KIT 582+583	30 kV	80 µA	NORMAL LAB

To confirm the hypothesis that the Unit Cell is cubic, the length of side must be established in the 'b' direction.

In order to achieve this the crystal must be oriented to ensure that the 'b' planes are parallel with the primary beam when $2\theta = 0^\circ = \theta$.

D25.1 Unlock the crystal jaw-clamp and rotate the crystal itself through 90°.

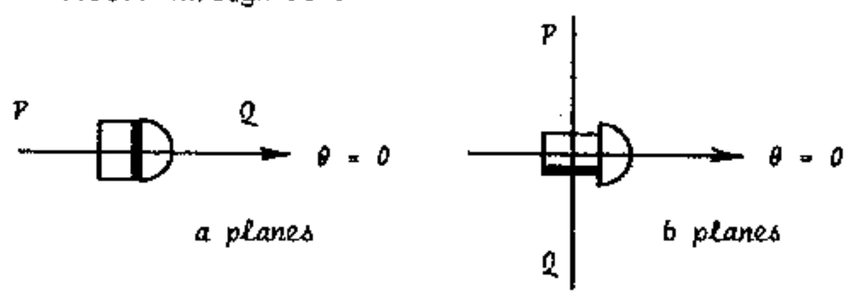

The 'b' planes can be drawn on the graph of D24.9 by constructing at right angles to PQ; it is assumed that the Unit Cell is cubic and since a = b nm a cursory investigation shows that identical 2θ angles will be predicted.

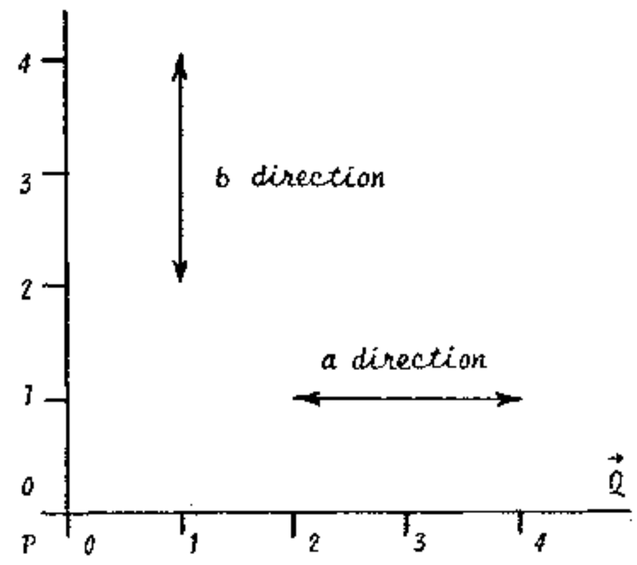

D25.2 Set up for Bragg reflection as in D24.7, D24.8 and D24.9 and verify that the angle 2θ for diffraction peaks and "extinctions" are the same for the 'b' direction as for the 'a' direction.

The crystal has now been mapped in two of the three major apparent axes, 'a' and 'b'; sufficient information now exists to predict the reflections from planes perpendicular to other axes which are not major.

D25.3 Construct a lattice by projecting the perpendiculars to the integer points in both the 'a' and 'b' directions.

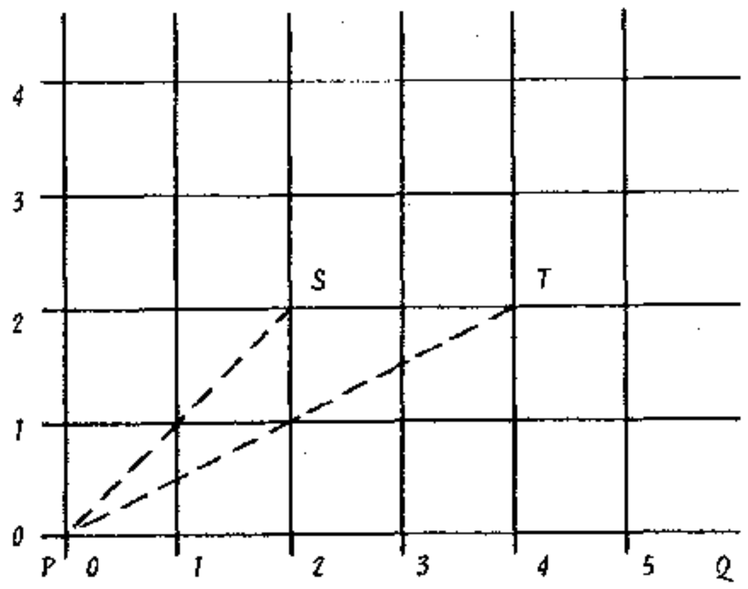

Any point on the lattice such as S now has co-ordinates (2,2) and T has (4,2).

These points represent PLANES within the crystal; since the graph is constructed from reciprocal dimensions it is called the Reciprocal Lattice and co-ordinates are usually referred to in terms of (hk), the Miller indices.

In terms of two dimensions, the reference for point S is (22) where $h = 2$ and $k = 2$ and in real terms within the crystal the co-ordinates are $(\frac{a}{2}, \frac{b}{2})$.

D25.4 In considering a three-dimensional structure the equivalent Miller index for the 'c' direction is the letter 'ℓ'; the crystal has been located in the Crystal Post with the 'c' planes horizontal and parallel to the primary beam and with no additional orientation the index 'ℓ' is zero.

The spatial co-ordinates for the S planes and T planes are thus (220) and (420) respectively.

D25.5 The spacing of the (220) planes is PS and therefore PS represents the direction of the normal to the planes; again this normal must be set perpendicular to the primary beam when $2\theta = 0$.

The k planes were oriented through 90° with respect to the h planes in D25.1; in this instance, the crystal must be oriented through $S\hat{P}Q$ when the carriage arm is set at $2\theta = 0$.

D25.6 Draw the line SP on the constructed diagram of D25.1 and, using the Calculator as a protractor, measure the angle $S\hat{P}Q$.

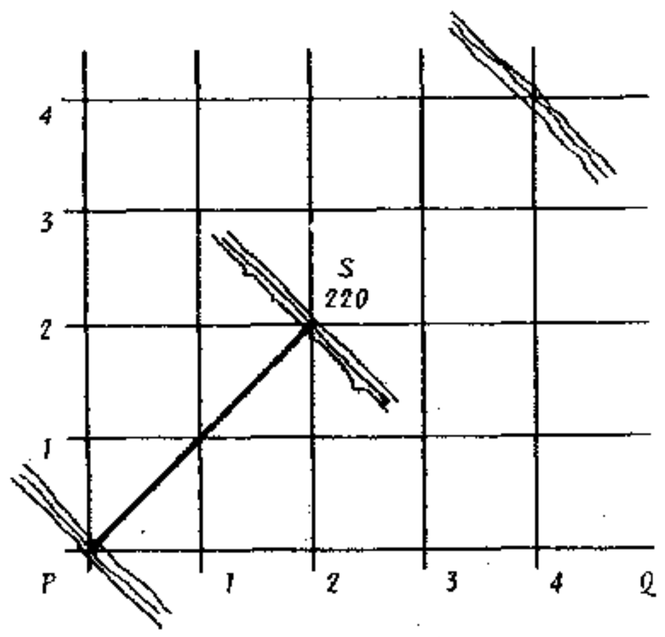

D25.7 Set up for Bragg reflection as in D22.1 and D22.3.

D25.8 Unlock the 2:1 drive by turning the Knurled Clutch Plate in an anti-clockwise direction; with the Carriage Arm accurately held at zero, rotate the crystal in a clockwise direction through the measured angle $S\hat{P}Q$ as precisely as possible and lock up the Knurled Clutch Plate.

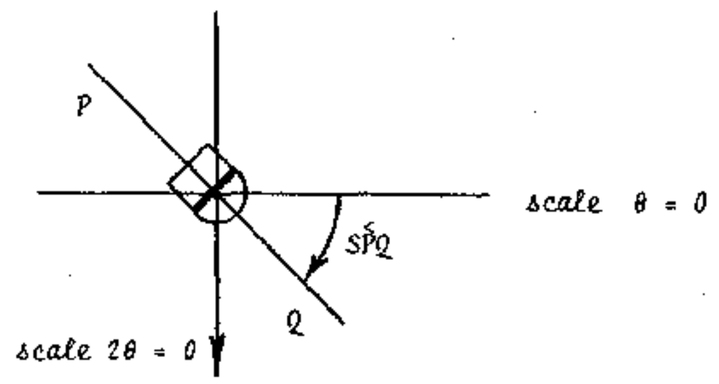

The normal to the (220) planes has been set perpendicular to the primary beam when the carriage arm is at zero.

D25.9 The normal to the (220) planes is also that for the (110), (330), (440), etc. and so 2θ angles can be read-off the constructed Reciprocal Lattice by using the Calculator; tabulate the measured angles.

$\angle SPQ$	*planes (hk0)*	*2 θ*	
		theoretical	*actual*
	110		
	220		
	330		
	440		
	430		
	320		
	640		
	210		
	420		
	630		
	310		
	620		

Observe that 2θ for the (110) planes is smaller than SPQ and considerable absorption of the primary beam might be expected.

D25.10 Unlock the jaw clamp and carefully displace the crystal such that the corner nearest the primary beam is about 1mm from the axial centre line scribed on the Crystal Post.

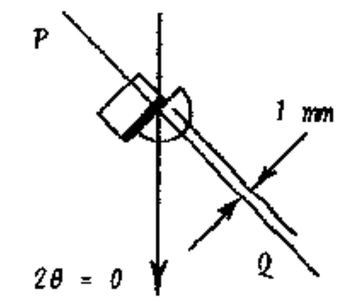

D25.11 Using a Ratemeter, search for the predicted diffraction peaks and tabulate the results, always noting any "extinctions", in the table of D25.9.

Observe that, as with Table D24.6, whenever h or k is odd there is an extinction.

D25.12 The length of PS, diagram D25.6, from simple trigonometry is

$$\sqrt{(2^2 + 2^2)}$$

or in three-dimensional terms

$$\sqrt{(h^2 + k^2 + \ell^2)}\ .$$

In real terms within the crystal

$$d_{220} = \frac{a}{\sqrt{(2^2 + 2^2 + 0)}} \quad \text{nm}$$

and in general , for an isometric (cubic) system

$$d_{hk\ell} = \frac{a}{\sqrt{(h^2 + k^2 + \ell^2)}} \quad \text{nm}$$

Evaluate the 20 largest possible spacings of sets of planes within the Unit Cell by allocating suitable integers to h ,k and ℓ such that $h^2 + k^2 + \ell^2 = 1$, 2 etc

$h^2 + k^2 + \ell^2$	h	k	ℓ	Reflections R Extinctions X
1	1	0	0	
2	1	1	0	
3	1	1	1	
4	2	0	0	
5	2	1	0	
6	2	1	1	
7	—	—	—	—
8	2	2	0	
9	2	2	1	
	3	0	0	
10	3	1	0	
11	3	1	1	
12	2	2	2	
13	3	2	0	
14	3	2	1	
15	—	—	—	—
16	4	0	0	
17	3	2	2	
	4	1	0	
18	3	3	0	
	4	1	1	
19	3	3	1	
20	4	2	0	

Observe that the seventh and fifteenth terms of the series are absent since 7 and 15 are not possible combinations of $h^2 + k^2 + \ell^2$.

D25.13 Compare the results with Table D24.6 for $(h\ 0\ 0)$ planes and table D25.9 for $(h\ k\ 0)$ planes, noting in the last column the observed presence or absence of reflections.

To verify the presence or absence of reflections from the 9 planes where ℓ is not zero it is first necessary to establish that the "space-lattice" is indeed cubic by evaluating the length of the side of the Unit Cell in the 'c' direction.

The geometry of the Tel-X-Ometer will not allow the G. M. Tube to be rotated in a vertical direction; furthermore the construction of the Crystal Post does not allow the crystals to be conveniently oriented to present an adequate area to the primary beam.

An alternative technique can be used where a photographic record is made of reflections from a small rotating single crystal.

D26 — THE UNIT CELL, THIRD DIMENSION (6 HOURS)

KIT 582+583 + TEL 587	30 kV	80 µA	NORMAL LAB

As the crystal is rotated about the 'c' axis reflections will occur for planes $(h\ k\ \ell)$ when ℓ is not zero only when the Bragg condition is satisfied, but the direction of the reflection will have a vertical component; when ℓ is zero, as in all experiments so far performed, the G. M. tube is rotated around the crystal in a plane parallel and co-incident with the X-ray beam; this is the Equatorial Plane or zero layer.

If constructive interference is to be achieved from the 'c' planes, parallel to the X-ray beam, then the path lengths of the scattered rays must differ by a whole number of wave-lengths, $n\lambda$.

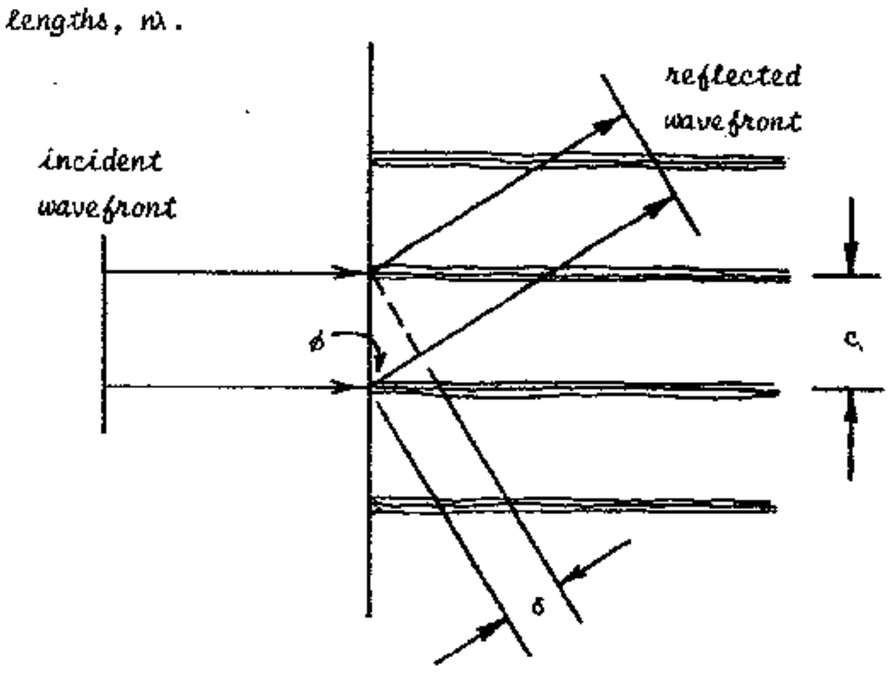

Thus $\delta = c \cos \phi = n\lambda$.

X-rays are scattered in all directions, but for a given 'c', n and λ the angle ϕ is constant and so only those rays emitted in a cone of semi-vertical angle ϕ will co-operate.

But the Bragg equation must also be satisfied and there will therefore be discreet reflections around the cone as the crystal is rotated; in the Equatorial Plane ϕ is 90^0 and hence only the Bragg condition applies, but with different integer values for n other cones are defined with decreasing semi-vertical angles ϕ as n increases.

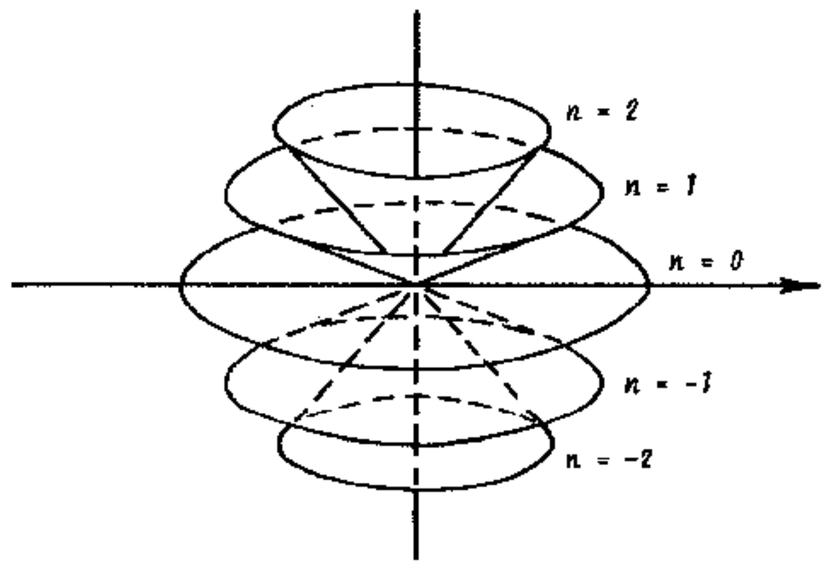

The directions of the discreet reflections in each cone can be predicted from an analysis of the Reciprocal Lattice.

In para D25 a Circle of Reflection was used in conjunction with a Reciprocal Lattice based on the h and k planes; a similar construction for the k and ℓ planes would require a circle centred at R but perpendicular to the paper and still rotated about P; for a fixed λ the radius of the circles, PR is constant and for reflections involving all three co-ordinates h, k and ℓ the Bragg equation must apply and hence the locus of Q $(h\ k\ \ell)$ is a sphere centred at R, of radius PR and rotated in the plane of the paper about P.

D26.1 On centimetre graph paper construct a Reciprocal Lattice to the scale a = b ≡ ½ cm, as in D25.3, up to h = k = 6.

On the k axis construct the Circle of Reflection for *LiF* (a = b = c = 0.403 nm) such that RP is 5.21 cm radius. The reason for using *LiF* and not *NaCl* is discussed at D26.9.

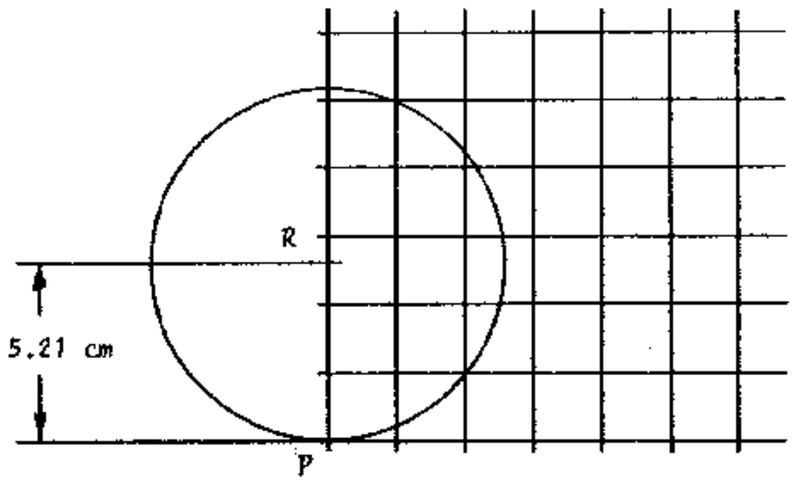

D26.2 On a second piece of centimetre graph paper construct an elevation view of the Sphere of Reflection to the same scale as in D26.1 and draw in lines representing the edge view of the h k lattice at ℓ = 1, =2, =3.

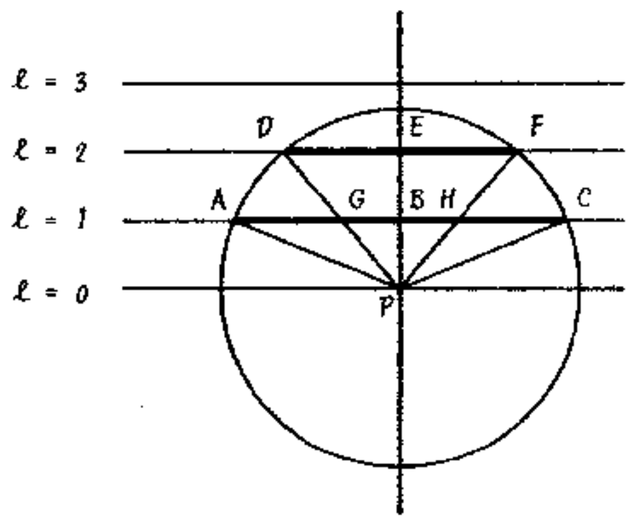

Observe that the Sphere does not intercept the (h k 3) lattice and therefore no reflections are possible for planes where ℓ = 3 or more for *LiF* and CuKα radiation.

The sphere intercepts the (h k ℓ) lattice at the circle AC and the cone of reflections APC can be constructed by joining AP and PC.

Similarly DPF is the cone for the (h k 2) reflections.

D26.3 To predict the discreet directions of possible reflections in these cones, the Sphere must be rotated about P in the plane of the paper of graph D26.1.

Measure the radius of the lattice/sphere intercepts AB and DE and draw equivalent circles on the graph D26.1 concentric with the (h k 0) circle of reflection already constructed.

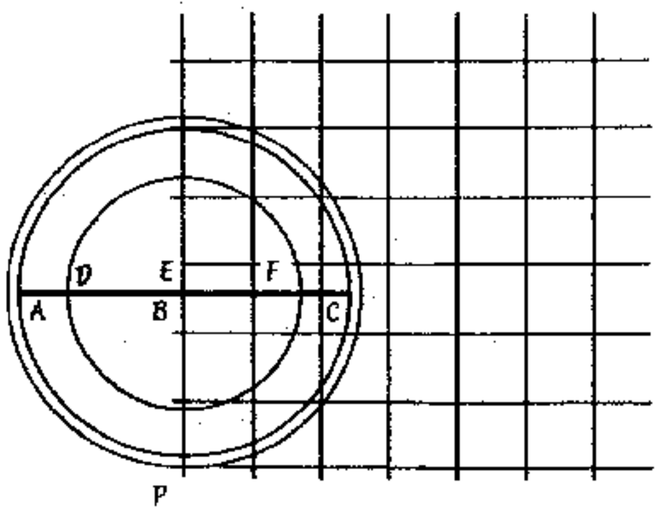

D26.4 Simulate rotation of the lattice by scribing arcs, centred at P, for all lattice points; these arcs should be drawn to intercept the three concentric circles.

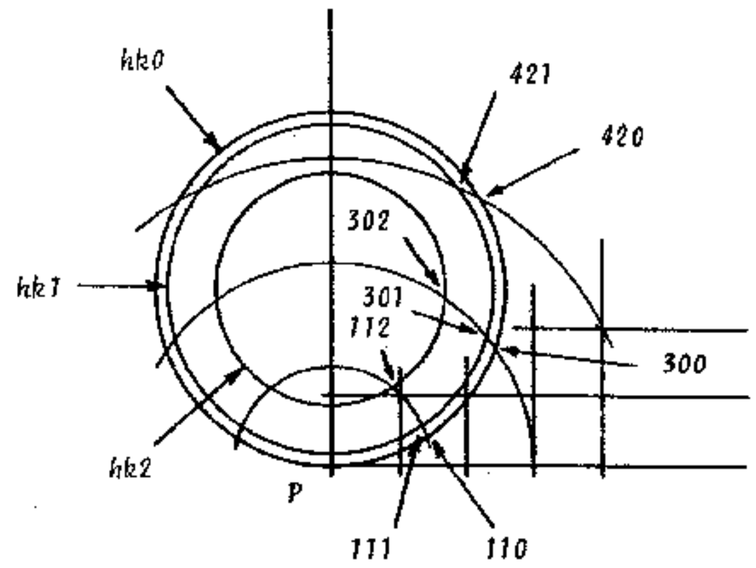

All these points of interception represent theoretically possible reflections.

Observe that there are 28 possible reflections on the circle for (h k 0), 26 on the circle for (h k 1) and only 22 on the circle for (h k 2). Reflections on the left hand side of the circles can be obtained by drawing arcs from lattice points where h is classically negative; half of the above reflections are thus for ($\bar{h}$ k ℓ) planes.

D26.5 If a flat film were placed above the crystal in the plane (001) i.e. at ABC in Diagram D26.2, the reflections in cone APC would lie on a circle of diameter AC; but reflections in the cone DPF would be recorded as a circle of diameter GH.

Measure the radius BG and construct an equivalent circle on the diagram of D26.4 concentric with the existing circles.

D26.6 Join the centrepoint to each of the 22 intercepts on the circle for (h k 2). Where these radials intercept the circle of diameter GH possible reflections will be recorded on the film.

D26.7 Draw small circles about 4mm in diameter at each of the 26 intercepts on the circle for (h k 1) and the 22 intercepts on the circle GH, the transferred intercepts on the circle for (h k 2).

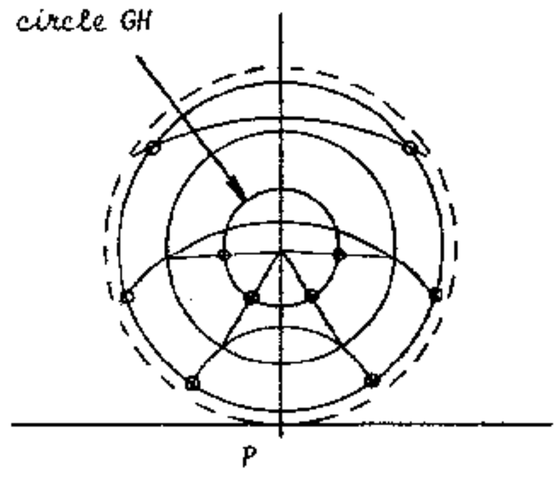

The constructed diagram now represents a large scale version of a theoretically possible photographic record on a flat film placed above (or below) a rotating crystal, in the 'c' direction and parallel to the 'ℓ' planes; the small 4mm circles will be filled in when reflections have been recorded.

To achieve this a small crystal must be 'bathed' by the incident beam; there is clearly a limit to the size of the crystal in order that reflections will not be completely absorbed within the crystal.

D26.8 In experiment D10.14 the Linear Absorption Co-efficient μ is defined by the equation

$$I = I_0 e^{-\mu t} .$$

As the thickness of the crystal increases the radiation transmitted is reduced in accordance with this equation; but at the same time the intensity of each diffracted beam increases as the volume of the crystal, thus as t^2 .

The intensity of the diffracted beam with the longest path is therefore proportional to

$$I_0 e^{-\mu t} t^2 .$$

The condition for this to be a maximum is that

$$t = 2/\mu .$$

In paragraph D16.11 the Linear Absorption Co-efficient was defined in terms of the Mass Absorption Co-efficient, μ_m as

$$\mu = \rho \mu_m$$

where ρ is the mass density of the material.

For a chemical compound

$$\mu = \rho \Sigma p \mu_m$$

where p is the proportion of each element present in the compound.

D26.9 To cleave and mount very minute crystals requires expensive apparatus and considerable skill; the *LiF* crystal is chosen for the Upper Layer Reflection experiment as having the smallest Mass Absorption Co-efficients and thus the least diminutive crystal.

Reference to Standard Tables reveals that for *LiF*, $\rho = 2.601 \times 10^3$ Kg per m^3 and μ_m for *Li* is 0.07 and for F is 1.64 m^2 per kg. for CuKα radiation.

The percentages can be deduced from the Atomic Weights.

Li , $p = 6.94/25.94 = 0.27$

F , $p = 19.00/25.94 = 0.73$

whence $\Sigma p \mu_m = (0.27 \times 0.07) + (0.73 \times 1.64)$

$= 1.22 \ m^2$ per kg.

$\mu = 2.601 \times 10^3 \times 1.22$

$= 3.18 \times 10^3 \ m^{-1}$

and $t = 0.63 \times 10^{-3}$ metres.

To perform an experiment to verify the theoretical reasoning an *LiF* Minicrystal, TEL 582.007, of dimensions of the order 0.6 x 0.6 x 8.0 mm is mounted in a Powder Camera.

D26.10 Withdraw the Sample Post from the top of the Powder Camera TEL 586.

Unscrew the chuck and using tweezers locate and lock in position a Mini Crystal of *LiF*, such that the crystal protrudes 4mm beyond the end of the chuck. Ensure that the crystal is co-axial with the chuck.

D26.11 Remove the lid from the Powder Camera and extract the metal backstop which is spring loaded into a recess in the lid.

Slide the backstop over the end of the primary beam collimator inside the camera such that the X-ray beam is reduced to 0.5mm in height by the cross-slot in the backstop.

D26.12 The film should be loaded into the Powder Camera in a DARK ROOM POSSESSING A SUITABLE SAFELIGHT (E.G. WRATTEN SERIES 6B).

The following items are required in the dark room:

Powder Camera and Lid.
Sample Post with crystal loaded.
Flat Film Envelope, TEL 586.002.
Filmpak, TEL 750/2.
Sharp pair of scissors.

D26.13 Cut off the flat end of the Filmpak and carefully withdraw the film; handle the film only by the edges and avoid creasing or scratching the surfaces (see Introduction to Radiography, page 39).

D26.14 Place the film in the Flat Film Envelope. Trim the film to the size of the Envelope.

D26.15 Locate the loaded Envelope in the bottom of the Powder Camera, under the primary beam collimator; the Envelope should lie flat with the withdrawal tag located in the recess in the wall of the camera opposite the collimator, narrow backing strip uppermost.

D26.16 Replace the lid, ensuring that the keyslot on the periphery of the lid correctly locates on the key protruding from the top of the body of the camera.

Verify that the lid is fully seated.

D26.17 Carefully place the Sample Post, loaded with the crystal into its bore in the lid and ensure that it is fully seated in its bearing.

Do not replace the Lid with the Sample Post in position as the piston action of pushing the lid down will propel the Sample Post out of its bore.

Transport the loaded camera out of the dark room to the Tel-X-Ometer; open the Tel-X-Ometer by sliding the Scatter Cover to the same side of the Instrument as the Power On Indicator Lamp.

D26.18 Locate the 1mm Diameter Collimator TEL 582.002 into the Basic Port as in Part I, para 10.2.

D26.19 Remove the Crystal Post and Jawclamp and rotate the Carriage Arm to $2\theta = 90^\circ$; it covers the kV selector switch which should be set at 30kV.

D26.20 Unlock the Clutch Plate and, keeping the Carriage Arm at $2\theta = 90^\circ$, rotate the Slave Plate until the flat on the central shaft is at right angles to the X-ray beam and facing away from the X-ray tube.

D26.21 Locate the Powder Camera between the Lead Glass Dome and the central shaft such that the U-shaped projection on the camera body is supported by the outer diameter of the Primary Beam Collimator and the underside of the camera rests on the Clutch Plate; the central shaft locates in a recess under the Powder Camera; the Camera should lie horizontal and be a good fit in this position.

D26.22 There is a screw in the shaft recess under the powder camera; adjustment of this screw will ensure that the camera is held lightly against the Primary Beam Collimator.

This screw should only need adjustment the first time the Camera is located; thereafter the camera will slip-fit into its self-aligning position.

D26.23 The Clutch Plate should be screwed down until the top of the central shaft just butts up against the

plastic of the camera; now screw-up the Clutch Plate by about half a turn to ensure that the outer skirt of the camera is resting on the Clutch Plate and thereby preventing the camera from rocking.

NOTE: If the Clutch Plate will not screw down sufficiently to achieve this, unscrew it completely, remove the cross-shaped spring and replace the Clutch.

When replaced, the centre-bore of the spring should locate on the bearing and the tips of the four arms should press on the underside of the Clutch Plate.

D26.24 The Motorised Drive Unit TEL 587 is used to rotate the crystal in the camera at about 6 revolutions per minute. Locate the 4mm plug on the base of the Drive Unit in socket B, situated close to $\theta = 45^{o}$ on the spectrometer table.

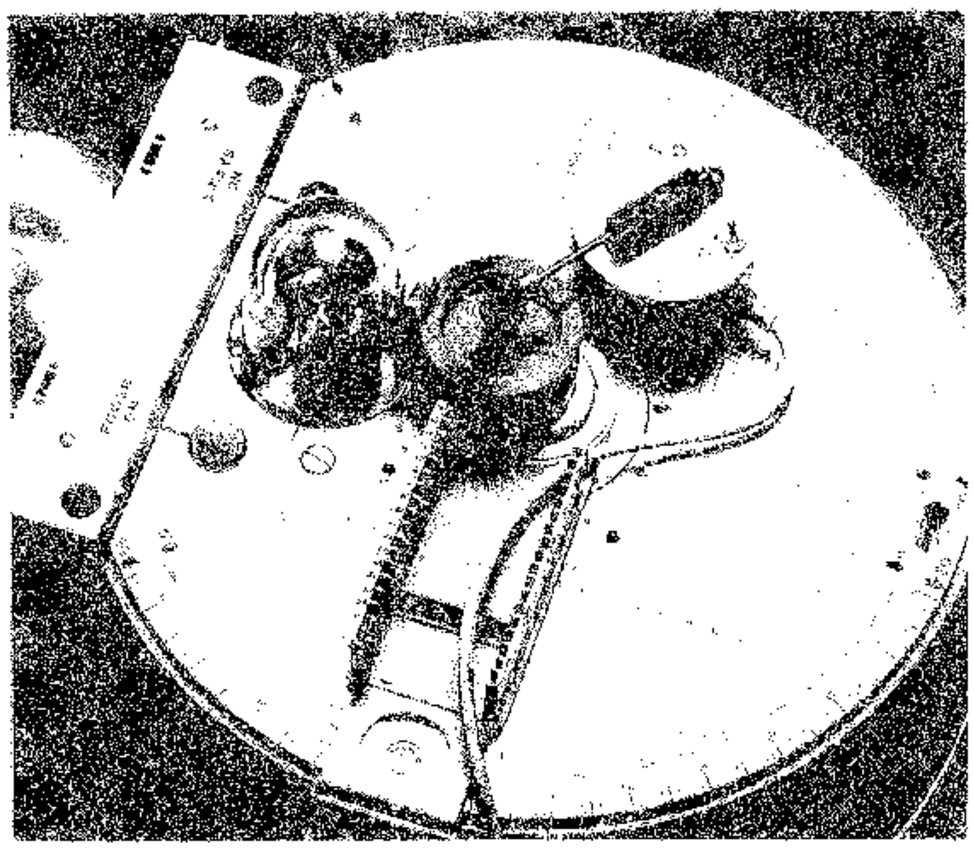

Turn the Drive Unit until the extension shaft points to the centre of the Sample Post in the Powder Camera; use the Allen Key affixed to the mains cable to adjust the position of the bevelled gear on the extension shaft to establish correct meshing of the gears.

It may be necessary to raise the Drive Unit slightly; the friction of the 4mm plug in the socket will suffice to maintain the raised position.

D26.25 Hold the Drive Unit in position and trail the mains cable down the Carriage Arm and outside the Scatter Shield; switch on the Drive Unit and ensure that the Sample Post is rotating.

D26.26 Close and centralise the Scatter Shield. Depress the X-rays On button (30kV already selected).

Adjust tube current to 80 μA.

D26.27 Set the Time Switch to maximum. EXPOSE FOR 4 HOURS.

NOTE 1: Meaningful results can be obtained in 3 hours but the {311} and more especially the {351} reflections will be very faint; however the {111} $\{\bar{1}11\}$, {h k 2} and {$\bar{h}$ k 2} reflections are sufficiently intense for further analysis.

NOTE 2: If it is required to filter out the CuKβ reflections (see para. D26.29) a thin piece of Nickel foil should be affixed, using adhesive tape, on the 1mm Diameter Primary Beam Collimator; exposures of about 6 hours are required.

D26.28 In the Dark Room, extract the Sample Post before removing the lid of the Powder Camera.

Take out the Envelope by means of the lifting tab.

Process and dry the film.

D26.29 There should be six intense elongated spots on an inner ring and six on the outer ring; each elongated spot is accompanied by a less intense Kβ reflection on the shorter wavelength side of the Kα reflections (i.e. on that side which is closest to the forward direction of the primary beam).

The direction of the primary beam can be ascertained from the shadow of the collimator system.

With a pin, pierce a hole through the film at the centre of each Kα elongated spot; ignore the Kβ reflections. Observe also the hyperbolae caused by the white radiation.

D26.30 Place the film in a Superslide TEL 585.007 and load into a Slide Projector having an 8.5cm, f 2.5 lens (e.g. Rank Aldis Tutor 500).

D26.31 Project the image onto the diagram constructed at D26.7 backed by a piece of stiff card and mounted in a retort stand (or similar).

Orient the diagram until the 12 bright spots each coincide with one of the small "predicted" locations; the diagram will be about 40 cms from the lens of the projector. Pencil in the small circles which are illuminated.

Establish by means of the diagram the co-ordinates (h k ℓ) for each of the reflections and tabulate these new results in the table D25.12.

Observe that, if zero is assumed to be an even number, only whenever h, k and ℓ are either all odd or all even does a reflection occur.

D26.32 The comparison between the geometrical construction and the experimental photographic image provides evidence that the crystal structure of LiF is of cubic form where a = b = c for the unit cell.

D26.33 To experimentally evaluate the size of the unit cell an estimate should be made, as precisely as possible, of the diameter of the (h k 1) and (h k 2) circles on the exposed film; these are the diameters 'ac' and 'df' in D26.2.

D26.34 Replace the Film Envelope in the Powder Camera, without the film inside it; as accurately as possible measure the height of the centre of the 0.5mm slot on the collimator from the surface of the Film Envelope.

This is the dimension 'bp' in D26.2.

D26.35 The semi-vertical angle, ϕ for each case is calculated from

$$\tan \phi_1 = \tfrac{1}{2}ac/bp \quad \text{and} \quad \tan \phi_2 = \tfrac{1}{2}df/bp$$

and 'c' is determined from the equations

$$\lambda = c \cos \phi_1 \quad \text{and} \quad 2\lambda = c \cos \phi_2$$

(LiF is cubic, face-centred, a = b = c = 0.403 nm).

The crystal has been rotated about a vertical axis perpendicular to the X-ray beam; the axis of rotation does not have to be vertical but it must be perpendicular to the beam.

If therefore the crystal were to be further rotated about the axis of the primary beam as well as about an axis perpendicular to the beam then the locus of each observed reflection would be a cone concentric with the X-ray beam.

The intersection of this cone and the Sphere of Reflection is a circle, co-axial with the X-ray beam and in a plane

perpendicular to it; viewed in plan, as in D26.7, the intersection is a straight line, the edgewise view of the circle, parallel to the 'h' axis of the diagram.

D26.36 Draw two lines, parallel to the 'h' axis, one through the (220) intercept and one through the (420) intercept. Observe that these lines pass through the real intercepts, on the theoretical circle DEF, of the reflections (202) and (402).

The reflections (220) and (202) thus lie on a cone co-axial with the X-ray beam and they are both referred to as (*h*,*k*,0) type reflections, as are the (420) and (402) reflections.

An apparatus to impose simultaneous rotations in these two directions would prove expensive; but by powdering a crystal of LiF a very large number of minute crystals could be presented to the beam and it is reasonable to expect that these crystals would randomly lie in the correct orientation to produce reflections from all possible planes; these reflections would lie on cones co-axial with the X-ray beam.

D27 – POWDER ANALYSIS (4 + 3½ + 4½ HOURS)

Remove Crystal Post and Jaw.

KIT 582+583	30 kV	80 µA	NORMAL LAB

If, on the Diagram of D26.7, a strip of film were wrapped around the equatorial plane of the Sphere of Reflection then part of all the co-axial cones of reflection from an irradiated powder source would impinge on the film.

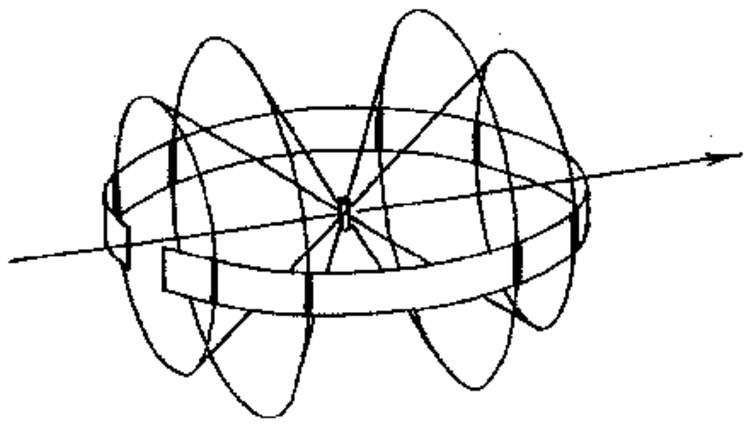

The success of powder analysis frequently depends on the manual expertise of the experimenter in preparing the sample for radiation and in correctly setting up the Powder Camera.

The Powder Camera 586 has been designed to provide automatic precision alignment once the Tel-X-Ometer has been correctly set (as for Bragg type experiments) and the camera adjusted as in para. D26.22.

Powder samples can be prepared in the conventional manner by making a paste of the powder to be analysed and gum. Roll the paste in the palm of the hand into a small bead about 4mm in diameter; select a Glass Fibre 567.004 and push this through the centre of the bead. Now roll the bead about the axis of the fibre until the paste "grows" along the fibre to a length of about 10mm and a diameter of not greater than 1mm. Trim the sample to be 15mm long with the glass fibre protruding 5mm from one end.

The preparation of such samples requires considerable dexterity and evidence of correct preparation is only available after a lengthy exposure in the camera; if the proportions of powder and gum are incorrect then not only is the student exasperated and disillusioned but valuable experimental time is wasted. Nevertheless, it is important that the student should learn to prepare his own samples for irradiation and therefore the ensuing relatively simple technique is recommended.

D27.1 Pierce the end of the tube of Acetate Cement 585.009 with a pin 1mm in diameter.

Mount a Sample Tube Wire 586.003 in the Sample Post of the Powder Camera such that 5mm of the wire is secured in the chuck.

Insert the wire nearly to its full length into the tube of Acetate Cement, rotate it once or twice and then extract it in one smooth movement. Allow the cement to dry very thoroughly, preferably in an oven or over a radiator.

When dry, remove the wire from the Sample Post, place one end in a vice and hold the other end with a pair of serrated jaw pliers; pull the wire along its length until it yields ; the acetate 'capillary tube' will be released from the copper wire.

Using sharp cutters, remove one 'spoiled' end of the wire; the capillary tube should suffice for three sample tubes each 15mm long.

Care should be exercised to ensure that the Sample Tube Wire is kept very straight throughout this preparation; allowing 30 minutes drying time the preparation will take 40 minutes.

Slide the Acetate Tube off the end of the wire until it projects by about 10mm.

D27.2 Place the *LiF* Powder, TEL 582.008, on a watch glass and lightly thrust the projecting capillary tube into the powder. Allow the tube to touch the watch glass itself as this action forces the powder up into the capillary.

Continue this tamping process until the projecting length of 10mm is filled with powder. Seal the open end of the tube by the application of a small amount of Acetate Cement, TEL 585.009.

When dry, lightly push the copper wire to pack the powder and, using sharp wire cutters, cut the tube/wire assembly to contain about 5mm of copper wire.

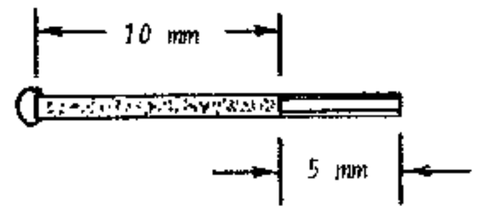

D27.3 Extract the Sample Post from the Powder Camera Lid and mount the *LiF* powder sample into the chuck; the end of the sample tube containing the copper wire should be inserted into the chuck thus ensuring that 10mm of *LiF* sample will be irradiated and none of the copper wire.

D27.4 Remove the Lid of the Powder Camera and establish that the metal backstop is mounted in the recess in the lid and is NOT acting as a beam limiter on the internal primary beam collimator.

D27.5 The film should be loaded into the Powder Camera in a DARK ROOM. The following items are required in the dark room:

Powder Camera and Lid.
Sample Post with Sample Loaded.
Filmpak, TEL 750/4.
Sharp pair of scissors.

D27.6 Cut off the end of the Filmpak across the two fixing holes at the 'injection' end and carefully withdraw the film; do not withdraw the film quickly as this can create electrostatic effects which mar the film.

D27.7 Insert the film around the inner periphery of the Powder Camera; the ends of the film should be on each side of the internal primary beam collimator. Ensure that the film is held against the wall of the Powder Camera by the two small posts which protrude from the floor of the camera near the internal collimator. These posts cast shadows on the film which provide identification of the top and bottom and of the left and right hand sides of the camera in the event that the processed film indicates some form of camera fault.

D27.8 Replace the lid and ensure that it is fully seated.

D27.9 Carefully place the Sample Post loaded with the *LiF* sample tube into its bore in the lid and ensure that it is fully seated in its bearing.

Transport the loaded camera out of the dark room to the Tel-X-Ometer and proceed as in D26.17 to D26.26 but use the 1mm Slot Collimator TEL 582.001 in the Basic Port instead of the 1mm Diameter Collimator; the 1mm slot should be vertical.

It is not necessary to use the Motorised Drive Unit TEL 587 but with it the quality of the photographic record is much improved (see D28.4).

D27.10 Expose for 3 hours.

D27.11 IN THE DARK ROOM, extract the Sample Post before removing the lid of the Powder Camera.

Take out, process and dry the strip of film.

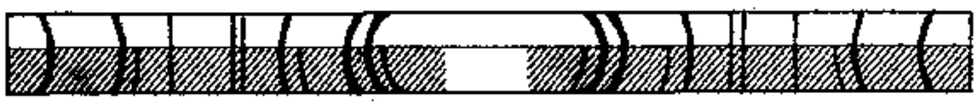

D27.12 The film reveals the familiar arcs typical of this technique, developed by Debye & Scherrer in 1916.

The top half of the film is less exposed than the lower half; this is due to the presence around the camera lid of a strip of Nickel foil which absorbs the Kβ radiation.

The Kβ arcs can thus be readily identified and ignored.

D27.13 Using internal calipers measure the diameter of the Powder Camera with and without the film in position. Calculate the Mean Diameter, D.

D27.14 Calibrate the Powder Camera:

$$\pi D \text{ mm} = 360 \text{ degrees.}$$

$$1 \text{ mm} = 360/\pi D$$

$$= K \text{ degrees.}$$

D27.15 The forward direction of the X-ray beam is apparent from the shadow of the backstop. The cones of reflection impinge on the film on each side of the X-ray beam where $2\theta = 0$; there are thus arc pairs, "lines", which represent identical reflections.

D27.16 Select the 5 or 6 strongest pairs of lines and measure the distance between them along the centre line of the film; ignore the weaker reflections and also the Kβ reflections.

A convenient way of measuring these distances, equivalent to the angle 4θ, is to pin-prick through the film onto a piece of white paper at each line and measure the distance between the corresponding pairs.

Tabulate the results and calculate $d/_n$ to three significant figures.

Line Pairs	4θ	θ	$\theta \times K$	$\sin\theta$	$d/n = \lambda/2 \sin\theta$
	mm	mm	θ^o		$\lambda/2 = 0.077$
A					
B					
C					
D					

D27.17 Neither d nor n is known, but from D25.12, n^2 must be an integer and the length of side of the unit cell as well as the co-ordinates of the reflecting planes can be extrapolated from the following table when completed to 4 significant figures.

Line Pairs	$\frac{d}{n}$	$\frac{d^2}{n^2}$	d^2							
			$\times n^2 =$ 2	3	4	5	6	8	9	10	etc to 20
A											
B											
C											
D											

It is not necessary to work laboriously through all the calculations, because an approximation of the common value for d^2 emerges after the first three or four lines are resolved; thereafter the use of a slide rule enables the nearest integer for n^2 to be rapidly selected and accurate calculations for d^2 can be worked out for this nearest integer only.

D27.18 From the equation $n^2 = h^2 + k^2 + \ell^2$ allocate Miller indices $(h\ k\ \ell)$ for all lines where d^2 is most nearly identical.

For the respective integers of n^2 calculate the mean value for d^2; since angular errors are greatest for small angles, it is recommended that d^2 for lines of smallest 2θ are ignored when calculating d.

Alternatively, since angular errors progressively decrease as the angle increases, plot θ against d^2 and extrapolate the intercept of the curve on the *y*-axis, where $\theta = 90^o$.

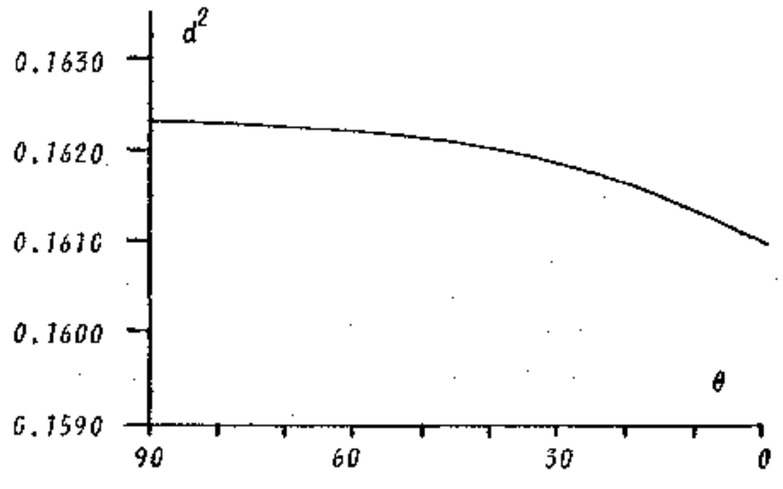

Observe that, as in the completed table of D25.12 the only reflections present are those where the indices are all odd or all even.

The size of the unit cell is

$$a = b = c = \sqrt{d^2} \text{ nm.}$$

Note that this technique gives an accuracy of better than 1%; for *LiF*, a = b = c = 0.403 nm.

D27.19 *This iterative technique illustrates the advantages of making use of computers in crystallographic analysis; the alternative method of plotting 'a' against 'd' for some 16 planes and indexing the film on the diagram does not lend itself to any great accuracy for a camera of such small geometry.*

D27.20 Repeat D27.1 to D27.18 but use *NaF* Powder (99.0%) TEL 585.001 in place of the *LiF* powder.

Expose for 3 hours.

D27.21 Observe that, as expected following D23.4 because *Na* has a higher Atomic Number than *Li*, the length of side of the Unit Cell for *NaF* (0.462 nm) is greater than that for *LiF*.

D27.22 Observe also the "extinction" of all reflections with odd indices, (111) (311) (331).

Careful observation of the LiF photograph will reveal that these reflections with odd indices are all weaker than the even indices.

The contacting sphere models from D22 could equally well serve for LiF (instead of NaCl) and NaF (instead of KCL) since the difference is merely a question of scale.

Examination of the models reveals that for the (111) reflection, waves from the Fluorine ions are in phase but the waves from Lithium ions oppose those of Fluorine ions, being mid-way between the Fluorine planes. Similarly for Sodium and Fluorine, but the effective population of electrons in the Lithium ion is only 2 whilst that of both Sodium and Fluorine is 10, one electron being 'shared' in the ionic bond.

LiF ..... Li^+ 3-1, F^-9 + 1
NaF ..... Na^+11-1, F^-9 + 1

The opposing waves from Lithium, having less electrons and thus less diffracting power than Fluorine, will only weaken the reflection from Fluorine ions. Sodium and Fluorine ions have equal diffracting power, hence the opposition of the waves from Sodium ions will extinguish the Fluorine reflection.

D27.23 This is strong evidence that the alkaline halide compounds are, as Bragg predicted, face-centred cubic systems; the metallic ions form, by themselves, a perfect face-centred lattice interlinking in absolute cubic symmetry with an equal number of halogen ions forming, by themselves too, an equally perfect face-centred lattice..

D27.24 Repeat D27.1 to D27.18 but use *SiC* powder, TEL 585.002, in place of the *LiF* powder (or *NaF* Powder).

In preparing the sample it will be noted that the *SiC* powder, being very dry, tends to fall out of the tube when using the tamping technique; If however the sample tube is pushed horizontally into the powder a few millimetres of the tube is filled; invert the tube and tap gently; the powder will progress to the copper wire. Repeat the process until about 10mm of the sample tube is filled and seal the end as in D27.2.

Expose for 4 hours; meaningful results can be obtained in 3 hours but the important (111) reflection will not be very intense.

D27.25 It is apparent from the results that *SiC* has a face-centred cubic lattice of Unit Cell length 0.438 nm but there are obvious anomalies.

D27.26 The reflections (200) (222) and (400) are absent (also the (331) but this is usually weak in any case); further inspection of the film reveals that in the region where the (400) and (331) reflections are expected there is a series of many more than two weak reflections.

There are also relatively strong reflections present, one close to the (111) line and one between the (422) and (511, 333) reflections.

Reviewing the total number of equivalent reflections for the (111) and the (200) planes it is reasonable to expect type (200), with 6 possible reflections, to reflect with only a marginal difference in intensity with respect to type (111), with 8 possible reflections, namely 111, 11$\bar{1}$, 1$\bar{1}$1, $\bar{1}$11, 1$\bar{1}\bar{1}$, $\bar{1}$1$\bar{1}$, $\bar{1}\bar{1}$1, and $\bar{1}\bar{1}\bar{1}$.

A difference in the anticipated intensity of reflections frequently provides a lead to the type of possible structure.

For cubic systems the theoretical number of equivalent reflections is:

Type of reflection	*h00*	*hh0*	*hk0*	*hhh*	*hhl*	*hkl*
Number of reflections	*6*	*12*	*24*	*8*	*24*	*48*

There is thus evidence that the holosymmetry observed for LiF and NaF is not present in the SiC lattice; also that some material is present which is not cubic and face-centred.

D27.27 *An iterative analysis of why (200), (222) and (400) reflections are absent can be found in standard text books in references to the structures of CuCl and ZnS; SiC is also of this type exhibiting the tetrahedral configuration, usually preferred by carbon bonds, wherein each Carbon atom is tetrahedrally surrounded by four Silicon atoms.*

D27.28 *Chemical analysis of the powder indicates that it is relatively pure so the only other possible explanation of the additional non-cubic reflections is that SiC can take up alternative lattice configurations or phases; reference to standard works reveals that this is true. The fourth phase is cubic but the other phases are all hexagonal.*

Judging by the relative strength of the reflections due to cubic lattice, there is a predominance of SiC (IV) in the powder sampled.

D27.29 *Powder photographs usually exhibit a general reduction in intensity with increasing angle 2θ (equivalent to decreasing planar spacing 'd') and this phenomenon is also observed in single crystal Bragg experiments.*

Some variation of intensity from one type of reflection to another is to be expected as a result of the different diffracting powers of atoms (the crystal structure amplitude) and of the possible number of equivalent reflections.

For a complete treatment of other factors affecting the intensity of reflections, high electron density for high order diffractions, thermal vibration and absorption, reference should be made to standard text books.

D27.30 *For single crystal Bragg experiments however the relative purity of the crystal has an effect on the intensity of reflections.*

To obtain diffraction of a parallel beam of X-rays, the Bragg equation must be satisfied exactly; if the crystal is perfect then the incident beam will be diffracted only when the angle is exactly $\sin^{-1}\lambda/2d$.

In practice, the collimated beam is not truly parallel but diverges slightly so that if a perfect crystal is irradiated, only a small proportion of the beam can satisfy the Bragg condition.

If, however, the surface layers of such a crystal are "dislocated" to create a mosaic of crystallites tilted slightly at random, then the proportion of rays that will satisfy the Bragg equation is significantly increased, resulting in enhanced intensity of reflection.

The four crystals used in this programme of instruction are especially groun, cleaved and dislocated for use with the Tel-X-Ometer; one major cleavage face is dislocated by an abrasion technique and can be recognised from the "flat matt" appearance of the face.

The crystals LiF and NaCl are particularly pure and exhibit a marked improvement in intensity of reflections from the dislocated surfaces compared to the opposite, as cleaved, face; to obtain crystals of KCl and RbCl of near perfection is very difficult and the REDUCTION of intensity of reflections from the dislocated faces indicates that the process has merely created even further imperfection.

An additional cause of lack of intensity using a near perfect crystal is "extinction" where the phase and angle of certain reflections contribute to annihilate a proportion of the incident beam, as distinct from the reflected beam; this effect is relatively small but it nevertheless is ameliorated by dislocating the surface layers.

In some humid climates the crystals may deliquesce profusely in spite of the presence of silica-gel in the phials; the crystals may be protected with a light coating of colourless nail varnish; care should be exercised to avoid dissolving the colour code by which the crystals are recognised. The varnish will also camouflage the matt appearance of the dislocated face which must be thereafter determined by intensity measurements.

D27.31 The *SiC* Debye-Scherrer photograph reveals that variations in the symmetry within a cubic lattice are possible although *LiF* and *NaF* both exhibit holosymmetry.

The experiments illustrate that within a face-centred cubic "space-lattice" different types of pattern-unit or "space group" exist which give rise to reflections, discreet both in direction and in intensity; an iterative analysis of these reflections leads to an understanding of the space-group, space-lattice and size of the unit cell for the material under investigation.

There are fourteen types of space lattice, the Bravais lattices; this programme of experiments is intended to familiarise the student with the basic principles of crystallography and so only the most simple systems are examined, the three cubic systems.

D28 — CRYSTAL SYSTEMS (3½ + 4 + 4 HOURS)

KIT 582+583	30 kV	80 μA	NORMAL LAB

The material under investigation does not have to be in powder form; the crystalline structure of a solid solution can be determined using the Debye-Scherrer technique.

D28.1 Repeat D27.1 to D27.18 but use Aluminium Wire (Purity 99.9%) TEL 585.005 as the sample, in place of *LiF*. Expose for 3 hours.

The results show that Aluminium, even in wire form, has a face-centred cubic structure of Unit Cell length 0.405 nm.

Observe that the high order (511) lines show evidence of doublet structure (see Para D19).

D28.2 In place of Aluminium, the Copper wire TEL 586.003 may be conveniently used, cut to a length of 15mm and similarly exposed for 3 hours; Copper has a face-centred cubic lattice of Unit Cell length 0.362 nm. Observe the blackening of the film towards the ends due to fluorescent scattering of the short wavelength white radiation, from the side of the copper sample facing the beam.

D28.3 Repeat D27.1 to D27.18 but use Niobium Wire (Purity 99.9%) TEL 585.003, as the sample in place of *LiF*.

Expose for 3½ hours.

The results show that Niobium has a Unit Cell of length 0.330 nm, but a study of the Miller indices reveals that, instead of being either all even or all odd, the planes which give rise to constructuve interference have

$h + k + \ell$ always EVEN

This typifies a body-centred cubic system.

D28.4 Repeat D27.1 to D27.18 but use Ammonium Chloride, NH_4Cl, TEL 585.004 as the sample in place of *LiF*.

NH_4Cl (99.5%) is very crystalline in powder form and does not respond to being finely divided by pestle and mortar; however it does readily sublime to a fine powder.

Mount a small diameter test tube, filled to about one third with cold water, inside a larger test tube (about twice the diameter) containing a few grammes of NH_4Cl; the water filled test tube should be about 20mm above the surface of the powder.

Gently apply heat from a blue flame in the area of the NH_4Cl.

The compound readily sublimes to condense on the water filled test tube; after a few minutes sufficient fine powder should be created to scrape onto a watch glass and the Sample Tube can be prepared as in D27.2.

Expose for 3½ hours.

The results show that NH_4Cl has a Unit Cell of length 0.388 nm, but a study of the indices reveals that ALL planes give rise to constructive interference.

This typifies a primitive or simple cubic system.

Note 1: The (100) smallest angle reflection can be observed, but it is very faint.

2: The cell is considered as being constructed of ammonium and chlorine ions.

The reason for recommending the sublimation process is that if the size of grain in the sample is too large, there are insufficient particles present for the specimen to possess random orientation; the resultant photograph appears 'spotty' and usually a longer exposure is necessary than for fine grain powders.

If a powder sample is stationary, the maximum grain size should not exceed 10 microns if 'spottiness' is to be avoided.

If a powder sample is rotated using the Motorised Drive Unit, the limit of particle size may be increased to 45 microns.

The presence of 'spottiness' on a photograph can also be useful in revealing the 'state' of the specimen.

D29 — MATERIAL STATE (4½ + 1 HOUR OR + 2½ HOURS)

KIT 582+583 + TEL 587	30 kV	80 µA	NORMAL LAB

D29.1 Prepare a mixture of Aluminium Powder 585.008 and Lithium Fluoride Powder 582.008 in equal volumes.

D29.2 Repeat D27.1 to D27.18 and expose in two parts, stationery for 2 hours followed by rotation for 2 hours using the Motorised Drive Unit, 587.

D29.3 A cursory analysis of the processed film reveals that lines can be attributed to each of the constituents of the mixture merely by distinguishing between "spotty lines" and "clean lines".

Make side by side comparisons using the photographic results of D27.11 and D28.1 to provide an "index" of identification for Al and LiF.

The "spottiness" of the reflections from the Aluminium Powder indicates that the grain size of the metal powder is much larger than that of the halogen compound.

This technique is frequently used to assist in "separating" groups of reflections prior to further analysis, especially in work involving the development and manufacture of metallic alloys and of ceramics.

Laue type patterns can be used to not only indicate the 'state' of granularity but also the 'state' of stress endured by a crystalline structure.

D029.4 Set up for the Laue photograph as in D12 but use a Polyethylene Monofilament 585.006 in place of the Mini-Crystal.

Ensure that the axis of the monofilament is vertical and that the monofilament is centralised over the 1mm diameter port.

Select 30kV, 80 µA.

Expose for 20 minutes, at E.S.2 or 1 hour at E.S.3 depending on time available.

D29.5 Remove the monofilament and manually stretch the central portion of the filament until it obtains a clearly 'drawn' form.

Replace the monofilament over the 1mm aperture with the drawn portion centralised over the port.

D29.6 Replace the exposed film with a fresh Filmpak 750/2.

Expose for 20 minutes or 1 hour as chosen for D29.4.

D29.7 Compare the photographs of the "amorphous" polyethylene (D29.4) with the "oriented" material (D29.6).

In the amorphous state the long molecular chain of polyethylene is coiled up like a spring and the X-ray diffraction pattern bears a resemblance to a flat-film Debye-Scherrer photograph resulting from random orientation.

But in the stressed state the molecular chain is drawn out and the diffraction pattern resembles that of a single crystal with reflections in the equatorial plane; when performed with greater precision this technique also reveals upper layer reflections. From such precision photographs it is often possible to estimate the unit cell dimensions, to construct a reciprocal lattice and deduce the crystalline properties of the stressed polymer chain.

The diffraction patterns revealed in these experiments and in those of the previous paragraphs are unique to the particular material being irradiated; it is this uniqueness that permits X-ray diffraction techniques to not only identify single crystals but also to determine the composition of mixtures.

D30 — MATERIAL COMPOSITIONS (7 HOURS)

KIT 582+583	30 kV	80 µA	NORMAL LAB

The unique nature of diffraction patterns has led to Debye-Scherrer type techniques being widely used for the identification and analysis of mixtures where the component parts exist as separate crystals. The identification of mixtures does not differ in principle from that of single substances, wherein the component parts of the mixture are identified by the spacing of the strongest lines and the composition by weight is estimated by measuring the intensity of those lines.

The technique is however not very sensitive and to detect even a 5% composition requires careful analysis of the effects of absorption and angular differences.

If it is of didactic importance, the student can perform identification and analysis experiments using the Tel-X-Ometer.

Mixtures of powders already used in the previous part of the programme will allow the student to refer to the single substance photographs and numerical calculations already achieved and thus simulate the Uppsala Photographic Index and the Powder Data Card Index published by the American Society for Testing Materials.

In order to obtain adequate line separation, mixtures of NH_4Cl with LiF and of MgO with NaF are recommended ; exposures of up to 6 hours are required for compositions in the ratio 2:1 by weight.

The experimental results illustrate the need for maximum line separation and thus the requirement to employ the longest possible wavelengths, large diameter cameras and small diameter specimens.

NOTE : The elements Fe , Cr and V , all cubic and body centred have not been recommended either in wire or powder form for this series of experiments ; these elements are highly excited by both CuKβ and CuKα radiation resulting in such a radical loss of Cu characteristic radiation that no significant structure information is revealed on photographs made during exposures of up to four hours.

The reason for recommending the sublimation process is that if the size of grain in the sample is too large, there are insufficient particles present for the specimen to possess random orientation; the resultant photograph appears 'spotty' and usually a longer exposure is necessary than for fine grain powders.

If a powder sample is stationary, the maximum grain size should not exceed 10 microns if 'spottiness' is to be avoided.

If a powder sample is rotated using the Motorised Drive Unit, the limit of particle size may be increased to 45 microns.

The presence of 'spottiness' on a photograph can also be useful in revealing the 'state' of the specimen.

D29 — MATERIAL STATE (4½ + 1 HOUR OR + 2½ HOURS)

KIT 582+583 + TEL 587	30 kV	80 µA	NORMAL LAB

D29.1 Prepare a mixture of Aluminium Powder 585.008 and Lithium Fluoride Powder 582.008 in equal volumes.

D29.2 Repeat D27.1 to D27.18 and expose in two parts, stationery for 2 hours followed by rotation for 2 hours using the Motorised Drive Unit, 587.

D29.3 A cursory analysis of the processed film reveals that lines can be attributed to each of the constituents of the mixture merely by distinguishing between "spotty lines" and "clean lines".

Make side by side comparisons using the photographic results of D27.11 and D28.1 to provide an "index" of identification for Al and LiF.

The "spottiness" of the reflections from the Aluminium Powder indicates that the grain size of the metal powder is much larger than that of the halogen compound.

This technique is frequently used to assist in "separating" groups of reflections prior to further analysis, especially in work involving the development and manufacture of metallic alloys and of ceramics.

Laue type patterns can be used to not only indicate the 'state' of granularity but also the 'state' of stress endured by a crystalline structure.

D029.4 Set up for the Laue photograph as in D12 but use a Polyethylene Monofilament 585.006 in place of the Mini-Crystal.

Ensure that the axis of the monofilament is vertical and that the monofilament is centralised over the 1mm diameter port.

Select 30kV, 80 µA.

Expose for 20 minutes, at E.S.2 or 1 hour at E.S.3 depending on time available.

D29.5 Remove the monofilament and manually stretch the central portion of the filament until it obtains a clearly 'drawn' form.

Replace the monofilament over the 1mm aperture with the drawn portion centralised over the port.

D29.6 Replace the exposed film with a fresh Filmpak 750/2.

Expose for 20 minutes or 1 hour as chosen for D29.4.

D29.7 Compare the photographs of the "amorphous" polyethylene (D29.4) with the "oriented" material (D29.6).

In the amorphous state the long molecular chain of polyethylene is coiled up like a spring and the X-ray diffraction pattern bears a resemblance to a flat-film Debye-Scherrer photograph resulting from random orientation.

But in the stressed state the molecular chain is drawn out and the diffraction pattern resembles that of a single crystal with reflections in the equatorial plane; when performed with greater precision this technique also reveals upper layer reflections. From such precision photographs it is often possible to estimate the unit cell dimensions, to construct a reciprocal lattice and deduce the crystalline properties of the stressed polymer chain.

The diffraction patterns revealed in these experiments and in those of the previous paragraphs are unique to the particular material being irradiated; it is this uniqueness that permits X-ray diffraction techniques to not only identify single crystals but also to determine the composition of mixtures.

D30 — MATERIAL COMPOSITIONS (7 HOURS)

KIT 582+583	30 kV	80 µA	NORMAL LAB

The unique nature of diffraction patterns has led to Debye-Scherrer type techniques being widely used for the identification and analysis of mixtures where the component parts exist as separate crystals. The identification of mixtures does not differ in principle from that of single substances, wherein the component parts of the mixture are identified by the spacing of the strongest lines and the composition by weight is estimated by measuring the intensity of those lines.

The technique is however not very sensitive and to detect even a 5% composition requires careful analysis of the effects of absorption and angular differences.

If it is of didactic importance, the student can perform identification and analysis experiments using the Tel-X-Ometer.

Mixtures of powders already used in the previous part of the programme will allow the student to refer to the single substance photographs and numerical calculations already achieved and thus simulate the Uppsala Photographic Index and the Powder Data Card Index published by the American Society for Testing Materials.

In order to obtain adequate line separation, mixtures of NH_4Cl with LiF and of MgO with NaF are recommended ; exposures of up to 6 hours are required for compositions in the ratio 2:1 by weight.

The experimental results illustrate the need for maximum line separation and thus the requirement to employ the longest possible wavelengths, large diameter cameras and small diameter specimens.

NOTE : The elements Fe , Cr and V , all cubic and body centred have not been recommended either in wire or powder form for this series of experiments ; these elements are highly excited by both CuKβ and CuKα radiation resulting in such a radical loss of Cu characteristic radiation that no significant structure information is revealed on photographs made during exposures of up to four hours.

scattered radiation is apparent in the Debye-Scherrer photograph of experiment D28.2, the exposure of which takes 3 hours at 30kV and 80 µA.

The blackening towards the ends of the film are tending to obliterate the black diffraction lines which are the very features which require detailed analysis.

It can be again deduced, from the Law of Reciprocity, that equivalent blackening would be present in a film exposed for only 8.64 seconds at 100mA and 30kV.

Scattered radiation is a hazard to adequate contrast in industrial and in medical diagnosis and both disciplines have developed masks, grills, screens and blocking media which, when suitably placed, minimise the effects of scattered radiation.

Crystallographers, however, can rarely use elimination techniques and, when measuring the intensity of reflections with densitometer instruments, the contribution due to scatter must be estimated from the surrounding film.

D32 — DEFINITION (45 MINUTES)

The Definition or sharpness of images depends to a very large extent on the size of the focal spot of the X-ray tube.

KIT 582+584	kV as specified	50 µA	NORMAL LAB

D32.1 Place the Pin-Hole 582.006 centrally in the Crystal Post adjusted such that the beam passes through the centre line both of the collimator and of the Carriage Arm (i.e. $\theta = 90^{\circ}$ and $2\theta = 0^{\circ}$).

D32.2 Load Film Cassette 562.013 with a Filmpak 750/2 and locate at E.S.21; note that E.S.21 is 16 cms from the focus, twice that of the collimator at 8 cms and the set-up thus represents a Pin-Hole Camera.

Select 30kV and 50 µA and expose for 1 minute.

Process the film.

Observe that the apparent focus is about 1mm in diameter; the actual focus at the anode is 1mm by 5mm, being the image of the filament, but the foreshortened view of this represents the apparent focus, which is seen at closer inspection to be a 1mm square with rounded corners.

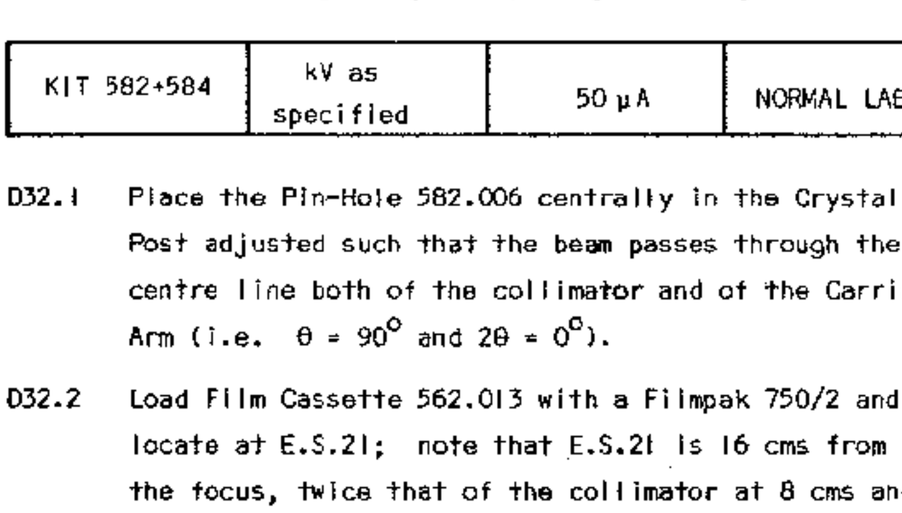

D32.3 Remove Collimator, Crystal Post and Jaw.

Place Cracks 584,004 at E.S.29 with a pin trapped in the surrounding slide as in D31.2.

D32.4 Locate Film Cassette 562.013 loaded with a Filmpak 750/2 at E.S.30.

Select 30kV and expose for 1 minute.

Process the film.

The slide comprises a thin piece of glass covered on both sides by paper adhesive tape; radial cracks have been induced by stressing the glass to yield at the centre.

The developed film reveals these cracks as dark lines on a lighter background; the X-rays have penetrated the paths of the cracks and are less absorbed than through the body of the glass.

D32.5 Select the quadrant with the greatest number of cracks and mark the paper covering the slide accordingly by referring to the datum pin; remove the pin.

Throughout all the following eight exposures rotate both the Cracks Slide and the Lead Mask such that the marked quadrant is always radiographed.

The ratio of the subject/focus distance to the subject/film distance is also an important factor influencing definition.

D32.6 Place the Lead Mask 584.006 at E.S.29 to expose the first quadrant.

D32.7 Locate the Cracks 584.004 at E.S.28 with the marked quadrant in the same angular mode as the Lead Mask.

D32.8 Locate Film Cassette 562.013 loaded with a Filmpak 750/2 at E.S.30.

Select 30kV, 50 µA.

Expose for 1 minute.

D32.9 Rotate the Lead Mask and Cracks to quadrant 2.

Select 20kV, 50 µA.

Expose for 1 minute.

D32.10 Rotate the Lead Mask and Cracks to quadrant 3, replace Cracks in the correct angular mode at E.S.21.

Select 30kV, 50 µA.

Expose for 1 minute.

D32.11 Rotate the Lead Mask and Cracks to quadrant 4, replace Cracks in the correct angular mode at E.S.14.

Select 30kV, 50 µA.

Expose for 1 minute.

Process the film.

Quadrant 2 reveals that 20 keV radiation is not sufficiently energetic to produce a radiograph.

Quadrants 1, 3 and 4 show that maximum definition is obtained when the subject/film distance is a minimum; the presence of penumbra is not obvious in these images but it is apparent that the larger the ratio between subject/focus and subject/film distances the smaller will be the penumbra and consequently the "geometric unsharpness" will be reduced.

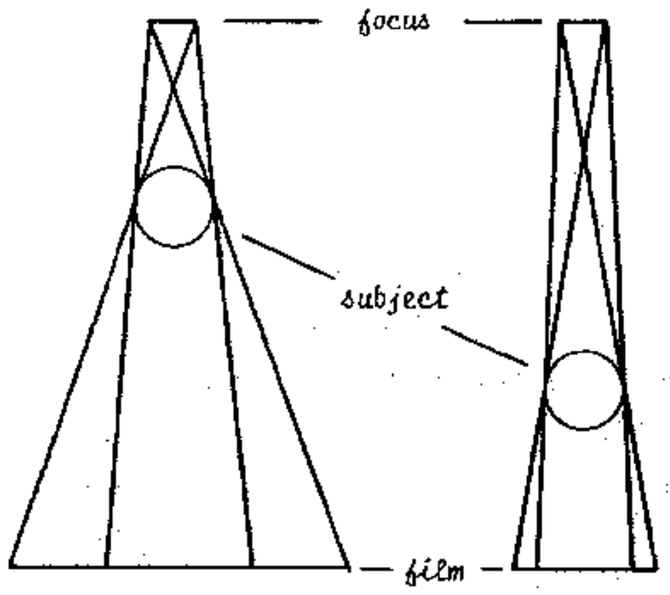

Magnification such as exhibited by quadrants 3 and 4 may be desirable and optimum conditions must be established for maximum definition; the greater the focus/film distance the longer the exposure (or the greater the intensity). Industrial radiographers can accept relatively large exposures but for medical applications this may result in further unsharpness due to 'blur' caused by the movement of the subject;

optimum conditions must again be based on the maximum tube current available and the Law of Reciprocity.

Sharpness can also be seriously effected by viewing angle.

D32.12 Rotate Cracks to the same angular mode as in D32.3 and locate it at an angle to the primary beam across E.S.28 and E.S.25.

D32.13 Locate Film Cassette 562.013 loaded with a Filmpak 750/2 at E.S.30.

Select 30kV, 50 µA.

Expose for 1 minute.

Process the film.

Compare the film with that of D32.4.

Observe that some cracks have been accentuated whereas others, although still apparent, have lost their sharp definition.

A technique used by industrial radiographers is to mount either the subject or the X-ray tube head such that it can be oriented relative to the other; by using the "fluoroscopy" method and electronic image intensification, any cracks located can be angled to give the sharpest definition. Such cracks often occur where there is a major change of section in a casting and the inspector may increase the voltage on the X-ray tube to provide greater penetration through the thicker sections, especially if the crack is a surface crack and has not propogated through the material. The inspector thus adjusts the 'sensitivity' of the investigation.

D33 – SENSITIVITY (2¾ HOURS)

Remove Crystal Post and Jaw.

KIT 582+584	kV as specified	50 µA	NORMAL LAB

When, on viewing a radiograph, no anomalies are evident, it cannot be inferred that no defects or inclusions are present; they may be there but the practical parameters may not be sufficiently sensitive for their detection. Information that any defects that are present cannot exceed a maximum thickness is a valuable guide to the efficiency of the radiographic technique.

D33.1 Remove the circular frame from a Film Cassette 562.013 and load a Filmpak 750/2.

Remove the keeper plate from magnets 562.008 and place a magnet on each side of the film cassette such that the magnet on the 'exposure' face is masking exactly one half of the filmpak.

Locate the assembly at E.S.30; the magnet should mask the left-hand vertical side of the filmpak, as viewed from the back of the cassette.

D33.2 Locate Lead Mask 582.006 at E.S.28 to expose the top right-hand quadrant of the film.

D33.3 Affix the two 0.1mm thick strips of aluminium to the flat back of the Aluminium Wedge 562.014, using adhesive tape, as illustrated.

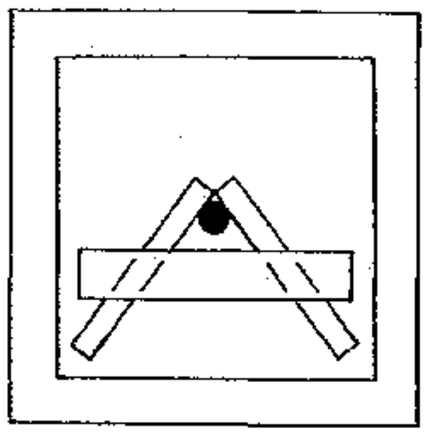

Locate the assembly at E.S.27 with the strips forming an inverted V; raise the slide about 5mm from the bottom of the slot of the carriage arm:

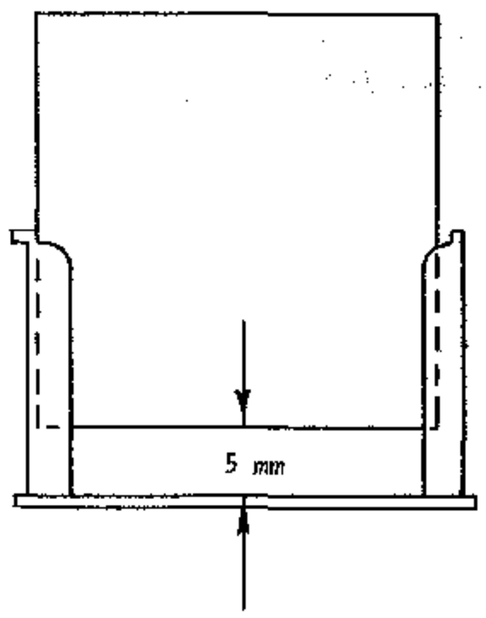

D33.4 Select 20kV.

Expose for 10 minutes.

D33.5 Remove the Lead Mask from E.S.28.

Expose for a further 10 minutes.

D33.6 Slide the Magnets across the cassette to now mask the already exposed right-hand side of the film.

Select 30kV.

Expose for 1½ minutes.

D33.7 Replace the Lead Mask at E.S.28 to expose only the top left-hand quadrant of the film.

Expose for a further 20 minutes.

Process the film.

A comparison of the quadrants reveals the importance of penetration (kV) and intensity (exposure time or tube current) in providing adequate 'contrast' to detect a 0.1mm difference in the various thicknesses of the Aluminium Wedge.

Observe that 20 keV radiation is not sufficiently energetic to penetrate more than the back plate and the first step of the wedge (Quadrant 1).

In quadrant 2 the 0.1mm strip is clearly discernible through the back plate but barely through the first step.

In quadrant 3 the strip is revealed through the first and second steps as well as the back plate.

The strip is visible through even the third step and just discernible in the fourth and thickest step.

D33.8 The steps and back plate are 0.75mm thick and the 'sensitivity' exhibited by the quadrants can be expressed as a percentage of the thickness penetrated.

$$Sensitivity = \frac{0.1\ mm\ (strip)}{Thickness\ of\ strip + wedge} \times 100$$

Quadrant	Thickness in mm				
	Back Plate	Step 1	Step 2	Step 3	Step 4
	0.85	1.60	2.35	3.10	3.85
1	-	-	-	-	-
2	12 %	6 %	-	-	-
3	12 %	6 %	4 %	-	-
4	-	-	4 %	3 %	2½ %

Observe, in quadrant 4, that during the longest exposure the image of the central hole is blurred due to scatter from the film itself with some contribution from the aluminium of the wedge.

The contrast at Step 4 in quadrant 4 is poor (similarly Step 1 in quadrant 2 and Step 2 in quadrant 3) and any further loss of 'definition' would cause the image of the strip to be indiscernible.

D33.9 Load the cassette with Filmpak and magnets as in D33.1.

D33.10 Locate the Lead Mask at E.S.28 to expose the top right-hand quadrant.

D33.11 Locate Aluminium Wedge (with strips) at E.S.20 in the normal manner and not raised by 5mm.

Select 30kV.

Expose for 10 minutes.

D33.12 Remove Lead Mask from E.S.28.

Expose for a further 10 minutes.

D33.13 Remove both Magnets - the film is now unmasked.

Expose for 20 minutes.

D33.14 Replace Lead Mask at E.S.28 to expose the top left-hand quadrant.

Expose for further 30 minutes.

Process the film.

Observe that even after 50 minutes exposure (Quadrant 4) it is very difficult to distinguish the end of the strip and in the third step discernibility is at its limit in quadrants 2 and 3.

The increase in film to object distance and the consequent loss of definition has thus reduced the sensitivity of the diagnosis from 2½% to 3 or even 4%.

The qualitative measurement of sensitivity is mainly practised by industrial radiographers using flat, step and wire type penetrameters or Image Quality Indicators (I.Q.I).

$$I.Q.I\ Sensitivity = \frac{dimension\ of\ thinnest\ step\ or\ wire}{thickness\ of\ specimen} \times 100$$

It is more difficult to employ similar indicators in medical diagnosis, where sensitivity is referred to as 'good', 'bad', 'better', 'worse', etc. when assessing the extent of Negative Diagnosis.

The employment, in the foregoing two experiments, of the progressive exposure technique has reduced the total exposure time for this section, 53 + 140 (193) to 43 + 70 (113) minutes.

D34 — RESOLUTION (45 MINUTES)

Remove Crystal Post and Jaw.

KIT 582+584	20 kV	50 µA	NORMAL LAB

Even when a defect has been detected, a knowledge of the 'resolution' of the radiographic process is necessary in order to estimate the real nature of the fault.

D34.1 Mount Porosity, 584.003, at E.S.27. Locate Film Cassette, 562.013, without the circular frame and loaded with a Filmpak 750/2, at E.S.28.

D34.2 Select 20kV, 50 µA.

Expose for 5 minutes.

Process the film.

The included iron filings are revealed as white dots and the trapped bubbles as dark dots.

D34.3 Remove Porosity, 584.003, to E.S.24. Place Lead Mask 584.006 at E.S.27 to expose one quadrant.

Reload a Filmpak 750/2.

D34.4 Select 20kV, 50 µA.

Expose for 5 minutes.

D34.5 Remove Porosity to E.S.21, E.S.17 and E.S.13 in turn and rotate the Lead Mask to expose successive quadrants alternatively.

Expose each quadrant for 5 minutes.

Process the film.

Observe the progressive loss of resolution; the inclusions become more fused as the object to film distance increases.

The resolution of a radiograph can be quantised by using special grids which enable the inspector to determine the number of 'lines' per millimetre which can be seen as discreet images.

STUDENT ENQUIRY

Faulty Weld, 584.005 is included as a practical test for the student; based on the programme D31 to D34 the student might measure the thickness of the subject and then

* assess the quality of radiation required (30 kV),
* estimate the tube current and exposure time to give the required intensity (125 µA min),
* determine the location of the defect (use pin datum) and
* estimate the size and nature of the defect (the method used to induce the fault in the otherwise high quality butt weld always produces inclusions and frequently some porosity but not with each and every fault).

RADIATION UNITS AND MEASUREMENTS, D35 TO D40 (3 HOURS)

Throughout the entire series of experiments, from D1 to D34 , the X-ray emission has been defined by its wavelength and intensity, the latter in effect being the power of X-rays to produce ionisation, whether in a photographic emulsion, a Geiger- Müller tube or an Ionisation Chamber; a similar state of affairs existed from the time of Professor Wilhelm Röntgen's discovery in 1895 until the First International Congress of Radiology was convened at Stockholm in 1928. Then, in honour of the Professor's work, the "power of X-rays to produce ionisation" was defined as the 'roentgen' and given the symbol R where

1 R ≡ 1 esu of ionic charge liberated per cm^3 of air at STP.

Since the CGS system is no longer generally preferred, the esu is replaced by the Coulomb, where 1 Coulomb = 3×10^9 esu and the volume of air at STP is defined by mass which for 1 cm^3 of air is 1.293×10^{-6} kg.

$$1\ R = \frac{1}{3 \times 10^9} \cdot \frac{1}{1.293 \times 10^{-6}} = 2.58 \times 10^{-4}\ C\ kg^{-1}.$$

In experimental programme D3 an Ionisation Chamber is used to detect the presence of ionising events in the enclosed volume of air; the results are recorded in terms of amperes, A and making use of the definition 'Coulombs per second', the above equation may be rewritten

$$1\ R\ sec^{-1} = 2.58 \times 10^{-4}\ A\ kg^{-1}.$$

This is the "exposure dose rate" and the term is applied only to electro-magnetic radiation; thus it is also used when measuring exposure to gamma radiation.

D35 -- EXPOSURE DOSE RATE (1 HOUR, OPTIONAL):

Ionization chamber, picoammmeter, and 5 KV power supply required
Remove Crystal Post and Jaw.

KIT 582+584 + TEL 588	kV and μA as specified	NORMAL LAB

D35.1 Remove the plastics window which incorporates the evacuation manifold from the Ionisation Chamber, 588 and measure the internal diameter, d and length, L of the chamber.

Calculate the enclosed volume of air, $\pi d^2 L/4$ cm^3.

Calculate the mass of this volume.

$$M = (\pi d^2 L/4) \times 1.293 \times 10^{-6}\ kg.$$

Specifically for an Ionisation Chamber of the volume of TEL 588 therefore the calibration factor, F is given by

$$1\ ampere \equiv \frac{1}{2.58 \times 10^{-4} \times M} \times 60\ R\ min^{-1}.$$

whence $F = 4.58 \times 10^9\ R\ min^{-1}$

and conversely

$$1\ R\ min^{-1} \equiv 21.85 \times 10^{-11}\ A,$$

but this is not an absolute equivalent since the air in the Ionisation Chamber is not at STP.

D35.2 Do not replace the evacuating plastics window but mount the Ionisation Chamber with the plastics flange supporting the anode at E.S.26 and the alternative plastics flange with the central hole supporting the front of the chamber at E.S.13.

Connect up the circuit as illustrated at para. D3 to a DC Amplifier with a facility to measure currents down to 10^{-12} amps and polarise the Ionisation Chamber using a power supply with a dc output variable to 500 volts.

D35.3 Set the polarising voltage V_p at 300 volts and select 20 kV.

Tabulate the collector current I_c for increments of X-ray tube current I_a, monitoring this by means of an external meter; complete the Table and plot the graph.

I_a x 10^{-6}	I_c x 10^{-11}	Dose rate $I_c \times F$
A	A	$R\ min^{-1}$
10		
20		
30		
40		
50		
60		
70		
80		

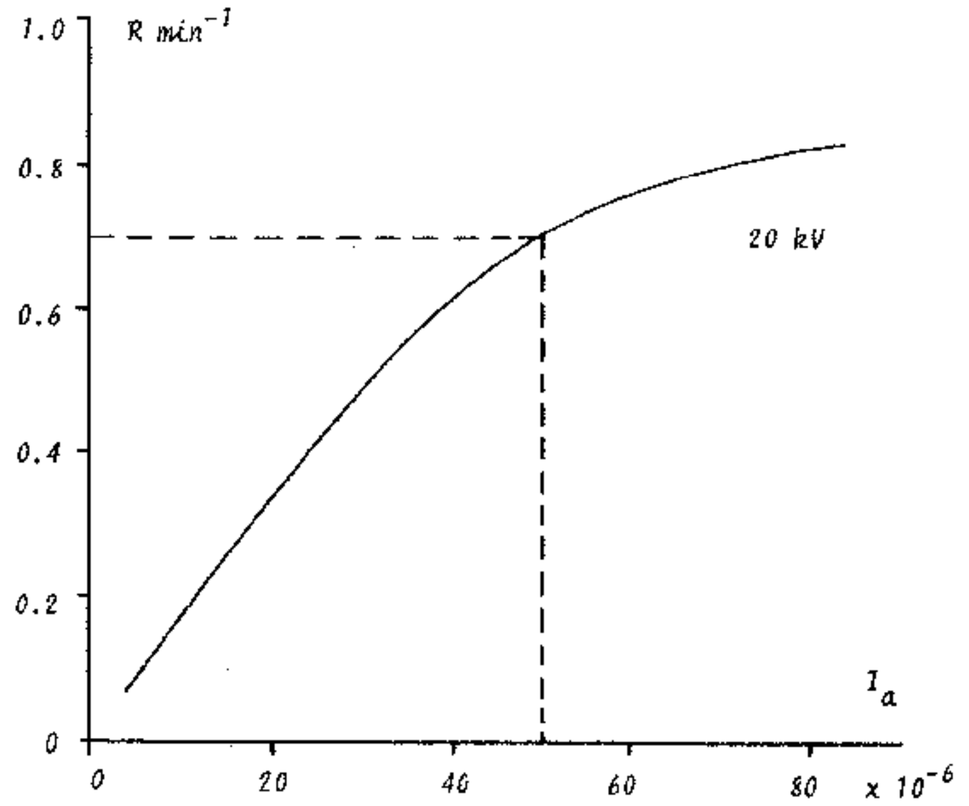

The non-linearity of the graph is due to the finite regulation of the high voltage supply; as the tube current is increased so the e.h.t. drifts slightly and consequently the radiation emitted will be marginally less energetic and thus more absorbed by the glass of the X-ray tube and by the air traversed.

The non-linearity is not so apparent with the harder radiation emitted for 30 kV anode voltage , see next paragraph..

The graph represents the dose rate at the mid-point of the Ionisation Chamber, some 15 cm from the X-ray source (about 0.7 $R\ min^{-1}$ at 50 μA tube current and 20 kV).

D35.4 In 1968 the International Commission on Radiological Protection adopted a report (ICRP Publication 13) which recommends that the exposure under maximum operating conditions does not exceed 0.5 *mR* in one hour at a distance of 5 cm from the shielding, measurements being averaged over an area of 10 cm^3 (about 3.6 cm diameter).

The X-ray beam impinges on the scatter shield about 25 cm from the anode; the theoretical exposure 5 cm beyond this and without the scatter shield can be calculated by applying the Inverse Square Law, see D8.

Select 30 kV and record the collector current, I_c at tube currents, I_a of 20, 40, 60 and 80 µA.

I_a	I_c	$I_c \times F$
$\times 10^{-6}$A	$\times 10^{-11}$A	$R\ min^{-1}$
20		
40		
60		
80		

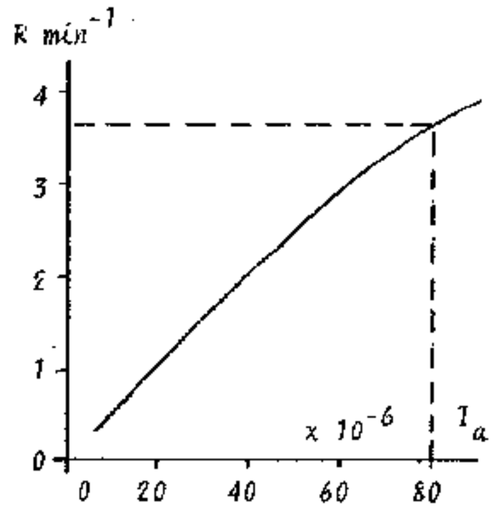

The theoretical exposure at 30 kV and 80 µA (maximum operating conditions) and 5 cm beyond the scatter shield thus is $R \times (15/30)^2$, typically 55 R in one hour and averaged over an area of $\pi d^2/4$ cm.

The radiation of the primary beam must therefore be severely attenuated.

D35.5 Rest the Shielding Plastic 562.029 in front of the open end of the Ionisation Chamber to attenuate the beam.

Select 30 kV, 80 µA.

Measure the collector current, I_c allowing time for the amplifier to stabilise; currents of the order of 1.5×10^{-12} A are typical.

D35.6 Calculate the reduced exposure and determine the percentage transmission, T relative to the dose rate at 80 µA recorded in D35.4 (typically 0.25 %).

D35.7 Estimate the reduced dose rate at 5 cm from the scatter shield as in D35.4.

This is in excess of 100 $mR\ hr^{-1}$ and so the plastics material of the scatter shield by itself does not provide adequate attenuation of the primary beam.

D35.8 Remove the Shielding Plastics and place the Lead (0.5mm) 562.028 in front of the open end of the Ionisation Chamber.

Observe that the collector current is reduced to zero.

The primary beam backstop affixed to the scatter shield comprises a sheet of lead, 1 mm thick sandwiched between the plastics material and the aluminium external plate ; the primary beam is thus totally absorbed by the backstop3.

D35.9 The Shielding Plastic has been shown to have attenuated the primary beam by some 55 $R\ hr^{-1}$. The photons not only ionise the plastics material but they also experience Compton and coherent scattering; the roentgen, by definition applies only to a mass of air and hence cannot be used for the plastics material.

There is therefore a need to express not only the ionisation effect but also the total energy extracted from the X-ray beam by a particular material.

D36 — RADIATION ABSORBED DOSE, THE *RAD*.

In 1953 the *rad* was introduced as strictly a measure of the absorbed dose in a specified material without reference to the type and energy of the radiation, not just X-rays.

1 *rad* = 100 ergs per gramme

and in contemporary units

1 *rad* = 10^{-2} Joules per kilogramme.

The average energy required to produce an ion pair in air is 34 eV or $34 \times 1.6 \times 10^{-19}$ Joules, since 1 eV = 1.6×10^{-19} J ; the radiation absorbed by the air in the Ionisation Chamber can therefore be readily calculated in terms of *rad* .

D36.1 If n is the number of ions resulting from an exposure of 1 R in air then

$$n = \frac{R}{e} \quad (= 2.58 \times 10^{-4} / 1.6 \times 10^{-19}\ )\ kg^{-1}.$$

The energy thus absorbed

$$E_{abs} = n \times 34 \times 1.6 \times 10^{-19}\ J\ kg^{-1}$$

or 0.877 *rad* per roentgen.

D36.2 The energy absorbed by a medium other than air is given by the equation

$$E_{abs} = \frac{\mu_m \text{ medium}}{\mu_m \text{ air}} \times 0.877\ rad\ R^{-1}$$

where μ_m is the mass energy absorption co-efficient.

This ratio is dependent on the wavelength where X-rays are concerned and also on the atomic number Z of the medium.

However the *rad* was primarily introduced as a practical unit for radiation protection and for soft tissue the relationship is reasonably constant at 0.98 *rad* R^{-1}.

This is very nearly 1 *rad* and for most practical purposes relating to biological protection a measure of exposure in air expressed in roentgens can be taken as giving the absorbed dose in soft tissue in *rad*.

For materials other than soft tissue the energy absorbed cannot be taken as the roentgen air equivalent due to the often very marked difference in the mechanism of the absorption process.

The absorption properties of elements of similar atomic numbers and hence electron densities reveal substantial differences for 'qualities' of radiation even as similar as CuKβ and CuKα.

D37 — THE QUALITY FACTOR, *QF* (50 MINUTES, OPTIONAL):

Ionization Chamber, picoammeter, and 5 KV power supply required

K T 582	30 kV	80 µA	NORMAL LAB

The main characteristic radiations of Copper can be segregated from the 'white' radiation using the diffraction properties of a crystal, see para. D14.

D37.1 Mount an *LiF* crystal, 563.005 in the crystal post with the matt face of the crystal in the primary beam.

D37.2 Zero set the Carriage Arm and Slave Plate as precisely as possible.

D37.3 With the Ionisation Chamber located between E.S.13 and E.S.26, rotate the carriage arm to $2\theta = 45^\circ$.

D37.4 Connect the Ionisation Chamber to the amplifier circuit and polarise to 300 volts.

D37.5 Select 30 kV, 80 µA.

Observe that the current in the chamber is about 10^{-12} A and with further attenuation accurate measurements would require the use of an expensive DC Amplifier.

There is clearly a need for improved detection sensitivity.

If it is intended to continue with experiments using different pressures or gases then it is recommended that the evacuating plastics window flange be mounted, the percentage transmission determined and the calibration curve of D35.4 corrected accordingly.

For the purposes of this programme a G. M. Tube is used for improved sensitivity, see D5.

D37.6 Switch off the polarising supply to the Ionisation Chamber and remove the chamber from the Carriage Arm.

D37.7 Mount G.M. Tube 546 with the Tube Holder 547 located at E.S.22 and connect to a Ratemeter capable of integrating up to 5000 counts per second.

D37.8 Locate Collimator 562.015 at E.S.13 with the 1 mm slot vertical to discriminate for the CuKα radiation at $2\theta = 45^{\circ}$.

Select 30 kV, 80 μA.

Record the count rate, I_o in the collimated beam of CuKα radiation.

D37.9 Rotate the Carriage Arm to $2\theta = 40\frac{1}{2}^{\circ}$ to intercept the CuKβ radiation and likewise record the count rate.

D37.10 Locate in turn the filters of *Zn, Cu, Ni* and *Co* at E.S.14 and tabulate the results.

	Transmission			
	CuKβ		*CuKα*	
	cps	I/I_o %	*cps*	I/I_o %
I_o		—		—
I Zn				
I Cu				
I Ni				
I Co				

The presence of the absorption edges of *Ni* and *Co* introduce abrupt differences in the progressive increase or decrease in transmission with atomic number, see paras D16, D17 and D18.

Relative to biological exposure only these 'quality' effects are not very prominent for X- and gamma radiation but they are very different for the absorption of particle radiation.

D37.11 In making health physics measurements a Quality Factor *QF* is introduced in order to assess the biological effect of different radiations.

Radiation	*QF*
X- and gamma rays	*1*
Electrons (and beta radiation)	*1*
Thermal neutrons	*3*
Fast neutrons	*10*
Protons	*10*
Alpha radiation	*10*
Heavy ions	*20*

For equal doses of alpha and X-radiation, the alpha particles cause 10 times more damage per *rad* to biological tissue and in 1955 the term Relative Biological Effectiveness, **RBE** was introduced. this term relates the absorbed dose of defined X- and gamma radiation to that of other radiation producing identical biological damage and since 1962 the **RBE** has been generally confined to radiobiology and furthermore the conditions of measurement must be precisely recorded.

The term **QF** is currently preferred for the analysis of radiation protection; both the **RBE** and **QF** depend on the Linear Energy Transfer, **LET** of a particle in traversing a medium and this effect is already taken into account in the Table.

Different radiations may be present at any one time, for example, outside the shielding of a cyclotron and it is necessary to equate the effects of the various exposures.

D38 — RADIATION EQUIVALENT MAN, THE *REM* (50 MINUTES)

KIT 582	kV and μA as specified	NORMAL LAB

The dose equivalent can be defined as the probability of the development of a particular biological effect; in *rem* it represents the absorbed dose, in *rad* multiplied by all appropriate factors such as QF.

D38.1 Calculate the dose equivalent of the following combined radiations detected in the vicinity of a cyclotron.

Radiation	*Dose rate*	*QF*	*m rem* hr^{-1}
Gamma-rays	*0.5 mR* hr^{-1}		
Thermal neutrons	*0.2 mrad* hr^{-1}		
Fast neutrons	*0.1 mrad* hr^{-1}		
Total monitored dose rate	*0.8 mrad* hr^{-1}	*Total dose equivalent*	

For X-rays and relevant only to health physics measurements

$$1\ R \equiv 1\ rad \equiv 1\ rem$$

The maximum intensity outside the primary beam of the Tel-X-Ometer is associated with CuKα radiation; in order to estimate the dose equivalent beyond the scatter shield the G.M. Tube must be calibrated.

D38.2 With the Carriage Arm in the primary beam, mount the G.M. Tube and Holder assembly at E.S.22; the mid-point of the G.M. Tube is 15 cms from the anode of the X-ray tube, as was the Ionisation Chamber.

Ensure that the crystal jaw and post are removed.

The G.M. Tube will saturate when exposed to the full beam and severe attenuation is required, see D4.

D38.3 Locate Collimator 562.015 at E.S.13 with the 1mm slot vertical.

Locate Collimator 562.016 at E.S.14 with the 3mm slot horizontal.

The primary beam is thus reduced to a rectangle 0.1 x 0.3 cm at the end window of the tube.

Select 20kV.

D38.4 Ensure that the G.M. Tube is correctly polarised, see D.4 and tabulate the count rate I_g for increments of X-ray tube current I_a monitoring this by means of an external meter.

D38.5 The dose rate has been reduced from that of D35.3 by the crossed collimators.

Calculate the collimator factor, f.

$$f = \frac{\text{Area of collimated beam}}{\text{Area of Ionisation Chamber}}$$

Complete the Table and plot the graph.

I_a	*Dose rate from D35.3*	x f	I_g
x 10^{-6}A	*R min^{-1}*	*mR min^{-1}*	cps
10			
20			
30			
40			
50			
60			
70			

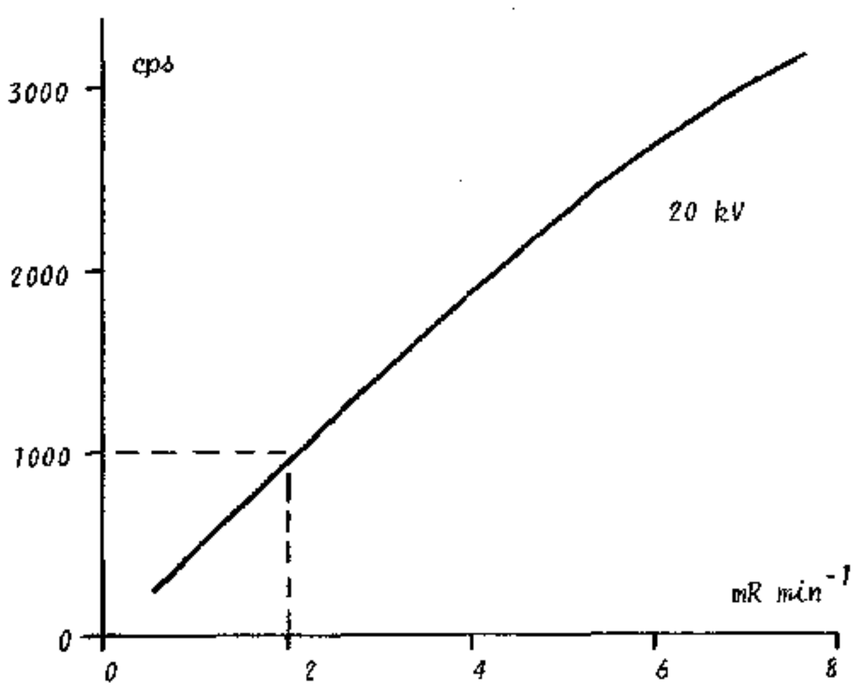

D38.6 Remove the collimators and replace the LiF crystal in the crystal post.

Rotate the Carriage Arm to $2\theta = 45^{\circ}$.

Select 30kV and close the Scatter Shield.

Mount the G.M. Tube and Holder outside the Scatter Shield using a retort stand or similar device at a height and direction to intercept the CuKα radiation; the mid-point of the G.M. Tube should be 5 cm from the surface of the plastic.

Select 80 µA and, using a Scaler, record the total number of counts over 100 seconds; 3 cps is typical and therefore a ratemeter is not suitable.

Such a count rate is too small to read the exposure on the graph of D38.5. However, the graph is nearly linear up to 2000 cps and the exposure can be deduced from the equivalent exposure at 1000 cps.

Adequate safeguard against excessive exposure can be obtained, as in the case of the Tel-X-Ometer, by both working at a large enough distance from the source and by using shielding materials.

But most instruments used to monitor the exposure in a working area sample only a narrow portion of the radiation and when estimating working times or shielding parameters an account must be made of the area of the primary beam.

D39 – BUILD UP FACTOR (20 MINUTES)

KIT 582+584	30 kV	50 µA	NORMAL LAB

In standard works of reference the shielding efficiency of a range of constructional materials is given in terms of "narrow beam" or "broad beam" conditions.

D39.1 Locate the G.M. Tube and Holder at E.S.22.

Mount the Collimator 562.015 at E.S.13 with the 1mm slot vertical and Collimator 562.016 at E.S.14 with the 3mm slot horizontal.

Select 30kV, 50 µA.

Record the count rate.

D39.2 Insert Collimator, 1mm tubular, 582.002 into the Basic Port.

Record the count rate and calculate the percentage reduction of the exposure.

D39.3 Clamp one edge of the Shielding Plastic 562.029 on the crystal post and rotate the slave plate until the shielding plastic intercepts the primary beam at right angles to the beam axis.

Record the counts over a period of 10 seconds using a scaler.

D39.4 Withdraw the collimator from the Basic Port.

Record the counts over a period of 10 seconds using a scaler and calculate the percentage reduction of exposure.

Compare with D39.2.

The build-up of radiation monitored in the broad-beam (typically 20%) is due to the collection of radiation scattered by the absorber; the methods of calculation of build-up factors are complex and it is usually sufficient to refer to published tables and charts.

It is nevertheless standard practice, whenever possible, to perform an experimental measurement of dose rate at the shielded position and then review this in terms of the geometrical relationships of the source, any shielding and the detector.

VERY IMPORTANT NOTE:

IT SHOULD BE NOTED THAT THE CALIBRATION OF THE G.M. TUBE IN THIS PROGRAMME IS NOT ABSOLUTE AS IT IS RELATED TO A VERY SIMPLE IONISATION CHAMBER WHICH HAS BEEN DESIGNED FOR DIDACTIC PURPOSES ONLY; FURTHERMORE, THE APPROXIMATE CALIBRATION IS VALID ONLY FOR THE PARTICULAR G.M. TUBE, SINCE THEY VARY QUITE CONSIDERABLY AND, DUE TO THE PREVAILING GEOMETRICAL CONDITIONS, IT IS ONLY VALID FOR TEL-X-OMETER MEASUREMENTS.

THIS CALIBRATION SHOULD NEVER BE USED FOR EXPERIMENTAL WORK WITH OTHER X-RAY UNITS OR FOR α , β AND γ RADIATION MEASUREMENTS.

D40 — INTRODUCTION OF S.I. UNITS

Most of the definitions given in this instructional programme are still commonly quoted although the International Commission on Radiological Units and Measurements (I.C.R.U.) issued Report No. 19 in July 1971 recommending that the following definitions be adopted in or by 1978.

D40.1 Exposure, — X.

The roentgen, R is accepted as a special unit of exposure, X.

$$X = \frac{dQ}{dm}$$

where dQ is the absolute value of the total charge of the ions of one sign produced in air when all the electrons (negatrons and positrons) liberated by photons in a volume element of air whose mass is dm are completely stopped in air.

The word 'dose' is deliberately omitted and retained only for the term absorbed dose.

D40.2 Exposure rate, — $\dot{X}$.

The quotient of roentgen by a suitable unit of time ($R\ min^{-1}$, $mR\ hr^{-1}$ etc.) is accepted as a special unit of exposure rate, $\dot{X}$.

$$\dot{X} = \frac{dX}{dt}$$

where dX is the increment of exposure in the time interval dt .

D40.3 Absorbed dose, — D.

The *rad* is accepted as a special unit of absorbed dose, D.

$$D = \frac{d\bar{\varepsilon}}{dm}$$

where $d\bar{\varepsilon}$ is the mean energy imparted by ionising radiation to the matter in a volume element and dm is the mass of the matter in that volume element.

As with exposure and exposure rate so

$$\dot{D} = \frac{dD}{dt}$$

where $\dot{D}$ is the Absorbed Dose Rate.

where D is the Absorbed Dose Rate.

D40.4 Quality Factor, — Q.

The symbol Q is preferred to the former QF; for X-rays this factor is 1.

D40.5 Dose equivalent, — H.

The *rem* is accepted as a special unit of dose equivalent, H.

$$H = D \times Q \times N$$

where N is the product of any other modifying factors such as those allowing for distribution of absorbed dose in space and time. This factor is currently assigned a value of 1 for external sources such as the Tel-X-Ometer.

D40.6 Maximum permissible level, — MPL.

For radiation protection relative only to X-rays and to soft tissue

$$X = D = H .$$

ICRP Publication 13, 1968 recommends the following maximum permissible levels per year for school exposure:;

Gonads and red bone marrow	*50 mrem*
Skin, bone and thyroid	*300 mrem*
Thyroid for children under 16	*150 mrem*
Leg and arm extremities	*750 mrem*
Other single organs	*150 mrem*

Adherence to these *MPL* figures will "prevent or minimise somatic injuries and minimise the deterioration of the genetic constitution of the population".

The duration of the entire programme D1 to D39 is about 75 hours, including some 42 hours film exposure time. Presuming therefore that the student will be working in close proximity to the Tel-X-Ometer, even during film exposures and thus be exposed to a maximum exposure rate of 0.5 *mR* per hour, the total absorbed dose will not exceed 38 *mrem*.

EXPERIMENT NUMBER	DESCRIPTION OF EXPERIMENT		STUDENT ATTENDED TIME	UNATTENDED EXPOSURE TIME	RECOMMENDED ACCESSORIES												
					KIT	KIT	KIT	MOTOR DRIVE	ION. CHAMBER	G.M. TUBE AND HOLDER		SCALER	RATEMETER	DC AMPLIFIER	KV UNIT	FILMPAK	
			HR MIN	HR MIN	582	583	584	587	588	546	547	806	807	808	813	750/2	750/4
DETECTION (2 Hours)																	
D1	The Röntgen Observation		- 15	-	x		x										
D2	The Spark Gap		- 10	-	x										x		
D3	The Ionisation Chamber		1 , 0	-					x					x	x		
D4	The Geiger-Müller Tube		- 20	-						x	x		x				
D5	Photographic Detection		- 15	-	x											2	
D6	The Photographic Process		- 5	-	x		x									1	
PROPERTIES (2 Hours)																	
D7	Rectilinear Propogation		- 10	-	x											1	
D8	Inverse Square Law		- 15	-	x											1	
D9	Deflection Effects		- 15	-	x		x								x		
D10	Penetration and Absorption		- 45	-	x		x			x	x		x			1	
D11	The Phantom		- 40	-	x		x									3	
ELECTROMAGNETIC RADIATION AND THE QUANTUM THEORY (10 Hours)																	
D12	Diffraction of X-rays, Laue		- 15	1 , 0	x											1	
D13	Wavelength by Diffraction Grating		-	-													
D14	Wavelength measurement, Bragg		1 , 30	-	x					x	x		x				
D15	X-ray emission		1 , 15	-	x					x	x	x					
D16	X-ray absorption		1 , 0	-	x					x	x	x					
D17	X-ray scattering		- 50	-	x					x	x	x					
D18	Moseley's Law		- 30	-	x	x				x	x	x					
D19	Fine Structure		1 , 0	3 , 0	x	x										1	
CRYSTALLOGRAPHY (45 Hours)																	
D22	Atomic Size		- 20	-	x	x				x	x		x				
D23	Unit Cell, one dimension		-	-													
D24	Co-ordinates		- 30	-		x											
D25	Unit Cell, two dimensions		- 40	-	x	x				x	x		x				
D26	Unit Cell, third dimension		2 , 0	4 , 0	x	x		x								1	
D27	Powder Analysis		2 , 0	10 , 0	x	x		(x)									3
D28	Crystal Systems		1 , 30	10 , 0	x	x		(x)									3
D29	Material State		1 , 0	6 , 0	x	x		x								2	1
D30	Material Compositions		1 , 0	6 , 0	x	x		(x)									1
RADIOGRAPHY (4 Hours)																	
D31	Contrast		- 30	-	x		x									1	
D32	Definition		- 45	-	x		x									4	
D33	Sensitivity		2 , 15	-	x		x									2	
D34	Resolution		- 45	-	x		x									2	
RADIATION UNITS AND MEASUREMENTS (3 Hours)																	
D35	Exposure Dose Rate		1 , 0	-	x		x		x					x	x		
D36	The *RAD*		-	-													
D37	Quality Factor, QF		- 50	-	x				x	x	x		x	x	x		
D38	The *REM*		- 50	-	x					x	x		x				
D39	Build up factor		- 20	-	x		x			x	x	x	x				
D40	S. I. Units		-	-													

APPENDIX B TEL-X-OMETER ACCESSORIES

CATALOGUE NUMBER	DESCRIPTION		KIT 582	KIT 583	KIT 584	INTRODUCED SEPT. 1974
562.007	Maltese Cross				x	
008	Magnetic Field				x	
009	Plain Electrode (2)		x			
012	Phantom				x	
013	Film Cassette, no backstop		x			
014	Aluminium Wedge				x	
015	Collimator, 1mm slot		x			
016	Collimator, 3mm slot		x			
017	Aluminium, 0.1mm				x	
018	Aluminium, 0.25mm				x	
019	Aluminium, 0.50mm				x	
020	Aluminium, 1.0mm				x	
021	Aluminium, 2.0mm				x	
028	Lead, 0.5mm				x	
029	Shielding Plastic				x	
031	Film Cassette, with backstop		x			
033	Blank Slide		x			
563.005	Crystal, *LiF*		x			
564.001	Rotary Radiator & Actuator		x			
002	Filter, *Fe*			x		
003	Filter, *V*			x		
004	Filter, *Ni*		x			
005	Filter, *Mn*			x		
006	Filter, *Cu*		x			
007	Filter, *Cr*			x		
008	Filter, *Co*		x			
009	Filter, *Zn*		x			
567.004	Glass Fibres		x			
005	Powder, *Mgo*			x		
008	Spindle Clips (5)		x			
582.001	Collimator, 1mm slot		x			
002	Collimator, 1mm tubular		x			
003	Luminescent Screen		x			
004	Crystal, *NaCl*		x			
005	Auxiliary Slide Carriage		x			
006	Pin Hole				x	+
007	Mini-Crystal, *LiF* (2)		x			+
008	Powder, *LiF*		x			+
583.001	Crystal, *KCL*			x		
002	Crystal, *RbCl*			x		
003	Reciprocal Lattice Calculator			x		
584.002	Buried Elements				x	
003	Porosity				x	
004	Cracks				x	
005	Faulty Weld				x	
006	Lead Mask		x			
585.001	Powder, *NaF*			x		+
002	Powder, *SiC*			x		+
003	Wire, *Nb* (3 x 15mm)			x		+
004	Powder, NH_4Cl			x		+
005	Wire, *Al* (3 x 15mm)			x		+
006	Polyethylene Monofilament (10)			x		+
007	Blank Superslide			x		+
008	Powder, *Al*			x		+
009	Acetate Cement		x			+
586.000	Powder Camera		x			+
003	Sample Tube Wires (10)		x			+
546	G. M. Tube, MX168					
547	G. M. Tube Holder					
587	Motorised Drive Unit					+
588	Ionisation Chamber					+
750/2	Filmpak, for radiographs (20)					
750/4	Filmpak, for powder camera (12)					

© 1974 TELTRON LTD.

The Tel-X-Ometer instrument
is the subject of
DESIGN REGISTRATION NO. 961472

TEL-X-OMETER
is a registered trade mark.

TELTRON LIMITED 32/36 Telford Way London W3 England

Printed in England

PRINTED BY BUSINESSCARE · CROYDON CR0 4RQ · TELEPHONE 01-686 9651